THE PECULIAR POPULATION OF HELIUM EMISSION STARS AT THE GALACTIC CENTER

by

Peter Tamblyn

A Dissertation Submitted to the Faculty of the

DEPARTMENT OF ASTRONOMY

In Partial Fulfillment of the Requirements
For the Degree of

DOCTOR OF PHILOSOPHY

In the Graduate College

THE UNIVERSITY OF ARIZONA

1 9 9 6

INFORMATION TO USERS

This manuscript has been reproduced from the microfilm master. UMI films the text directly from the original or copy submitted. Thus, some thesis and dissertation copies are in typewriter face, while others may be from any type of computer printer.

The quality of this reproduction is dependent upon the quality of the copy submitted. Broken or indistinct print, colored or poor quality illustrations and photographs, print bleedthrough, substandard margins, and improper alignment can adversely affect reproduction.

In the unlikely event that the author did not send UMI a complete manuscript and there are missing pages, these will be noted. Also, if unauthorized copyright material had to be removed, a note will indicate the deletion.

Oversize materials (e.g., maps, drawings, charts) are reproduced by sectioning the original, beginning at the upper left-hand corner and continuing from left to right in equal sections with small overlaps. Each original is also photographed in one exposure and is included in reduced form at the back of the book.

Photographs included in the original manuscript have been reproduced xerographically in this copy. Higher quality 6" x 9" black and white photographic prints are available for any photographs or illustrations appearing in this copy for an additional charge. Contact UMI directly to order.

UMI

A Bell & Howell Information Company
300 North Zeeb Road, Ann Arbor MI 48106-1346 USA
313/761-4700 800/521-0600

THE PECULIAR POPULATION OF HELIUM EMISSION STARS AT THE GALACTIC CENTER

by

Peter Tamblyn

A Dissertation Submitted to the Faculty of the

DEPARTMENT OF ASTRONOMY

In Partial Fulfillment of the Requirements
For the Degree of

DOCTOR OF PHILOSOPHY

In the Graduate College

THE UNIVERSITY OF ARIZONA

1 9 9 6

THE UNIVERSITY OF ARIZONA ®
GRADUATE COLLEGE

As members of the Final Examination Committee, we certify that we have read the dissertation prepared by Peter Tamblyn

entitled The Peculiar Population of Helium Emission Stars at the Galactic Center

and recommend that it be accepted as fulfilling the dissertation requirement for the Degree of Doctor of Philosophy

George H. Rieke	1/31/96 Date
Fulvio Melia	1/31/96 Date
Donald W. McCarthy, Jr.	1/31/96 Date
Philip Pinto	1/31/96 Date
	Date

Final approval and acceptance of this dissertation is contingent upon the candidate's submission of the final copy of the dissertation to the Graduate College.

I hereby certify that I have read this dissertation prepared under my direction and recommend that it be accepted as fulfilling the dissertation requirement.

Dissertation Director 1/31/96 Date

George H. Rieke Fulvio Melia

STATEMENT BY AUTHOR

This dissertation has been submitted in partial fulfillment of requirements for an advanced degree at The University of Arizona and is deposited in the University Library to be made available to borrowers under rules of the Library.

Brief quotations from this dissertation are allowable without special permission, provided that accurate acknowledgment of source is made. Requests for permission for extended quotation from or reproduction of this manuscript in whole or in part may be granted by the head of the major department or the Dean of the Graduate College when in his or her judgment the proposed use of the material is in the interests of scholarship. In all other instances, however, permission must be obtained from the author.

SIGNED: 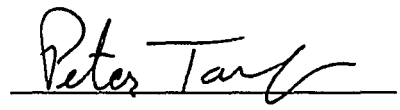

ACKNOWLEDGMENTS

This work would not have been possible without the continuous deadlines and floggings generously provided by my thesis advisors, Fulvio Melia and George Rieke. Their ideas, experience, enthusiasm, critical readings, and humor were equally valuable. But they will be most missed as friends. Essential scientific contributions were made by Laird Close, Margaret Hanson, Don McCarthy, Marcia Rieke, and Maximilian Ruffert. Valuable conversations with Peter Conti, Philippe Eenens, Joe Haller, and Phil Pinto improved the content and doubled the number of hyphens. Nadine Dinshaw, Richard Elston, Eric Hooper, and Evonne Marietta patiently listened to my confused ideas and helped convert them into readable proposals.

A NASA Graduate Student Fellowship and scholarships generously provided by the ARCS Foundation and the Spelman Prentice family had value beyond the resources they provided directly. They allowed me to concentrate on my thesis and were interpreted as votes of confidence. Observations reported in this paper were obtained with the Multiple Mirror Telescope, operated by the Smithsonian Astrophysical Observatory and the University of Arizona. Timely infusions of new data were provided by the mysterious workings of the Rieke TAC. The IRAF package and extensions were used for data reduction. IRAF is distributed by NOAO, which is operated by AURA under cooperative agreement with the NSF. This research has made use of the Simbad database, operated at CDS, Strasbourg, France. The local computer support provided by Alan Koski and Skip Schaller was excellent; pity about Solaris, though. Observing at the various telescopes was pure joy thanks as much to their support staffs as to their beautiful surroundings.

My parents and grandmother have provided continual encouragement. As did Sarah Blake, Robin Ciardullo, Gary DaCosta, John Hill, Pat Hogan, Steve Keil, Richard Kelly, Rob Kennicutt, Paul Krajovic, Brian Marsden, Larry November, Frank Wallace, and Michael Zeller at some of the critical junctures leading to this project. Assorted friends and my fellow graduate students were reasonably effective at keeping me sane through these years. Particularly supporting, diverting, and/or constructively critical were Anne, Barry, Charles, Chris, Crystal, Doug, Eric, Evonne, Grace, Joe, JRT, Kim, Laird, Lisa, Margaret, Mike, Nadine, Pat, Rex, Richard, RLM, Tamara, Tim, and the denizens of Hawthorne House.

Dedication

This work is dedicated to Andrew T. Shapiro,
who taught me to take pride in saying that
I am a professional geek.

"You have studied the Core. The stars of the Core are an average of half a light-year apart. They are even closer near the center, and no dust clouds dim their brightness. When stars are that close, they shed enough light on each other to increase materially each other's temperature. Stars burn faster and age faster in the Core.... Since the Core stars age faster, a much greater portion are near the supernova stage than in the arms. Also, all are hotter considering their respective ages. If a star were a few millenia from the supernova stage, and a supernova exploded half a light-year away, estimate the probabilities."

"They might both blow. Then the two could set off a third, and the three might take a couple more...."

At the Core by Larry Niven, 1966

Table of Contents

List of Figures

List of Tables

ABSTRACT

We show that extremely luminous, blue stars are present at the Galactic Center (GC) in numbers that are incompatible with normal stellar evolution. He I 2.058 μm images with a spatial resolution of 1″ show that the He I emission is concentrated on point sources, most of which are bright in the infrared, indicating they are warm and very luminous. Comparison with Monte-Carlo stellar population models demonstrates that normal evolution is incapable of producing this population. Near-infrared spectroscopy at high angular and spectral resolutions has been obtained, along with spectra of an extensive suite of other warm, luminous stars. These spectra provide new constraints on the mass in the central 1/2 parsec and the spectral comparisons confirm the peculiarity of the GC stars. The brightest have few, if any, analogues known in the Galaxy. Constraints from space-based observations on the blue light associated with nuclear populations in nearby galaxies demonstrate that the GC is unique or in a time-dependent phase. We have examined and rejected a number of models expected to produce this density of luminous, blue stars in the central parsec. A possibility remains that they are recently formed massive stars with unusual evolution forced by close binary companions. This model predicts similar populations of peculiar stars only in other dense galactic nuclei which have undergone very recent star formation.

CHAPTER 1

INTRODUCTION

1.1 Motivation

Galactic nuclei are among the most important and least understood astronomical objects. The unresolved center of an Active Galactic Nucleus (AGN) can outshine 1000 entire galaxies. Their importance stems not only from the hints they provide about physical processes in extreme environments, but also as beacons useful for probing the structure of the universe over cosmological distances and times. In addition to questions about the mechanism, fuel, and evolution of the central engine, astronomers struggle to understand why they turn off and where they are today.

One indirect approach to studying AGN is to study their quiescent colleagues, the Boring Galactic Nuclei (BGN). What leads some galactic nuclei to be active while the majority are boring? Do BGN share the engine but lack the fuel? Studies of BGN benefit from many local examples for detailed study, but frequently such studies identify previously unnoticed signs of low level activity. Is there a continuum of activity levels between BGN and AGN?

One of the dominant obstacles to study of the closest BGN, our own galaxy's nucleus, is that our perspective is through the intervening dust in the Galaxy's disk.

With 30 magnitudes of visible extinction, optical and ultraviolet (UV) studies are impossible. Fortunately, infrared (IR) photons can more easily penetrate the obscuring dust. Continuing improvements in IR technologies and their astronomical uses have brought us to a turning point in GC research. With IR arrays, spectrographs, adaptive optics, and space-based observations, we can study the nucleus of our Galaxy at a spatial detail unattainable beyond radio frequencies for other galactic nuclei. Recent studies have continually exceeded our expectations in showing the GC to be a peculiar, interesting, and active region. The region has the ingrediants thought to be critical to the activity in Seyferts and AGN, a large central mass and a large gas supply. Study of why this gas is separated from the engine is likely to be important to understanding the relation between Boring, low-level active, and Active nuclei.

1.2 The Galactic Center Region

A review of the GC region covering its remarkable features in radio, IR, X-ray, and γ-ray observations (Townes *et al.* 1983) indicates that two of the most interesting features are a point radio source, Sgr A*, which is unique in our Galaxy, and the densest stellar concentration in the Galaxy. The radio source Sgr A* has many of the characteristics expected of a relative of an AGN engine. It is associated with a large concentration of non-luminous matter (cf. Haller *et al.* 1996), located at the dynamical center of the Galaxy (Herbst *et al.* 1993), and has proper motion of less than 40 km s^{-1} (Backer & Sramek 1987). The spectrum has been successfully modeled as arising from a massive ($\sim 10^6\,M_\odot$), compact object with a low accretion rate (cf. Melia 1994). Further studies of the object are stymied by the large extinction, which prevents optical and UV observations, and by crowding in the IR. Observations with improved spatial resolution in the IR promise to determine which, if any,

of the coincident near-infrared (NIR) sources are associated with the radio source, and thereby improve the constraints on accretion models. Indirect measures of the object's mass and ionizing radiation will also be significantly improved in the near future. Demonstrating that Sgr A* is a massive black hole would be a significant step toward understanding the relation between our Galaxy and AGN.

The NIR from the GC is dominated by starlight, both an unresolved population and a large number of bright stars. The former is the aggregate contribution of the expected bulge population. The bright sources include older red giants and a surprising population of young stars which are more luminous than the older giants. Many of the bright stars are "blue" in NIR color maps. A broad emission line, He I 2.058 μm, is observed (Hall *et al.* 1982) to come from IRS 16, a dense concentration of these bright blue sources very near the dynamical center.

1.3 Preview

In this work, we focus on the young blue stellar population in the central 1/2 pc. Chapter 2 compares the observed population with that expected from a normal, large star formation event. Emphasis will be placed not only on matching the population's NIR color and brightness distributions, but on consistency with the constraints on the aggregate properties of the population. Chapter 3 tests a prediction of starburst models, that the bright "blue" sources are intermediate temperature supergiants. Follow-up observations are directed at understanding the bright blue sources and searching for fainter counterparts. Chapter 4 addresses the kinematics of the emission-line stellar population and confirms and improves the mass constraint on Sgr A*. Chapter 5 uses the information gained from these observations to compare the prominent stars with samples from the Galaxy and the Large Magellenic Cloud and to further constrain models of the stellar population. Finally, Chapter 6

examines in detail one of the conclusions of these models and comparisons, that the emission-line stars may result from stellar formation or evolution modified by the extreme conditions in the region. We find that the GC is an even more interesting region than expected.

Chapter 2

Stellar Population Models I: Are the IRS 16 Stars Expected to be Hot?

Peter Tamblyn & G. H. Rieke

Abstract

We have constructed burst models of the stellar population in the Galactic center. Many classes of models can be excluded entirely. Models with an age of 7 to 8 Myr and an initial mass of less than $4 \times 10^5\,M_\odot$ can reproduce the red supergiant stars and stars with the continuum characteristics of IRS 16 and provide the ionizing flux. We show that if IRS 16 is the product of normal stellar evolution associated with a recent star formation burst that currently dominates the energetics of the region, then IRS 16 itself is inconsequential to Galactic center energetics.

2.1 Introduction

The large amount of foreground extinction in the direction of the Galactic center (GC) has hampered investigations of the energy source for this region. However, it has become apparent that there are a number of very young stars in the area (e.g., Lebofsky, Rieke, & Tokunaga 1982) and it appears that energy is provided by more than one object (Rieke, Rieke, & Paul 1989). These observations suggest the hypothesis that a burst of recent star formation is the primary energy source. Unfortunately, infrared colors are uninformative in identifying hot stars that are candidates to supply this energy because they sample only the Rayleigh-Jeans tails of the energy distributions. In this chapter we combine the available spectral type information for the brightest sources with other observational constraints to investigate star formation burst models consistent with the observed characteristics of the GC.

IRS 16 is a collection of bright sources with relatively hot spectral energy distributions which some authors (cf. Allen, Hyland, & Hillier 1990) have suggested may be responsible for the majority of the ionizing radiation in the GC environment. The exact nature of IRS 16 is hidden by the obscuring dust; but by postulating that IRS 16 is a collection of normal stars associated with a recent burst of star formation, we can probe the characteristics of these sources indirectly.

In this study, we construct synthetic bursts with Monte-Carlo generated populations of stars, aged according to theoretical stellar evolutionary tracks. A model is judged successful if it explains the observed stars and meets the mass and ionizing radiation field constraints as described in Section 2.2. In Section 2.3 we detail the construction of the burst models. Section 2.4 uses the burst models to eliminate classes of solutions which are inconsistent with the observational constraints. Sections 2.5 and 2.6 describe the solutions we find and their implications.

2.2 Observational Constraints

2.2.1 Mass

A variety of techniques have been used to study the dynamics and mass distribution in the central 1–2 pc of the galaxy (Rieke & Rieke 1988; McGinn *et al.* 1989; Serabyn *et al.* 1988). Within a 1 pc radius, it is found that the total mass is $\sim 3.5 \times 10^6\,M_\odot$ of which $\sim 2.5 \times 10^6\,M_\odot$ is some form of centrally concentrated matter. Allowing for the mass of the old stellar population, we require that the recent burst of star formation involve a mass no greater than $4 \times 10^5\,M_\odot$.

2.2.2 Ionizing Radiation Field

The GC has a high density of UV radiation ($\gtrsim 10^{50}$ photon s^{-1}) with a soft ($T_{\rm eff} \lesssim 35,000$ K) spectral distribution (Lacy *et al.* 1980; Serabyn & Lacy 1985). A few stars hotter than 35,000 K could exist at the GC so long as their contribution to the total ionizing radiation field is small. We required that bursts have less than 20% of their ionizing flux from stars hotter than 37,000 K. The models are quite insensitive to the ratio selected.

2.2.3 IRS 16

IRS 16 seems to be a promising candidate for the ionizing source. Simons, Hodapp, & Becklin (1990) calculated that if IRS 16 is composed of 4 O7 supergiants with surface temperatures of order 35,000 K, it could provide all of the ionizing radiation and 20% of the total luminosity. IRS 16 has been resolved into 4 dominant components (Simon *et al.* 1990; Simons *et al.* 1990). The presence of He I emission from the gas surrounding these components lends credence to the theory that they are energetic.

IRS 16 components NE and NW have K magnitudes of 8.68 and 8.78 respectively (Rieke *et al.* 1989). Component C and the dominant source in SW are approximately

one magnitude fainter (Simons *et al.* 1990). At the distance to the GC (≈ 8 kpc) and with an extinction A_K of 3.47 (Rieke *et al.* 1989), these sources have absolute K magnitudes ~ -8.3 to -9.3. The high-resolution observations obtained during lunar occultations of IRS 16 by Simons *et al.* (1990) indicate that the dominant components have diameters less than 0.02″ which corresponds to 160 AU at the distance of the GC. Hence, it is extremely improbable that these components are themselves aggregates of stars. Their near-infrared colors are consistent with Rayleigh-Jeans tails from relatively hot sources. The absence of detectable CO absorption indicates a lower limit on the temperature of the sources (e.g., Allen *et al.* 1990). The precise temperature at which CO absorption would be undetectable at high metallicity with an allowance for unknown surface gravity is difficult to pin down, but 5,000 K is an adequately generous lower limit. The UV temperature constraint applies as an upper limit to the temperature of IRS 16 because if as hot as 35,000 K, IRS 16 would produce $\sim 10^{51}$ ionizing photons per second (based on model stellar atmospheres, as described in Section 2.3.4). These temperature limits allow considerable latitude in the nature of IRS 16. If near the upper end of the allowed temperature range, IRS 16 is one of the primary energy and UV sources in the GC; if at the low end its UV output would be negligible. We can estimate the total luminosity of each of these sources as a function of their effective temperatures by assuming a blackbody energy distribution. This defines a locus in the HR diagram in which stars would appear as IRS 16 components.

2.2.4 Red Supergiant Stars

In the inner 2 parsecs of the GC field there are 9 stars with spectral classifications M0 to M4 in luminosity classes I and II (Rieke *et al.* 1989). Comparison with bulge giants (Frogel *et al.* 1978; Schmidt-Kaler 1982; Frogel & Whitford 1987) with a generous allowance for metallicity effects suggests limits on $T_{\rm eff}$ of 4,170 K and

2,800 K for these stars. Luminosities of the GC red supergiants (RSGs) are in the range 10^4 to 10^6 $L_\odot$.

2.3 Models of the Stellar Population

A model of a stellar population is fundamentally a sum of the characteristics of a group of stars. The age distribution of stars in the models, normalization of the models, distribution of stellar types, and evaluation of the stars' characteristics are discussed in this section.

2.3.1 Age Distribution

The hypothesis for this analysis is that most of the energetic phenomena at the GC are caused by young stars. As these stars have short lifetimes a burst is most efficient at producing the stars of interest. A spread in ages might be a more appropriate model for real star formation, but would dilute our results in this analysis.

2.3.2 Stellar Distribution

The initial mass function (IMF) describes the relative numbers of stars created in an episode of star formation as a function of their initial mass. However, the IMF is an averaged distribution. If a small number of stars are created in a single event, sample statistics can distort the mass distribution of stars compared with the predictions of a smooth IMF. Sample variations are particularly evident in the upper mass ranges: even a large burst of star formation will have only a relative handful of the most massive and most luminous stars. Yet, the observable characteristics of a population of stars are often dominated by the few most luminous members. Hence, two bursts with identical average characteristics could have very different observational characteristics due to small sample statistics. To overcome this limitation, we have used the technique of Monte-Carlo integration. By repeating a set of tests

with many different randomly populated bursts, we can estimate the probability of a burst with given parameters leading to the observed GC population.

The initial masses of the stars were distributed randomly in accordance with a power-law approximation to a Miller-Scalo (1979) IMF extended to $100\,M_\odot$ [only relevant for the youngest bursts]. A randomly generated number (x) between zero and one was mapped to an initial mass M:

$$M = ((M_u^{-\alpha+1} - M_l^{-\alpha+1})x + M_l^{-\alpha+1})^{\frac{1}{-\alpha+1}} \tag{2.1}$$

where α is the IMF power law index (3.3 for a Miller-Scalo IMF). M_u is the mass of the most massive star still in existence at the specified burst age in accordance with the linear interpolation used between source tracks. M_l is the mass of the lowest-mass stars of interest, taken to be $10\,M_\odot$ for this analysis. Stars with masses 0.1–$10\,M_\odot$ contribute relatively little ionizing flux but were considered when computing the mass and luminosity of each burst.

2.3.3 Stellar Evolutionary Tracks

Rich (1990) has found a wide spread in metallicities of nuclear bulge giants with an average metallicity of approximately twice solar. The abundances in the interstellar medium in the GC (out of which the burst stars would have formed) are difficult to determine because of reddening and other effects, but are estimated to be roughly twice solar (Lacy *et al.* 1980).

The accuracy of any analysis of this sort is fundamentally limited by the accuracy of the input stellar evolutionary tracks. The dearth of easily observable stars in the relevant mass range, and observational ambiguities including distance and interstellar reddening (Conti 1988), have led to uncertainties in the tracks. Convective overshoot and mass loss are of great importance to the evolution of massive stars, yet their extent is unclear (Schaller *et al.* 1992, hereafter SSMM). The obser-

vational evidence that the GC has a metallicity well above solar compels us to use evolutionary tracks which are less well constrained than those for solar metallicity. Non-solar metallicity introduces uncertainties in abundance ratios, opacities, and mass-loss rates (Conti 1988). However, our analysis yields a well defined conclusion that is likely to be correct qualitatively despite uncertainties in the evolutionary tracks.

We based one set of models on Maeder's (1990) stellar evolutionary tracks for massive stars with Z=0.040. These tracks have metallicity-dependent mass-loss rates and moderate convective overshoot. The tracks are tabulated by evolutionary stage such that one can interpolate between similar stages of evolution in neighboring source tracks. For each model star, a track segment for the randomly generated mass was interpolated from the set of source tracks and, at the chosen age, the luminosity, temperature, and current mass were interpolated from this segment.

For comparison we repeated our modeling with stellar evolutionary tracks published by SSMM for solar metallicity. These tracks differ from the Maeder tracks in many respects as detailed by SSMM. Of most importance for this analysis are revisions to the nuclear cross-sections which affect the blue loops, reduction of various timescales due to a change in the method used to compute compositions which is especially important in the presence of convective overshoot, and the treatment of the optically thick winds of WR stars in accordance with Castor, Abbott, & Klein (1975) theory. These differences apparently dominate the metallicity differences for most of the behaviors relevant for this paper. Tracks for $20\,M_{\odot}$ and up are published with standard mass-loss rates [set C] and with doubled mass-loss rates in the post-main-sequence stages [set D]. SSMM favor the latter to match observations of WR stars. Stars at the GC are likely to have enhanced mass loss due to the high ambient UV field and super-solar metallicity. The mass-loss rate has a dramatic

impact on the parameters of interest in this analysis, so complete sets of models were run with both sets of tracks.

Figure 2.1 illustrates burst models at various ages based on the three sets of stellar evolutionary tracks. Comparison reveals the very different behaviors described by the tracks in the post-main-sequence stages of evolution. In particular, the very hot and luminous Wolf-Rayet stars at the left of the 6 and 7 Myr panels of the Maeder bursts are much less numerous (because of reduced timescales) in bursts based on the SSMM tracks. The fraction of stars in blue loop phases of evolution is greatly reduced in the models based on the SSMM tracks.

2.3.4 Ionizing Radiation

Each burst model was constructed by adding stars to the burst until the ionizing flux from the collection of aged stars was $\geq 10^{50}$ photon s^{-1}. The Lyman contributions of model atmospheres were integrated from Kurucz (1992) synthetic stellar spectra for Z=0.04. The optically thick winds of Wolf-Rayet stars have strongly wavelength dependent optical depth effects which distort the emergent spectrum dramatically. The Kurucz atmospheres are assumed LTE and planar, neither of which applies to these winds. Care must be taken to consider the large uncertainties when interpreting burst models in which these stars are prominent.

Maeder (1990) only has tracks for stellar masses 15 $M_{\odot}$ and greater. At early ages the relative contribution to the UV flux from lower-mass stars is negligible. However, as the burst ages, the fractional contribution of the lower-mass stars grows and dominates the UV flux at ages greater than about 8 Myr. To make models of bursts at these ages, it was necessary to estimate the UV contribution from stars less massive than the Maeder tracks described. From our results, bursts older than 8.5 Myr cannot fit the characteristics of the GC. By restricting our analyses to ages less than 9.6 Myr, we were able to ensure that all stars in the burst less massive than

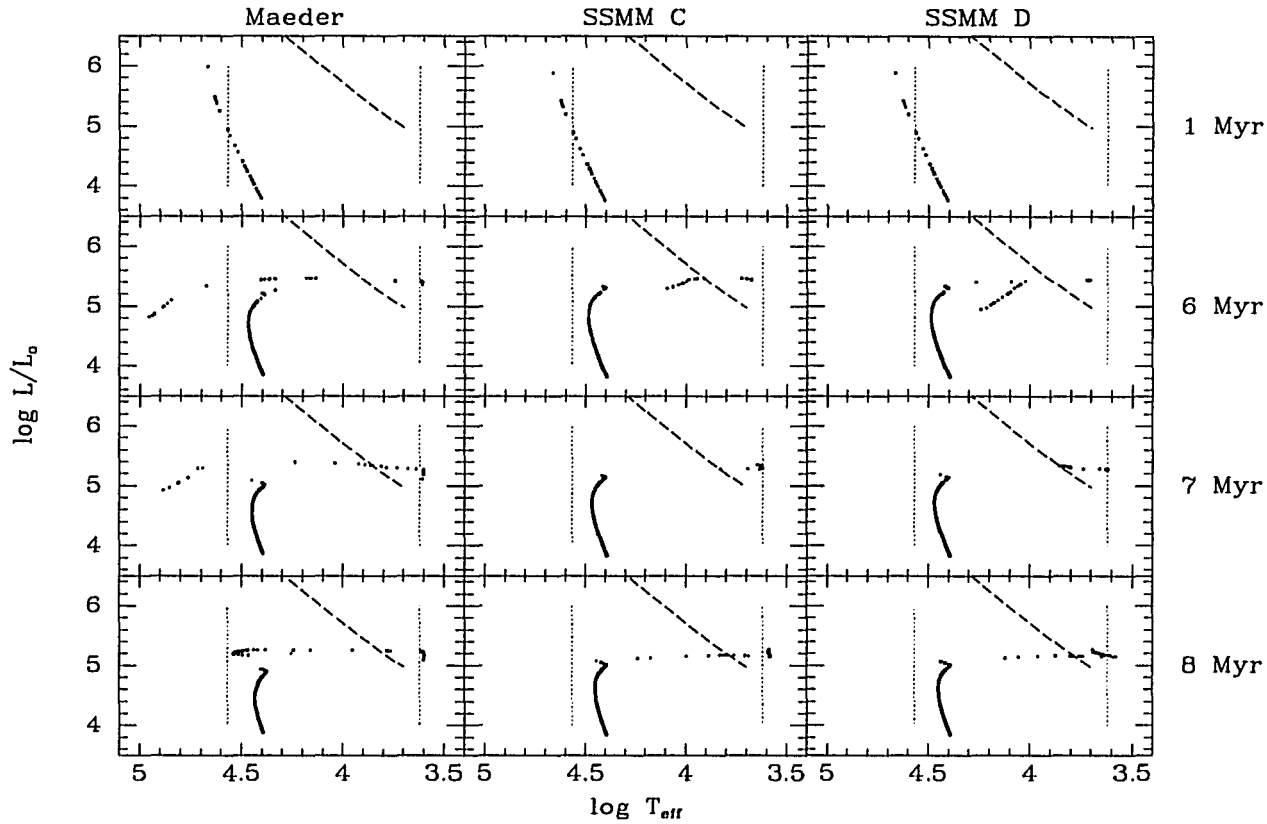

Figure 2.1: Synthetic Burst HR Diagrams at Various Ages. Dotted lines at $T_{\rm eff}$ = 37,000 K and at 4,170 K represent the cutoffs used for the UV temperature constraint and RSG counts. The dashed line is the locus of blackbodies with $M_K = -9.3$ (IRS 16-like sources). Note that many more stars are needed at later ages to produce the same Lyman flux and that candidate IRS 16 stars are progressively cooler in older bursts. It is also apparent that young bursts do not have the red stars observed at the GC. The differences in post-main-sequence evolutionary behaviors of the sets of tracks are quite apparent.

15 $M_\odot$ were still on the Main Sequence. A comparison of evolutionary tracks for 15 $M_\odot$ reveals that main-sequence evolution of SSMM tracks for Z=0.02 is similar to the evolution described by the Maeder tracks. An overall increase in luminosity of 8% and a decrease in main-sequence lifetime of 8% applied to the SSMM track made the main-sequence portions of the 15 $M_\odot$ tracks from these two sources essentially identical. To supplement the Maeder tracks, these same corrections were applied to the 12 and 9 $M_\odot$ tracks from SSMM and tracks interpolated in the 10 to 15 $M_\odot$ range in the same manner as with the Maeder tracks. Contributions from these stars were always tallied separately to make it apparent when errors in this procedure might influence results.

2.3.5 Burst Tests

Once the normalized burst population had been synthesized, a series of quantitative tests were applied to determine if the model burst matched the observed GC. The first of these tests was to check that the total ionizing photon fluxes from stars with $T_{\rm eff} < 37,000$ K was at least four times as great as the ionizing fluxes from hotter stars. The second test is that the total initial mass of the burst be less than 4×10^5 $M_\odot$. The number of stars in a burst model was determined by adding massive stars until the aggregate produced adequate UV output. The total mass of stars was determined by integrating the normalized Miller-Scalo (1979) IMF extended to 100 $M_\odot$:

$$M_{total} = \frac{N}{\int_{10}^{M_u} \psi(m) dm} \times \int_{0.1}^{100} \psi(m) m dm \qquad (2.2)$$

in which m has units of solar masses, N is the number of massive stars in a burst, and M_u is the same as in Equation 2.1.

Finally, the model burst must reproduce the observed stellar population. Model stars with blackbody-approximated M_K in the range -8.81 to -9.69 (0.67 to 1.5 times the luminosity of a bright IRS 16 component at the same temperature) were

tallied as IRS 16-like sources; four had to be in a synthetic burst for it to be considered a successful GC match. Model stars which get as cool as $T_{\rm eff}$=4,170 K have luminosities in the range observed for RSGs at the GC. A count of all stars in this temperature range was kept and required to be between 7 and 15 for a successful GC model. The star count restrictions are generous to compensate for the instantaneous star formation history we assumed for bursts. For example, although a burst model with a particular age might make more IRS 16-like stars than are observed, only a small spread in ages around this value would result in significantly reduced IRS 16 counts.

Table 2.1 lists the tests a burst model was required to pass to be counted as a successful model of the GC. Figure 2.2 summarizes the behavior of models using the Maeder Z=0.04 tracks. Figures 2.2*a-e* plot the average values of the portion of ionizing radiation from stars with $T_{\rm eff}$ above 37,000 K, the ratio and numbers of RSG and IRS 16 stars, and the total initial mass of stars. Figure 2.2*f* plots the percentage of bursts which satisfied these criteria as a function of age — in this case none. The models based on the Maeder Z=0.04 tracks fail primarily because of the UV $T_{\rm eff}$ constraint. As mentioned above, the $T_{\rm eff}$ of the WR stars which dominate the ionizing flux at the relevant ages is uncertain, so Figure 2.3 shows the same quantities without this test applied. Figures 2.4 and 2.5 show the same quantities for the full set of tests for bursts using the SSMM stellar evolutionary tracks. The UV $T_{\rm eff}$ criterion is a redundant constraint for these models.

The bolometric luminosities associated with a starburst population (including the late-type component) sufficient to produce the ionization were calculated to be $\sim 1 \times 10^7\,{\rm L}_\odot$ at 5 Myr and $\sim 8 \times 10^7\,{\rm L}_\odot$ at 8 Myr. These values are generally toward the high end of the estimated range (Werner & Davidson 1989) but they are compatible with observation if the solid angle subtended at the luminous stars by

Table 2.1: Criteria for Galactic Center-like Bursts

UV flux	$\geq 10^{50} \gamma\, s^{-1}$
UV $T_{\rm eff}$	Ionizing photon flux from stars with
	$T_{\rm eff} > 37,000\, K$ required to be $< 20\%$ of total
Initial mass	$\leq 4 \times 10^5\, M_\odot$
# RSG	7 to 15
# IRS 16	≥ 4

the dust torus is as small as indicated by the observations of Güsten *et al.* (1987).

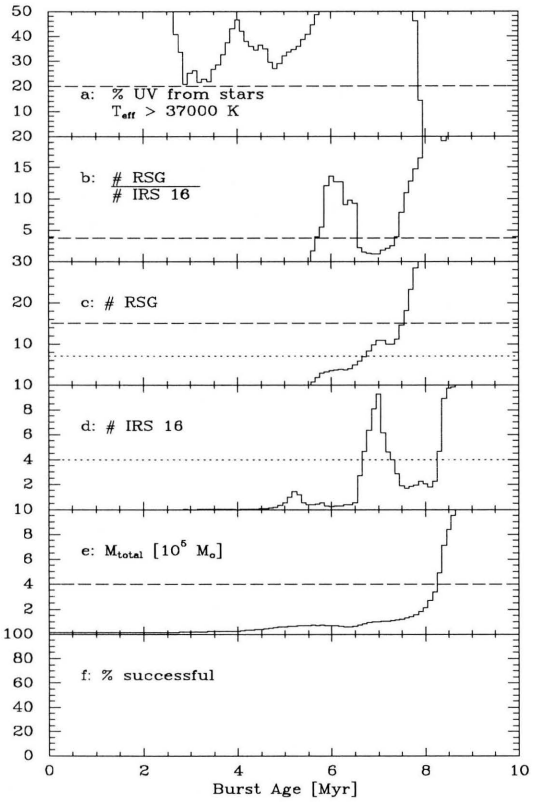

Figure 2.2: Average Quantities from 500 Synthetic Bursts Based on the Maeder Z=0.04 Stellar Evolutionary Tracks. Upper and lower limits are represented by dashed and dotted lines respectively. Panel *a* is the portion of the summed ionizing photon fluxes from stars hotter than 37,000 K; *b* is the ratio of RSGs to IRS 16-like sources; *c* is the number of RSGs; *d* is the number of IRS 16-like sources; *e* is the mass formed into stars in units of $10^5\,M_\odot$; *f* is the percentage of models that met all constraints.

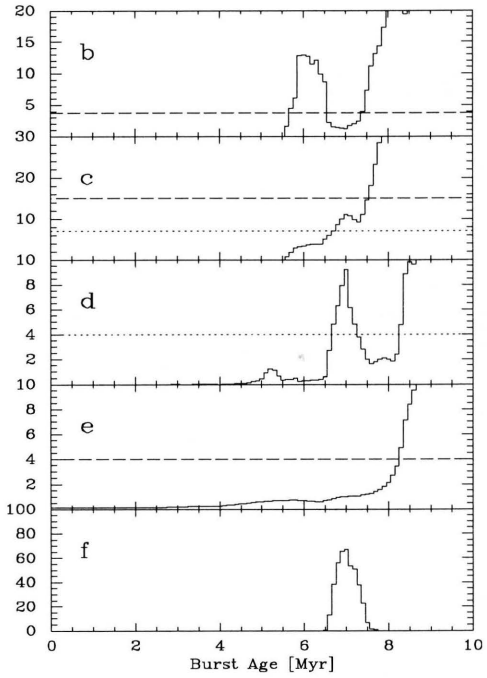

Figure 2.3: Same as Figure 2.2 with the UV $T_{\rm eff}$ constraint suppressed.

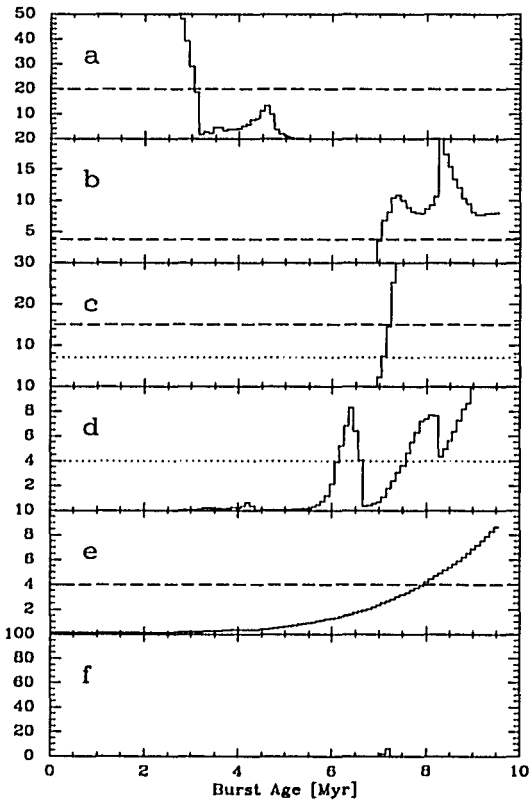

Figure 2.4: Same as Figure 2.2 with SSMM stellar evolutionary tracks with standard post-main-sequence mass-loss rates.

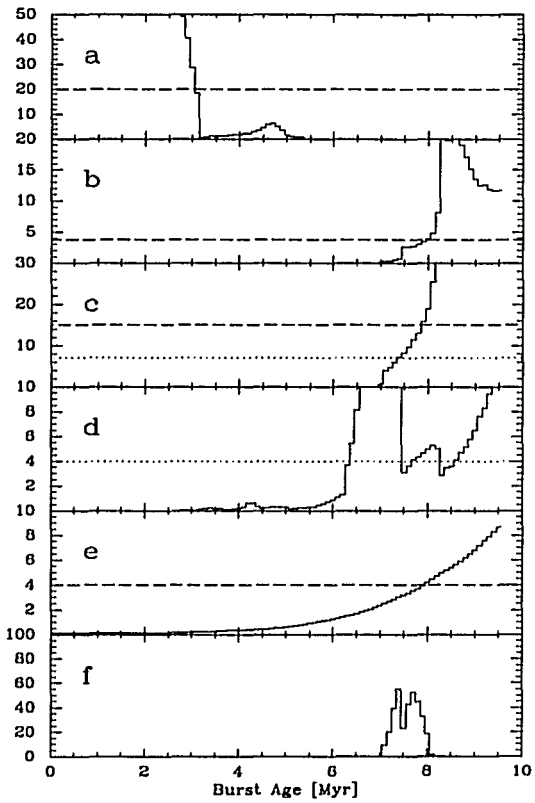

Figure 2.5: Same as Figure 2.2 with SSMM stellar evolutionary tracks with doubled post-main-sequence mass-loss rates.

2.4 Excluded Ages

2.4.1 Simple Star Formation History

Examination of Figures 2.2–2.5 allows us to exclude with confidence various ages of bursts. The youngest bursts are excluded by the constraint on the UV spectrum and because they do not produce any RSGs nor sources which would have IRS 16's observed characteristics. All three tests are independent of normalization and of each other. There continue to be no stars as cool as the GC RSGs until 5.5 Myr with the Maeder tracks and until 6.9 Myr with the SSMM tracks.

Bursts older than 8.5 Myr can also be dismissed. If stars are responsible for all of the Lyman photons, then these bursts require that more mass was converted into stars in the star formation episode than the dynamical observations allow and too many RSGs are present. Further, these bursts overproduce RSG stars relative to stars in the IRS 16 locus. Additional sets of models were computed with the SSMM tracks to confirm that this ratio remains well above the upper limit at ages later than shown in Figures 2.4 and 2.5. Note that this ratio is independent of normalization.

Although the mass, UV $T_{\rm eff}$, and IRS 16 count constraints confirm the result, the RSG count is sufficient to limit the ages of consistent bursts to a very narrow range (assuming that young stars provide the ionizing radiation). Even without this normalization assumption the models indicate that ages outside the range 5.5–8 Myr would not be likely to produce the stars observed at the GC. Therefore, our conclusions are unlikely to be affected by modifications in the IMF which might relax the mass constraint by reducing the proportion of low ($\sim$ solar) mass stars.

2.4.2 Complex Star Formation History

A more complex star formation history than just a single instantaneous burst could produce a different mix of stars observed at the present time. However, the uncer-

tainties in late stages of massive stellar evolution as illustrated by these three sets of stellar evolutionary tracks make it clear that any attempt to disentangle star formation history effects from stellar evolutionary effects would be mired in uncertainty. However, our basic conclusions do not seem to depend strongly on details of the star formation history. For example, consider models based on the tracks from set C of SSMM, which indicate the probability of a single burst reproducing the observed stellar population is very low. A mix of stars with ages 6.4 Myr, when IRS 16-like sources are relatively common, and 8.3 Myr, when RSGs are quite common, might be able to match the observed stellar population and slip in under the mass constraint. However, any such complex star formation history must still be dominated by star formation between $\sim$ 3 and 8 Myr ago to avoid having too much hard UV or mass.

2.5 Successful Models

2.5.1 Burst Parameters

The set of SSMM tracks with enhanced mass loss are the only set that yield formal solutions with high probability. The successful burst models have an age of 7–8 Myr, an initial mass of stars of a few times $10^5\,M_\odot$, and 1000–1900 stars more massive than $10\,M_\odot$ at the time of observation. Assuming $A_V = 30$ and a distance of 8 kpc, these stars have average integrated $m_K \sim 4.5$, 3.9, and 3.3 at 7.0, 7.5, and 8.0 Myr respectively, in agreement with the $m_K \sim 3.3$ within the central $1.8'$ (~ 2 pc radius) measured by Becklin & Neugebauer (1968). In successful models, the IRS 16 components are F or G supergiants with $L \sim 10^5\,L_\odot$ and $T_{\rm eff} \sim 6,000$ K. The ionization is provided by many late O or early B main-sequence stars with $T_{\rm eff} \sim 30,000$ K. The Maeder Z=0.04 tracks match all of the constraints at $\sim$ 7 Myr except the UV $T_{\rm eff}$ constraint. The WR stars left of the 37,000 K line in the relevant subpanel of

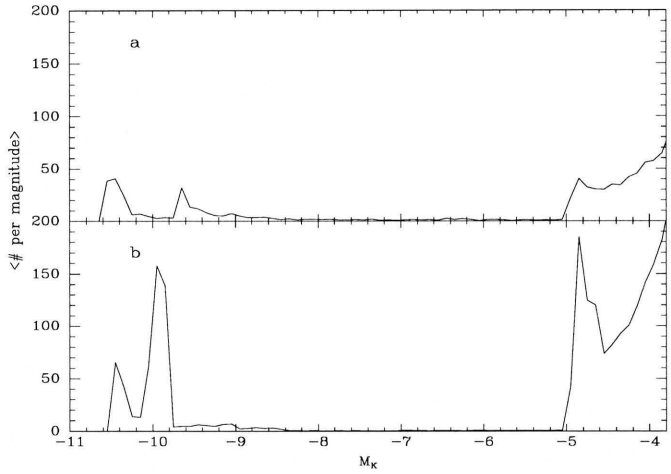

Figure 2.6: Averages of 100 Luminosity Functions. Panel *a*: models based on Maeder tracks at an age 7.0 Myr; *b*: models based on SSMM tracks at an age 7.7 Myr.

Figure 2.1 contribute only ~7% of the luminosity but most of the ionizing photons at these ages. As discussed above, the Lyman flux and characteristic temperature of WR stars are quite uncertain so it is not necessarily the case that the $T_{\rm eff}$ is correctly represented by the tracks. The SSMM tracks with the lower mass-loss rate give very low probabilities of burst solutions because model stars do not get as cool as the GC RSGs until after the first peak in the count of IRS 16-like sources.

Predicted luminosity functions for average bursts are given in Figure 2.6 based on the Maeder tracks at age 7.0 Myr and the enhanced mass loss SSMM tracks for an age of 7.7 Myr where the probability of a GC-like burst peaks. We conclude that the currently observed very high luminosity stars are likely to be the only ones observable, even with increased sensitivity and angular resolution, since the next most luminous stars are more than 4 magnitudes fainter and will tend to be heavily confused with the old stellar population.

2.5.2 Explosive Event

There exists a body of evidence pointing to a recent powerful explosion at the GC. Townes (1989) discusses the turbulent clouds near the GC and the evacuation of the GC region as possibly indicating an explosion in the region 10^5 yr ago. Mezger *et al.* (1989) detected a dust ring with radius ~ 5 pc around the synchrotron shell source Sgr A East. The source geometry suggests that an explosion inside a giant molecular cloud broke through the near side of the cloud and created a shell structure similar to a supernova (SN) remnant. Mezger *et al.* (1989) suggest this structure is due to a powerful event at the location of Sgr A* or to a SN inside a wind blown bubble. A difficulty with the latter explanation is that the formation of a wind blown bubble of this size requires $\sim 10^6$ yr without significant tidal disruption. Nonetheless, based on the radio brightness, Mezger *et al.* (1989) conclude that such a SN would have occurred 7,500 years ago. Our models predict one SN approximately every 70,000 yr and also have stars capable of creating substantial wind bubbles. Given the uncertainties in the estimate of the timescales involved, we consider it plausible that the Sgr A East structure is a SNR associated with the burst of star formation considered in this paper.

2.6 Conclusion

We can distinguish three different hypotheses for the activity in the GC:

2.6.1 Excitation by a Burst of Star Formation, with Normal Stellar Evolution

The primary conclusion of this paper is that, should all the activity in the GC be powered by a burst of star formation after which the stars evolved normally, then the bright (in the near infrared) blue stars that lie in IRS 16 are unlikely to be the objects that actually provide the UV flux and luminosity of the region. The time

since the episode of star formation must be roughly 7 Myr, the only epoch at which the observed numbers of UV photons and blue and red stars appear simultaneously. Given this age, however, a mix of objects that reproduces the observations within the current uncertainties in theoretical stellar evolution has a significant probability of forming.

2.6.2 Excitation by Non-Stellar Means, Recent Star Formation and Normal Evolution

The UV in the GC may be provided by some non-stellar source, with the observed population of stars arising as an incidental event. In this case, we find that the relative numbers of red giants and supergiants and IRS 16-like sources never reproduces the observations except during the same interval when the stars can provide the UV. Bursts of star formation that are more than 8 Myr old produce a larger ratio of red supergiants to IRS 16-like objects than is observed, and bursts less than 5.5 Myr old do not produce enough red supergiants. A separate UV source is therefore unnecessary if normal stellar evolution occurs; a burst of star formation that accounts for the components of IRS 16 and the red supergiants has no difficulty in producing adequate UV.

2.6.3 Abnormal Stellar Evolution

The presence of IRS 7 in the GC demonstrates that massive stars have formed in this region in the last $\sim$ 10 Myr. However, conditions in the GC may lead to stellar evolution that is significantly different from that observed elsewhere and represented by the evolutionary tracks used in our analysis. If the components of IRS 16 are hot enough to excite He I directly, for example, then we would conclude that the stellar evolution is highly abnormal or that these objects are not stars.

This work suggests a critical test for the hypothesis that a burst of star formation

with normal stellar evolution accounts for the energetics of the GC. The members of IRS 16 should not be hot enough to produce the emission of He I that is observed in close proximity to them; this gas must be ionized by hotter stars that are nearby. Applying this test may be difficult, since the unique conditions in the GC may result in excitation of He I in winds from relatively cool stars. For example, the He I imaging by Krabbe *et al.* (1991) shows strong He I from IRS 11, 12, 15E, and 17, all of which show CO bands in absorption and therefore must be dominated by red giants or supergiants. Very high resolution, spectrally resolved imaging should be used to see if the He I can be resolved separately from the continuum sources.

CHAPTER 3

EMISSION-LINE OBSERVATIONS

Peter Tamblyn[1], G. H. Rieke[1], Margaret Murray Hanson[2], L. M. Close[1], D. W. McCarthy, Jr.[1], & M. J. Rieke[1]

[1]Steward Observatory, University of Arizona, Tucson, Arizona 85721

[2]Joint Institute for Laboratory Astrophysics, Campus Box 440, University of Colorado, Boulder, Colorado 80309-0440

Abstract

Br γ and He I 2.058 μm images of the Galactic center reveal that most of the Br γ emission is associated with interstellar gas but that the He I is largely concentrated on individual, luminous stars that therefore must be hot. High-resolution spectra of these stars, emphasizing He I 2.058 μm through Br γ 2.166 μm, are compared with spectra of 98 hot, luminous stars from the literature and new spectra of 43 luminous galactic emission-line stars including late nitrogen-sequence Wolf-Rayet, Luminous Blue Variable, Oe, Of, and ON supergiant stars. Combining our data with other observations from the literature, the He I sources in the central parsec include $\sim$ 5 Ofpe/WN stars and one late-WC star. The inferred luminosity and detection of Mg II emission lines in the spectrum of IRS 16NE make it a likely LBV candidate. However, we find 6 stars with line widths $<$ 500 km/s which defy easy classification, even from the extensive library of comparison spectra we have compiled. Considering the ultraviolet constraints (cf. Serabyn & Lacy 1985; Shields & Ferland 1994) and the large number of peculiar hot stars, either we see this stellar population at a very distinctive moment in its evolution, or the conditions of formation or the evolution of the stars must be significantly altered by the environment in the central parsec.

3.1 Introduction

The center of the Galaxy is in many regards the most easily studied galactic nucleus, despite $\sim$ 30 magnitudes of extinction in the visual. A persistant puzzle is the region's power source. The interstellar gas is excited by $\gtrsim 10^{50}$ ionizing photon s^{-1} with a soft ($T_{\rm eff} \lesssim 35,000\,{\rm K}$) spectral distribution (Lacy *et al.* 1980; Serabyn & Lacy 1985). Although there has been considerable speculation that accretion onto a massive black hole is the dominant energy source, models (Hollywood & Melia 1995) which reproduce the faint infrared flux (Eckart *et al.* 1992; Close, McCarthy, & Melia 1995) indicate that accretion does not dominate the UV. The presence of red supergiants (Lebofsky, Rieke, & Tokunaga 1982) and the "blue" (near-infrared) colors of numerous point sources suggest that a population of young stars powers the region.

Broad He I 2.058 μm emission was detected from the IRS 16 region in the Galactic center (GC) by Hall, Kleinmann, & Scoville (1982). Allen, Hyland, & Hillier (1990) showed that the Br γ source 10″ SW of the dynamical center discovered by Forrest *et al.* (1987) is a strong He I source as well. Their tentative classification of this star, referred to as the AF star, as Ofpe/WN9 was confirmed with high-resolution spectroscopy (Najarro *et al.* 1994). Although it has generally been assumed that the IRS 16 complex could be a group of WR stars with the AF star an outlying example, Chapter 2 used the NIR brightnesses of these stars and a variety of constraints on the integrated properties of the stellar population to show that this would not be consistent with normal stellar evolution. Instead, we suggested that a normal young population consistent with the global constraints would have an ample supply of undetectable late-O main-sequence stars to excite nebular He I emission. Existing He I emission line images (Krabbe *et al.* 1991) can distinguish the AF star and $\sim$ 10 other strong and relatively isolated He I sources from the background. Higher

angular resolution is required to distinguish whether the bright, crowded IRS 16 components are also unusual He I 2.058 μm sources or whether they are the lower temperature supergiants predicted by the evolutionary calculations, with the emission lines originating in the surrounding nebulosity. As reported earlier (Tamblyn & Rieke 1993; Rieke & Rieke 1994), such images indicate the He I does in fact originate in the stars; these data are presented in greater detail here and in the context of their implications for population models of the central cluster.

Further insights to the nature of the hot stellar population can be obtained with spectroscopy, which can be compared with the near-infrared spectra of hot stars elsewhere in the Galaxy to classify the GC stars. We have obtained spectra at a resolution of $\lambda/\Delta\lambda \approx 2500$ of many of the He I sources apparent in our images and those of others. A number of the He I stars appear to be normal late-WN or Ofpe/WN stars. However, many others have relatively narrow lines and cannot be associated with any common stage in normal hot stellar evolution. Both our imaging and spectroscopy therefore indicate either that we see the GC at a very distinctive moment in its evolution or that there is some abnormality in the formation or evolution of massive stars in this region.

In Section 3.2, we describe our high-resolution images of the GC in the He I emission line and complementary Br γ images intended to determine whether the IRS 16 components are individual He I sources. Spectra of many of the He I sources and a large sample of comparison stars are described in Section 3.3. Section 3.4 discusses possible classifications for the population of narrow emission-line stars found in the region. Finally, Section 3.5 summarizes the results from these observations.

3.2 Emission-Line Images

These images test whether the IRS 16 components are hot, He I emission sources, contrary to the predictions of the starburst models with normal stellar evolution (Chapter 2).

3.2.1 Imaging Observations and Reductions

Narrow-band images of the GC south of IRS 7 were obtained in May 1993 and June 1994 at the Steward Observatory Bok (2.3 m) telescope. Atmospheric image degradation is a major concern for imaging the crowded GC field and is exacerbated by the low elevation at transit of the GC as seen from Kitt Peak. Tip-tilt correction for image motion, made possible by FASTTRAC (Close & McCarthy 1994), substantially improved the image quality. FASTTRAC uses a small probe mirror to pick off light from a bright guide star (IRS 7) and send it to an InSb camera read out at $\sim$ 50 Hz to determine the displacement of the stellar image centroid. The displacement is translated into an error signal to drive the tip-tilt telescope secondary to recenter the stellar image. The remainder of the field is imaged to 0.2″/pixel by the Steward Observatory NICMOS camera (Ricke *et al.* 1993) which has a 256x256 NICMOS3 array used for the longer-integration (120–300 s) science images. These images had a FWHM of 0.8–1.0″ in this experiment. A narrow bandpass interference filter was used in a system where the transmission function is tuned by tilting. The tilt of the interference filter was verified by observing a planetary nebula. For He I imaging, the filter transmission has a FWHM of 0.017 μm for a spectral resolution of 120. The Brγ data were measured with a resolution of about 200. Continuum images were obtained by changing the filter tilt to provide transmission with similar spectral resolution displaced slightly from the emission line.

Initial data reduction followed standard procedures. Pixel-to-pixel response variations were removed with dark and flat frames. Images of a blank sky field, taken

after each object image, were median combined in separate groups by night and filter setting. For each GC image, the appropriate blank sky frame was scaled to the same median as the single blank field image taken after the GC image and subtracted. The resulting images are quite flat except for the immediate area around the image of the probe.

Before summing, the images were co-aligned and bad pixel values replaced by interpolation from neighboring pixels. In none of the images were bad pixels located in the IRS 16 environs. In the case of the Brγ pair, the image in the nearby continuum had higher spatial resolution. It was degraded to the resolution of the on-band image by convolution with a Gaussian. The continuum images were scaled and subtracted from the on-band images to create the difference images presented in Figures 3.1*a* and 3.1*c*. In the case of the Brγ pair, there was little ambiguity (6%) about the scaling coefficient as an inappropriate coefficient clearly results in under- or over-subtraction of the stellar images. For the He I pair this uncertainty increases to 10%. In part this is due to the fact that the bulk of the He I emission is from point sources unlike the predominantly diffuse Brγ emission. A few stars (e.g., IRS 9 and IRS 12N) apparently suffer greater extinction or have H_2O absorption and appear over-subtracted when the scaling coefficient is adequate to subtract out the bulk of the stellar images. The over-subtracted stellar residuals were replaced with the local sky value before photometry was performed.

Simulated aperture photometry was performed on the images with the IRAF APPHOT package and compared to published aperture photometry (Wade *et al.* 1987). Our results agree allowing for uncertainty in aperture location. Large simulated apertures were used to estimate the contribution to the line flux from diffuse emission. Even in the difference image, the He I image is crowded and the sources incompletely resolved, so the stellar profile fitting photometry package DAOPHOT

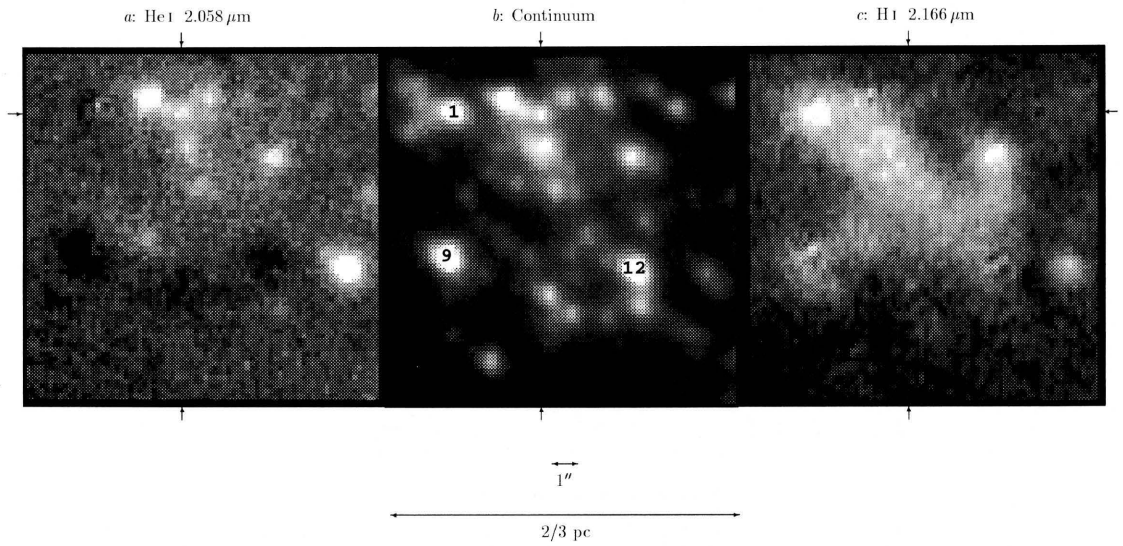

Figure 3.1: Emission-Line Images. The central 0.7 pc south of IRS 7 in *a*: He I 2.058 μm, *b*: nearby continuum, and *c*: H I Br γ. The location of IRS 16C ($17^h42^m29^s.4$ $-28°59'18''$, 1950.0) is indicated by arrows. Sgr A* is 1.1″W and 0.3″S of IRS 16C. IRS 1W, IRS 9, and IRS 12N are labelled for comparison with finding charts such as in Rieke *et al.* (1989). North is to the top and west is to the right.

in its IRAF implementation was used to measure He I fluxes. The two types of photometry could be compared with the isolated AF star. The resulting line fluxes are listed in Table 3.1. Because the He I emission is associated with bright stars, the uncertainty in the scaling coefficient combined with photometric calibration errors is enough to make our measured fluxes and even relative fluxes uncertain. However, the morphology described below is robust to these uncertainties and only sources which were prominent with either extreme of the subtraction coefficient are listed. A handful of fainter sources not associated with prominent stars in the continuum may exist in the region within the uncertainties. However, their number is small and they do not affect the conclusions of this paper.

Table 3.1: Unresolved Line Fluxes in Images

Source	Location	$F_{2.06\,\mu m}$ $10^{-16}\,W\,m^{-2}$	$F_{Br\gamma}$ $10^{-16}\,W\,m^{-2}$
AF (AHH)		2.4	1.8 ± 0.7
GCHe1	1.1″NE of AF	0.8	...
AHH-NW		0.6	...
GCHe2	0.7″N 2.6″W of IRS 9	1.0	0.9 ± 1
GCHe3	$\sim$ 4″S 1″W of IRS 16C	...	...
GCHe4	$\sim$ 4″N 1″W of AF	...	...
IRS 1W		...	2.1 ± 0.4
IRS 13		0.9	2.5 ± 1
IRS 16C+CC		1.8	...
IRS 16NE		1.8	...
IRS 16NW		1.5	...
IRS 29		...	...
GCHe5	$\sim$ 3″SW of IRS 7	...	...
IRS 15		...	...
Integrated		...	35 ± 8

3.2.2 Imaging Results – He I Star Cluster and Sgr A*

The Br γ image in Figure 1*c* has a few bright point sources (IRS 1W, IRS 13, and the AF star) and significant extended emission indicative of gas excited by the ambient radiation field. The morphology is very similar to the Br γ image presented by Lutz, Krabbe, & Genzel (1994) as well as the Br α image of Forrest *et al.* (1987) and radio images of the "mini-spiral" (Morris & Yusef-Zadeh 1987). In contrast, the 2.058 μm image (Figure 1*a*) clearly illustrates that the majority of the He I emission is from point sources, 5 of which are associated with stars prominent in broad-band images (Figure 1*b*) including 4 components of IRS 16. The contrast of He I and Br γ images clearly demonstrates that the He I is not from the surrounding nebula; its association with bright stars requires distinctive luminous stars which may be

difficult to reconcile with population models for the region (Chapter 2).

The observation by Krabbe *et al.* (1991) of He I emission from IRS 9, IRS 11, and IRS 15E is baffling because these objects are known to have CO absorption bands (IRS 9: Rieke, Rieke, & Paul 1989; IRS 11: Sellgren *et al.* 1987; IRS 15: Rieke & Rieke 1988). One of these sources, identified by Krabbe *et al.* (1991) as IRS 9, is in the field imaged in this experiment. With 1″ resolution, the emission-line source is clearly seen to be a star, near the background confusion limit in the continuum, located 2.6″ west of IRS 9. Images taken with the same instrument and a CO filter indicate IRS 9, which is a great deal brighter in the near infrared, has significant CO absorption and the previously unnoticed star to the west does not. Hence, this paradox was a result of insufficient spatial resolution blending the spectral diagnostics from a hot–cool source pair. Because it is not obvious how one star could exhibit both features, it seems likely that the remaining CO/He I identifications (IRS 11 and IRS 15E) by Krabbe *et al.* (1991) are also blends of the distinguishing He I feature from a hot star near a significantly cooler, and therefore brighter in the NIR, star with CO absorption.

We note that the He I image suggests the existence of an emission source at the same location (to an accuracy of 1 pixel) as the infrared source detected at H and K by Eckart *et al.* (1993) and at J by Close *et al.* (1995) coincident with the radio location of the black hole candidate Sgr A*. If this result is confirmed, it is likely to be useful in further studies of the nature of this object.

3.3 Spectroscopy

3.3.1 Spectroscopic Observations and Reductions

The confirmation that the He I emission line arises from a number of luminous stars leads to questions about their natures. To address these issues, spectra including

He I (2.058 and 2.112/3 μm), Br γ, and in some cases He II (2.189 μm) were obtained for many of the stars in the image. A large number of luminous galactic emission-line stars were also observed for comparison; many were selected for their high mass-loss rates. These spectra were all obtained with the Steward Observatory near-infrared spectrometer, Fspec, which is based on a NICMOS3 detector. Observations concentrating on the IRS 16 region were obtained on April 28 and 30, 1994 with the MMT, where the Fspec pixel scale is 0.37″, the slit is 1.2″ wide by 32″ long, and the spectral resolution measured from night skylines is 125 km/s. These were supplemented with observations of more isolated stars on June 26 and July 2, 1994 at the Steward Bok (2.3 m) telescope, with a pixel scale of 1.2″, slit 2.4″ by 96″, and measured resolution of 120 km/s. Spectra of the comparison stars listed in Table 3.2 were taken on those same nights and July 15 and 20 with the Bok telescope and in October 1993, April 1994, and October 1994 with the Mt. Bigelow 1.5 m telescope, where the slit width is 3.6″ and the measured resolution is 105 km/s. Observations and data reduction followed standard procedures. Two to three overlapping grating settings were used to cover the wavelength range. Distortion in the spatial axis was determined from the observations of the spectral reference stars which were stepped along the slit. Skylines are strong and common in this spectral region and could be used directly for wavelength calibration. Correction for atmospheric absorption was performed by dividing with a spectral reference observation obtained at the same airmass immediately before or after each object integration. Most of the spectral references were F5-G2V stars for which a correction for photospheric features (see Maiolino, Rieke, & Rieke 1996) was applied. A large number of sources with flat continuum spectra in the 2.058 μm region, not shown in this paper which focuses on the He I feature, confirm that this technique removes atmospheric residuals with a high degree of accuracy. The GC spectra presented have been corrected uniformly

for reddening assuming $A_K = 3.47$ (Rieke *et al.* 1989) and the reddening law of Rieke & Lebofsky (1985); no reddening correction has been applied to any of the spectra of the relatively unobscured comparison stars. No radial velocity corrections have been applied.

For the MMT observations of the GC, the slit was positioned by offsetting from IRS 7. An infrared guiding camera was available for the Bok observations, allowing precise placement of the slit. Although the position of the slit on the field can be determined fairly accurately by comparison of the intensity along the spatial axis with a high-resolution continuum image, many of the GC sources described here are not dominant continuum sources. With slit widths 1.2–2.4″ and pixel scales 0.4–1.2″/pixel, it is not always possible to determine the location of an emission source uniquely. In a few cases (e.g., AHH-NW), multiple slit positions allow an accurate determination of the source location. More generally, a best estimate was made from the source position on the spatial axis and the source was assumed to be the nearest He I source detected in our He I image or that of Krabbe *et al.* (1991) for sources north of IRS 16.

The slit angle on the sky was varied for optimal coverage of the most interesting sources. A nearby, heavily obscured region was used to monitor the sky level because of the extended nature of the GC stellar distribution. There is significant spatial structure in the background which is generally confused at the spatial resolution of these data, especially in the Br γ line. To minimize contamination, one-dimensional spectra were extracted using simulated apertures 2 pixels wide. It is noted in the text when subtraction of the stellar and nebular background is likely to have distorted the spectral features. The continuum level is generally significantly contaminated by cool stars; hence, the equivalent widths of the emission features are very uncertain. Similarly, because many of the sources were not centered on the slit, line fluxes can

Table 3.2: Comparison Star Features

Source	Type	HeI 2.06	CIV 2.08	HeI 2.11	NIII 2.12	MgII 2.14	HI... 2.17	HeII 2.19
HD 50896 (WR 6)	WN5	we		e	?		se	
HD 192163 (WR 136)	WN6	a		e			e	e
HD 191765 (WR 134)	WN6	a		wa			se	e
Roberts 89 (WR 120)	WN7	e^P		e			se	e
HD 177230 (WR 123)	WN8	se^P		se^P			se	e
AS 268 (WR 105)	WN8	se^P		e			se	we
AS 306 (WR 116)	WN8	se^P		se			se	we
HD 313846 (WR 108)	WN9	a	e	a			e	a
NaSt 1 (WR 122)	WN10	se		se			e	e
P Cyg	B2pe (LBV)	se^P		e		e	se	
HD 160529 [SN]	A3Iae (LBV)							NA
HD 15570	O4If+	wa	e		e	NA	e	wa
HD 14947	O5.5f	wa	e		e	NA	e	wa
HD 15558	O5.5III(f)		e		e	NA	a	
HD 190864	O6.5III(f)	a	e		e	NA	a	a
HD 36861	O8III(f)	a	we	a	e	NA	a	
HD 46150	O5V((f))				e	NA	a	wa
HD 15629	O5V((f))	wa	e		e	NA	a	wa
HD 229232	O5e				e		e	a
HD 39680	O6:pe	se		e		we	e	NA
HD 194334	O7.5Ve	a		a	e		e	a
HD 225160	O8e	a					a	
MWC 627	O8e	e^D					se	NA
HD 60848	O8V:pevar	e^D		NA	NA	NA	NA	NA
X Per	O9pe	e^D				NA	e	
SAO 20924	B0III/O9e			NA	NA	NA	NA	NA
HD 185859	B0.5Iae	we?		a			a	NA
HD 2905	B1Iae	e		a			a	NA
HD 207329	B1.5Ib:e	e		a			e	
HD 41117	B2Iaevar	e		a			a	NA
HD 206267	O6V				e	NA	a	
HD 199579	O6V	a		wa		NA	a	wa
V645 Cyg [SN]	O7			NA	NA	NA	NA	NA
HD 210809	O9Ib	a		a		NA		wa
HD 193322	O9V((n))	wa		a		NA	a	
HD 214680	O9V	wa		a		NA	a	
HD 209975	O9.5Ib	a		a		NA	a	
BD+36 4063 [R]	ON9.7Ia	e		a			e	
HD 191781 [R]	ON9.7Ib	we		a			we	
BD+59 2786	B0III			wa			a	NA
HD 38771	B0Iab:	e		a			a	NA
HD 37128	B0Iab:			a			a	NA
HD 14143	B2Ia	e		a			a	NA
HD 183261	B3II						a	NA
HD 14134	B3Ia			NA	NA	NA	NA	NA

e: emission a: absorption w: weak s: strong NA: not available

[SN] Relatively poor signal-to-noise. Weak features undetectable.

[R] Only R=500 spectrum available.

[P] P Cygni profile.

[D] Disk signature.

Table 3.3: Properties of Galactic Center Sources

Source	$W_{2.06\,\mu m}$ μm	FWHM km/s	$W_{2.112\,\mu m}$ μm
GCHe4	0.0035	1200	0.0006
AHH-NW	0.0046	1000	0.0020
IRS 15	0.0022	1000	...
GCHe5	0.0336	900	0.0054
IRS 13	0.0025	480	0.0009
IRS 16NW	0.0010	360	−0.0002
IRS 29	0.0006	320	...
GCHe2	0.0010	250	...
IRS 16NE	0.0009	180	−0.0001
GCHe3	0.0008	130	...
IRS 1	0.0004	< 120	...

be more accurately determined from the images.

3.3.2 Spectroscopy Results – Stellar Classifications

Figures 3.2 and 3.4 show the spectra of the GC sources observed. Table 3.3 lists measured properties of some of the prominent spectral features seen in the GC sources. The [Fe III] (2.145 and 2.218 μm) and H_2 (2.122 μm) lines are background features (cf. Lutz *et al.* 1994). Table 3.2 lists the comparison stars observed and Figures 3.3 and 3.5 show the spectra of the most relevant. The spectrum of NaSt 1 (WR122 in van der Hucht *et al.* 1981) has been truncated for presentation: the 2.058 μm line continues to 33 times the continuum level. Outside the late-WN sample, strong emission at 2.058 μm is clearly a rarity in the comparison sample despite preferential selection of spectral types most likely to exhibit this line. This is consistent with the expectation that this line is only strong in enriched stars undergoing strong mass loss and extends the result of Hanson & Conti (1994) in which only 1 of 19 O4–B3 stars had strong emission in this line.

Wide Emission Lines — Ofpe/WN9 Candidates

Four of the GC sources listed in Table 3.3 (GCHe4, AHH-NW, IRS 15, and GCHe5) have broad emission lines. The former two are seen in different spectra at close to the same location and may actually be a single source. The differences in the 2.058 μm profiles may be due to the subtraction of slightly contaminated backgrounds.

In regions crowded with emission sources, superposition of velocity-displaced profiles can mimic the appearance of a broad emission line (as seen in the low spatial resolution observations of Hall *et al.* 1982). However, these four are probably signatures of fast winds because these sources are not in the crowded IRS 16 region. P Cygni profiles seen in 3 of the spectra, most prominently for the source GCHe4, confirm this. The He I doublet at 2.112/3 is also seen in these sources. Their K magnitudes range from just above the background, $m_K \sim 12$, up to $m_K = 9.5$ (if the dominant continuum source in IRS 15 is the emission source). With correction for extinction, this corresponds to M_Ks of ~ -6 to -8.6.

These sources appear quite similar to the AF star (Allen *et al.* 1990; Najarro *et al.* 1994; Libonate *et al.* 1995) and to the later WN comparison stars, as WR116 in Figure 3.2 illustrates. Classification of late WN and extreme Ofpe stars is subject to debate (cf. Crowther, Hillier, & Smith 1995), made worse in this case by the unavailibility of optical or UV spectra of the GC sources. The comparison WN stars (also Figure 3.3) illustrate that the primary NIR criterion used to date, the He II 2.189 μm feature, is often relatively weak in the WN8–10 classes and the absence of this feature should not exclude a WN classification. It should be noted that although HDE 313846 (WR108) is the only Galactic WN9, it is considered a poor prototype of the class (Walborn 1982), and NaSt1 (WR122) has been compared to B[e] stars (Crowther *et al.* 1995). Until a meaningful differentiation of the late-WN and Ofpe classes in the NIR is identified, we will follow Allen *et al.* (1990)'s example and

classify these GC stars as Ofpe/WN9s with the note that they appear more in step with the WN progression than the Of or Oe examples in our comparison suite. The near-infrared brightnesses of these stars are in agreement with this classification.

Narrow Line Sources

Unlike the stars discussed above, seven sources have relatively narrow (< 500 km/s) 2.058 μm emission features which distinguish them from WRs and Ofpe/WN9s, including the AF star and the WC9 in the GC discovered by Blum, Sellgren, & DePoy (1995b). This distinction was first pointed out for IRS 13 and IRS 16NE by Libonate *et al.* (1995), who suggest an identification as LBV stars.

IRS 16NE: This is one of the brighter sources in the region and also one of the strongest He I sources, hence its spectrum is only lightly contaminated by the nearby stars. As Figure 3.4 and Table 3.3 show, this source has narrow (FWHM 160 km/s) 2.058 μm emission with P Cygni absorption. The 2.112/3 μm He I feature is in absorption. This source is fairly close to the strong Br γ source IRS 1W, so these spectral data do not allow us to determine if it has Br γ emission, but even before any background correction the He I 2.058 μm/Br γ flux ratio is 1.4. The Br γ images (this paper; Lutz *et al.* 1994) do not have a point source at this position bright enough to stand out against the nebular emission, but the Br α image of Forrest *et al.* (1987) does. Hence, IRS 16NE does still have hydrogen in its envelope. The detection of Mg II (2.137 and 2.144 μm) in the spectrum of IRS 16NE distinguishes it from all of the sources in our comparison sample except P Cyg (LBV) and HD 39680 (O6:pe). This doublet, also seen in other LBVs, is excited by fluorescence when Ly β is velocity broadened (McGregor, Hyland, & Hillier 1988b). The roughly equal fluxes seen in these lines in IRS 16NE and P Cyg argues for a fast stellar wind as the fluorescence requires doppler shifts of 73 and 116 km/s to populate the upper states. This is

confirmed by the measured widths of the He I 2.058 μm (less contaminated than Br γ) features of 160 and 175 km/s in IRS 16NE and P Cyg respectively. IRS 16NE is also one of the brighter infrared sources with an implied luminosity $\gtrsim 10^6 L_\odot$ (for $T_{\rm eff} \gtrsim 15,000$ K). These two characteristics in addition to the strong He I emission make it the most likely LBV candidate in the GC.

IRS 13: Our spectrum of IRS 13 illustrates the same, narrow emission features of He I, Br γ, and [Fe III] seen by Libonate *et al.* (1995) in this wavelength range. The [Fe III] features (2.145 and 2.218 μm) are nebular (Lutz *et al.* 1994). The broad base to the other emission lines is likely due to contamination from the large gas velocities in this region. The narrow line component (FWHM 175 km/s) peaks at the continuum location of IRS 13. This source has been resolved (Eckart *et al.* 1993) and the equivalent widths of the emission lines are certainly substantially diluted. Again, the relatively narrow lines distinguish this source from the AF star (emphasized by Libonate *et al.* 1995) and the broad-line sources discussed above. The relative strength of the He I 2.112/3 μm doublet and absence of Mg II features makes the comparison to P Cyg less compelling than for IRS 16NE. Other possible classifications will be discussed below.

IRS 16NW: Although the apparent Br γ absorption in this spectrum is just an artifact of background subtraction, the P Cygni signature in the He I line is real. The emission profile is certainly distorted by the background but is readily distinguishable from the wide lines discussed in the previous section: FWHM of the He I feature before and after background subtraction is 460 km/s and 360 km/s, respectively. There is a marginal emission feature at He II 2.189 μm, but with He I 2.112 μm in absorption, it seems unlikely that this is real.

IRS 1: Spectrally unresolved 2.058 μm emission weakly peaks in the IRS 1 region. We see the feature in spectra taken with both the MMT and Bok telescopes, but

no emission is evident in our 2.058 μm image. Emission with FWHM 540 km/s was reported by Krabbe *et al.* (1991), but only weak, diffuse emission was seen by Libonate *et al.* (1995) who discuss the possibility that the GC sources may have variable emission features. Alternatively, this source may not be detected in our image because the imaging is not as sensitive to weak emission as is the spectroscopy, and Libonate *et al.* (1995)'s coarser pixel scale may have made differentiation between the weak peak and surrounding nebulosity impossible. It is not clear why a much wider emission line was reported by Krabbe *et al.* (1991). IRS 1W is a bright red source with a blue core (Rieke *et al.* 1989) which has even been detected at 0.95 μm (Henry, DePoy, & Becklin 1984), so our data may apply to a hot star buried in the thermally reradiating dust. However, the level of emission and He I/Br γ ratio are also consistent with nebular emission from material of approximately solar composition and the lack of an obvious P Cygni feature makes identification with a stellar wind source uncertain. The spectrum presented has been background subtracted; a velocity displacement of the background Br γ line results in the peculiar Br γ profile.

IRS 29: IRS 29 is near the 10 μm source IRS 3, suggesting that this narrow emission feature may be similar to IRS 1. However, there is clear P Cyg absorption on the 2.058 μm feature. This spectrum has not been background subtracted and the absorption feature is well removed from the 2.0558 μm skyline, so this feature is not a false absorption from over-subtraction. Hence, this line probably does originate in a stellar wind. The thin peak of the He I line has a FWHM of 160 km/s. Comparison with a nearby spectrum along the slit shows that the more extended nebular component is responsible for the broader base.

GCHe2: As mentioned in Section 3.2, this is probably the source detected by Krabbe *et al.* (1991) which they identified with the red supergiant to the east, IRS 9. An emission peak 600 km/s to the blue of H I Br γ arising from blended He I (7-4) tran-

sitions (which span 2.158–2.165 μm, Najarro *et al.* 1994) is clearly distinguishable from H I Brγ; this He I emission feature is also distinguishable from Brγ in the spectrum of P Cyg and quite prominently in that of NaSt1 (WR122). This spectrum has not been background subtracted, and part of the 190 km/s FWHM and at least half of the flux is from the background. An extraction farther to the east has a similar but extended 2.058 μm feature displaced by $\sim$ 150 km/s; only emission from GCHe3 is seen to the west.

GCHe3: The location of this source is relatively poorly determined from these data. It is seen in two nearly perpendicular spectra, but the nearest source to the intersection in the 2.058 μm image is 1″ to the northeast. Both spectra were taken with the 2.4″ slit, so such a displacement is possible and we have assumed this identification. No background subtraction has been applied because other emission sources (GCHe2 and IRS 13) dominate nearby positions on the slit, but the main, unresolved peak of the He I feature is localized. No P Cyg absorption is seen. A feature at 2.143 μm due to Mg II 2.144 μm or [Fe III] 2.145 μm is seen. The [Fe III] identification is much more likely as this source is within the region bright in [Fe III] 2.218 μm (Lutz *et al.* 1994) and the 2.137 μm feature of Mg II is not seen.

Comparison Sample

In addition to the WN series discussed above, comparison stars observed for this project include a large variety of other spectral types as delineated in Table 3.2. Also included are two noteworthy ONIa stars observed on September 24, 1994 at R=500 with CRSP on the KPNO 1.3 m for another project. A few of the comparison stars have weak 2.058 μm features, but only P Cyg and subsets of the Oe/Be and ON stars are strong emitters. We have found no common class of star similar to the GC narrow-line stars. The literature already has a number of high-quality NIR spectra

of late-WC stars (Eenens, Williams, & Wade 1991; Eenens & Williams 1994); some WC9 stars (WR70, WR92, and WR103) have strong 2.058 μm emission lines, similar to the GC star discovered by Blum *et al.* (1995b). Our comparison sample does not duplicate this work nor does it include any Ofpe/WN9 stars. A number of these stars in the Magellenic Clouds also exhibit prominent He I 2.058 μm emission (McGregor, Hillier, & Hyland 1988a). The example in the GC, the AF star, has significantly wider emission lines than the majority of the GC He I stars which are likely a different type of star.

3.4 Discussion — The Collection of Stars

In the preceding sections, we have identified 3–4 Ofpe/WN9 candidates in the GC in addition to the AF star and 7 sources of narrow He I 2.058 μm emission. Table 3.4 lists these and the other stars in the region with published spectroscopy (Najarro *et al.* 1994; Libonate *et al.* 1995; Blum *et al.* 1995b). One of the narrow-line sources (IRS 16NE) is a likely LBV candidate and another (IRS 1) may be non-stellar, but the remaining 5–9 narrow-line stars pose a challenge to interpretation of the cluster of He I stars. Prior to this spectroscopic study, the assumption that the He I sources are WR-like stars (e.g., Krabbe *et al.* 1991) was difficult to reconcile with normal stellar evolution (Chapter 2). Recognition that some of these sources are readily distinguishable from WR and Ofpe/WN9 stars on the basis of line widths (Libonate *et al.* 1995) led to an appeal to less common stellar types (LBV). However, the finding that most of the GC hot stars are of this latter type, with narrow emission lines, demands comparison with a more common stellar class. Data in the literature indicate that the latest WC classes and Ofpe/WN9 stars have prominent but wider emission lines. The comparison sample indicates the same for late-WN stars and that LBV, Oe/Be, and ON supergiants are the only other classes of stars likely to

Table 3.4: Hot Stars with Published Spectroscopy

Name	Offset from IRS 16C	Spectral Type	m_K	Notes
Blum-WC9	−10.7″, −6.0″	WC9	10.6	C III, C IV
GCHe4	−9, −4	Ofpe/WN9	...	
AHH-NW	−9.4, −3.8	Ofpe/WN9	11.8	
AF	−8.2, −7.5	Ofpe/WN9	11.1	2 He I stars
IRS 6E-N	−6.3, +1	narrow	10.8	
GCHe5	−2, +2	Ofpe/WN9	...	
IRS 13	−4.7, −2.0	narrow	9.1	
IRS 34?	−4.5, +1	narrow	...	
IRS 29	−3.2, +1.0	narrow	...	
IRS 15	−2, +11	Ofpe/WN9	9.3	
IRS 16NW	−1.4, +0.8	narrow	10.1	
GCHe3	−1, −4	narrow	...	
IRS 16SW?	−0.1, −2	...	...	
IRS 16C+CC	0, 0	narrow	9.8+10.6	
IRS 16NE	+1.3, +0.7	LBV?, narrow	8.8	Mg II
GCHe2	+1.4, −6.0	narrow	...	
IRS 1?	+4, +0.2	narrow	9.3	weak He I 2.058

have prominent emission in this line.

3.4.1 Problems with LBV Classification

Is it reasonable to suppose that all of the GC narrow-line 2.058 μm sources are LBVs with IRS 16NE the most striking example? This seems unlikely for two reasons. First, the LBV phase of stellar evolution is very brief and experienced only by stars within a limited range of masses; there are only 5–9 known examples in the Galaxy (Humphreys & Davidson 1994). Hence, it is quite unlikely that a significant number inhabit this sub-parsec region. This argument is made stronger by considering that the 2.058 μm emission line used to pick out these stars should be inefficient at identifying LBV candidates. As HD 160529 in our comparison sample

indicates, many LBVs are not hot enough to be prominent sources of 2.058 μm emission. This implies that there should be many more LBVs in the region than those identified through this emission line. This can be directly ruled out: although main-sequence O stars would be lost in the confusion of the region, all of the LBVs listed in Table 4 of Humphreys & Davidson (1994) are luminous enough that they would be identified as blue sources in color maps (Rieke *et al.* 1989; DePoy & Sharp 1991; Eckart *et al.* 1993) of the region. However, almost all of the blue sources in these maps have been accounted for as He I stars. Second, the bulk of the He I sources are a factor of a few fainter in the near infrared than IRS 16NE, implying that they are either less luminous or hotter. The lowest luminosity LBV listed in Humphreys & Davidson (1994) Table 4 (R71) would have $m_K \approx 10.4$ if placed at the GC. AE And would be fainter, with $m_K \approx 11.6$, despite being more luminous because it is hotter than R71. In comparison, most of the GC narrow-line sources are fainter than would be expected for typical LBVs. For these two reasons, it is implausible that the bulk of the GC He I sources are LBVs.

3.4.2 A Collection of Oe Stars?

Although the one source in Hanson & Conti (1994) which exhibits significant He I 2.058 μm emission is the O7.5IIIe star, HD 155806, there are two arguments against the GC stars being of Oe/Be type. We have 8 Oe and 4 early-Be stars in our comparison sample including 3 selected for 2.058 μm emission seen in lower resolution spectra (Hanson *et al.* 1996). Even among this sample, only 6 share the trait of prominent 2.058 μm emission. As discussed above, limits on the number of blue stars without He I emission make problematic any identification with a blue stellar class in which this emission is not the norm. The emission-line profiles present another difficulty. Oe stars have high mass-loss rates and a disk or asymmetric mass-loss signature, similar to Be stars. As HD 2905 and HD 41117 illustrate, the emission

features can be fairly narrow and apparently Gaussian in profile, but the majority have obviously wider emission profiles, frequently including disk signatures not seen in the GC sources. Presumably this difference is a projection effect: HD 2905 and HD 41117 may be seen relatively face on to their mass-loss disks or asymmetric winds such that the velocity structures are not evident at this resolution. It is possible that some or all of the GC narrow-line sources are also face-on Oe stars, but it is not obvious why they would have a preferred orientation such that we would not detect any disk signatures in this sample of 5 (allowing for the possibilities that IRS 16NE is an LBV and that IRS 1's He I emission is nebular). Hence, although the relative line strengths are consistent with a minority of Oe stars, the line widths are not consistent given reasonable luck on projection angles for the disks.

3.4.3 ON Supergiant Stars

ON stars are a minority population of otherwise normal, H-burning O stars with enhanced surface abundances of CNO cycle products (Conti, private communication; Smith & Howarth 1994). BD+36 4063 (ON9.7Ia) and HD 191781 (ON9.7Ib) have emission at He I 2.058 μm and Br γ. A low-resolution spectrum of the former is included in Figure 3.5. Its equivalent width in the He I feature is comparable to the B1Ie stars in the comparison suite and the weaker GC narrow-line stars. HD 191781 has weak emission features, but if BD+36 4063 is more typical of the class, late-ON supergiants are an intriguing possible classification for the fainter GC He I stars. They have an appropriate brightness and are not expected to have the disk profiles exhibited by the Oe stars. As a minority population, they cannot explain the bright He I stars given the absence of a large number of equally bright blue sources without the He I feature as argued above. However, the contribution to the background from normal O stars remains largely unconstrained, and the sources such as IRS 29 may represent a subset with the ON characteristic.

3.4.4 Comparison with Nearby Populations

The cluster of hot stars in the central parsec can also be contrasted to the young, hot stars found within 40 pc of the GC. Cotera *et al.* (1996) have published infrared spectra of 17 hot emission-line stars which are found in this larger region. Unfortunately, these $\lambda/\Delta\lambda = 250$ spectra cannot distinguish the widths of the emission lines, but only three have prominent He I 2.058 μm emission. The population in the central parsec is considerably more biased towards stars with strong 2.058 μm emission. This indicates that the GC stellar cluster is of a very distinctive age or that conditions of formation or evolution are significantly different from those even just outside this region. For example, explanations for the GC population which rely on metallicity seem unlikely. The uniquely high stellar densities, location at the dynamical center, or possible presence of a central massive object may influence star formation or evolution in the central parsec and distinguish this region from other star formation regions nearby.

In the presence of so many apparently evolved, luminous stars, another surprising aspect of this population is the absence of earlier WR stars. At first appraisal, this may appear to be a selection effect because the hot stars have been identified through one emission line. As the sample of WN stars in Figure 3.3 illustrate, this 2.058 μm line is strongly in emission only in WN8 and later WNs. Also, earlier WRs are less luminous than LBVs and would be faint enough to escape detection as blue continuum sources. However, the He II features are strong in the earlier WN stars, and Werner *et al.* (1991) put a limit $W_{\mathrm{He\,II}\,3.09\,\mu\mathrm{m}} \lesssim 0.05\,\mu$m on 35 continuum sources in the central 20″. Also, the UV radiation field is inconsistent with a significant number of luminous stars hotter than $\sim 35,000$ K (Serabyn & Lacy 1985; Shields & Ferland 1994). Hence, there is not a large population of undetected WR stars of earlier type. This presents a significant constraint on starburst models of this

population.

Similarly, the He I emission line should be inefficient at detecting WC stars. Although a subset of late-WC stars exhibit strong 2.058 μm emission (Eenens & Williams 1994), of which the Blum *et al.* (1995) WC9 star is an example, most late-WC stars do not. However, the C IV triplet at 2.08 μm is usually very strong in these stars. Images of the region were also obtained in this emission feature using the same instrument as described in Section 3.2 in June 1994 with a spectral resolution of 150. They do not show any point emission sources above a 3σ detection threshold of 1.4×10^{-16} Wm^{-2}, indicating there is not a large population of undetected late-WC stars. This is apparently at odds with the Galactic trend with radius which would predict a high WC/WN ratio in the GC. However, this trend applies to constant star formation rate populations rather than burst populations for which age can be a dominant factor (Maeder & Conti 1994). Nonetheless, the observed dearth of WC stars is another important constraint on models of this population especially given the larger number of late-WN or Ofpe/WN9 stars found in this study.

3.4.5 Ultraviolet Contributions

Despite the identification of many luminous emission-line stars, it is still not clear that they dominate the UV field. The Ofpe/WN9-like stars are not luminous enough; IRS 16NE is quite luminous, but probably cooler. The He I 2.112 μm emission feature in IRS 13 suggests it is one of the hotter stars, but the brightness of the emission component of this resolved source is unknown. Hence, although the He I 2.058 μm flux is clearly dominated by these stars, the region's ionization still might be produced by a large number of undetected main-seqence O stars. These stars would be individually too faint to be detected in the near-infrared continuum, but in aggregate dominate the UV.

3.5 Summary

Emission-line images with 1″ resolution of the southern portion of the GC field indicate the following:

1. The Br γ line flux is predominantly from diffuse emission indicative of gas ionized by the ambient radiation field. There are three unresolved point sources: IRS 1W, IRS 13, and the Ofpe/WN9 AF star.

2. At least one of the sources reported to have He I emission and CO absorption is resolved into a hot/cool stellar pair.

3. The He I line flux is predominantly from nine or more point sources which dominate over the diffuse contribution. This result argues against the possibility that these sources are normal stars undergoing normal evolution.

4. The unambiguous association of the He I emission with stellar sources rather than with diffuse nebulosity, which likely would be subject to significant non-gravitational forces, indicates that these stars are useful dynamical test particles. Emission-line velocities for these early-type stars can provide a new dynamical constraint in the crucial central region where other probes fail (see Haller *et al.* 1996).

New 2 μm spectral observations of the GC He I stars and a sample of luminous emission-line comparison stars lead to these conclusions:

1. Four new Ofpe/WN9 (or late-WN) stars are identified in the central parsec.

2. We confirm that IRS 13 has relatively narrow emission lines including a He I 2.112/3 feature (Libonate *et al.* 1995).

3. IRS 16NE has very unusual Mg II features at 2.137 and 2.144 μm. These, its line widths, and its brightness make it a likely LBV candidate.

4. We find a number of GC sources with narrow 2.058 μm emission features which defy easy classification. He I 2.058 μm emission is a common feature of Oe stars, but the profile is frequently distinguishably different from the profiles exhibited by the GC narrow-line stars. ONIa is a possible classification for the fainter examples.

5. It is not obvious that these stars dominate the region's ionization.

These spectra emphasize the importance of spectral resolution in studying this population as the line widths and profiles have proven to be important distinguishing features. High spatial resolution is also required to avoid confusion even in the emission lines in the central region which is crowded with emission-line stars.

A current census of the known hot stars at the GC includes a WC9 star, 5 Ofpe/WN9s, 1 LBV candidate, and at least 5 additional stars of unknown type with narrow He I emission lines. Although it has been argued that the small number of WR and Ofpe/WN9 stars observed is consistent with a normal starburst (Schaerer 1994), an explanation must now be found for this extraordinary concentration of luminous stars, many of which are clearly very rare types.

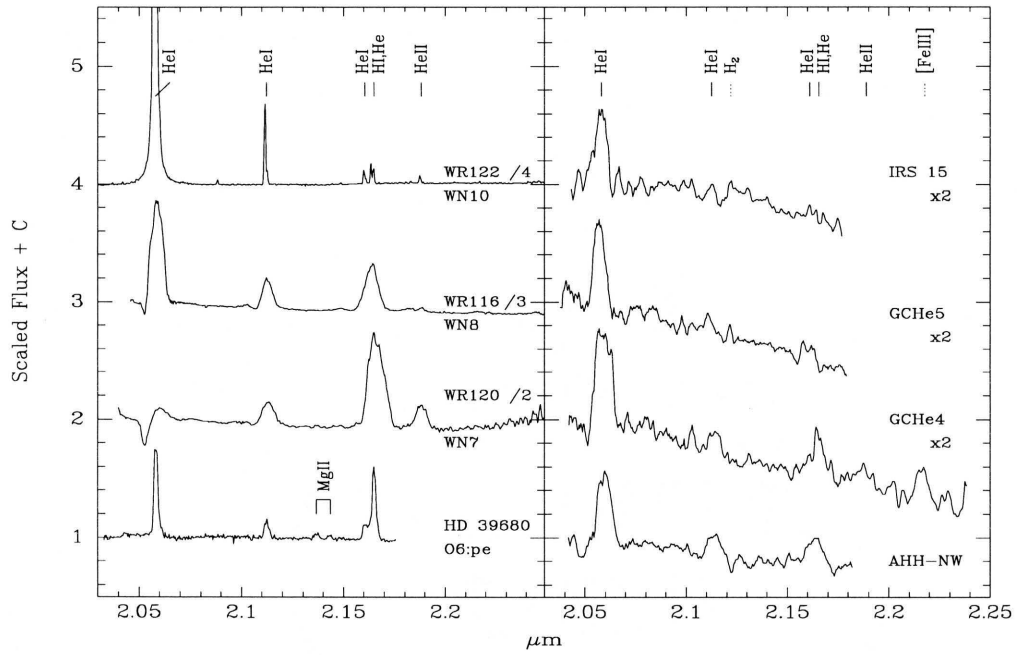

Figure 3.2: Candidate Ofpe/WN9 or Late-WN Stars with Selected Comparison Spectra. The comparison spectra illustrate that the 2.058/2.112 μm ratios and line widths are consistent with a late-WN classification. As Figure 3.5 illustrates, HD 39680 is the closest match among the non-WN stars in the comparison sample. The reader should also compare to the spectrum of the AF star (Najarro *et al.* 1994; Libonate *et al.* 1995), the Ofpe/WN9 stars in McGregor *et al.* (1988b), the GC WC9 star in Blum *et al.* 1995b, and the WC9 stars WR92 and WR103 in Eenens & Williams (1994) (in contrast to WR88). After normalization to the continuum level, these spectra have been scaled as indicated and shifted for convenient presentation. The GC spectra have had approximate background correction applied, dereddening for $A_K = 3.47$, and some smoothing. Br γ is likely to be severely distorted in all cases. Subtraction of background H_2 2.122 μm and H I 2.166 μm is responsible for the peculiar profiles of AHH-NW. [Fe III] 2.218 μm in GCHe4 is a residual nebular feature.

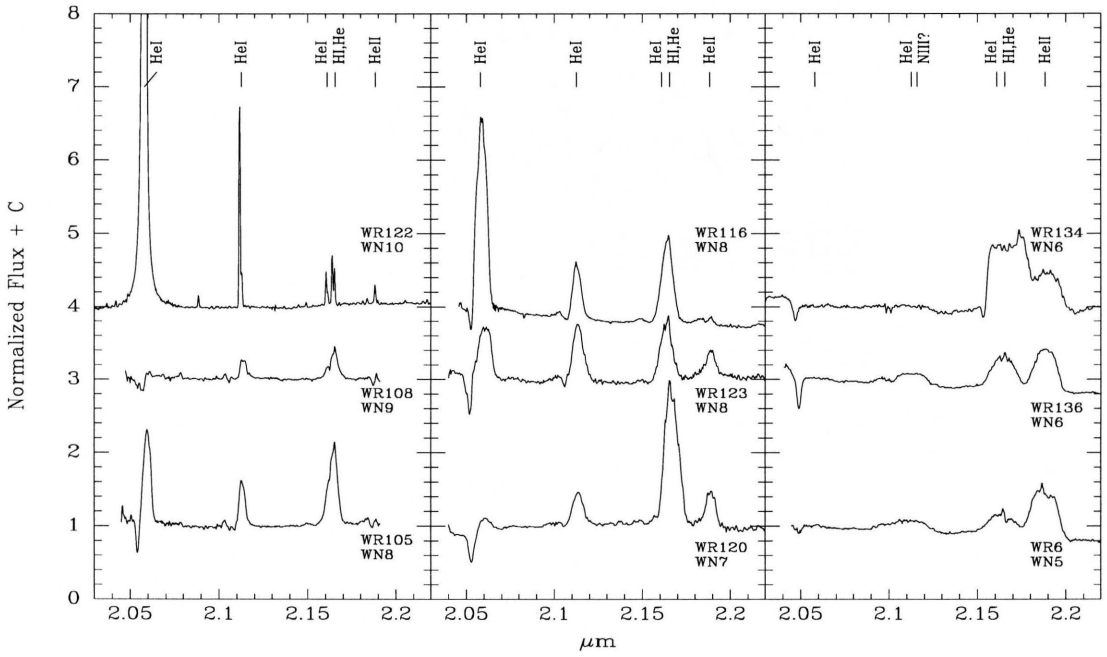

Figure 3.3: Comparison WN Stars. These spectra complement the atlas of NIR spectra of late-WC stars presented by Eenens *et al.* (1991). The 2.058 μm feature in WR122 continues to 33 times the continuum level. Note that apart from WR108 with the controversial classification WN9, there is a readily distinguishable progression with spectral type in the relative strenths of the various He I and then He II features. In particular, the 2.189 μm feature of He II is not prominent in most of the sources later than WN7.

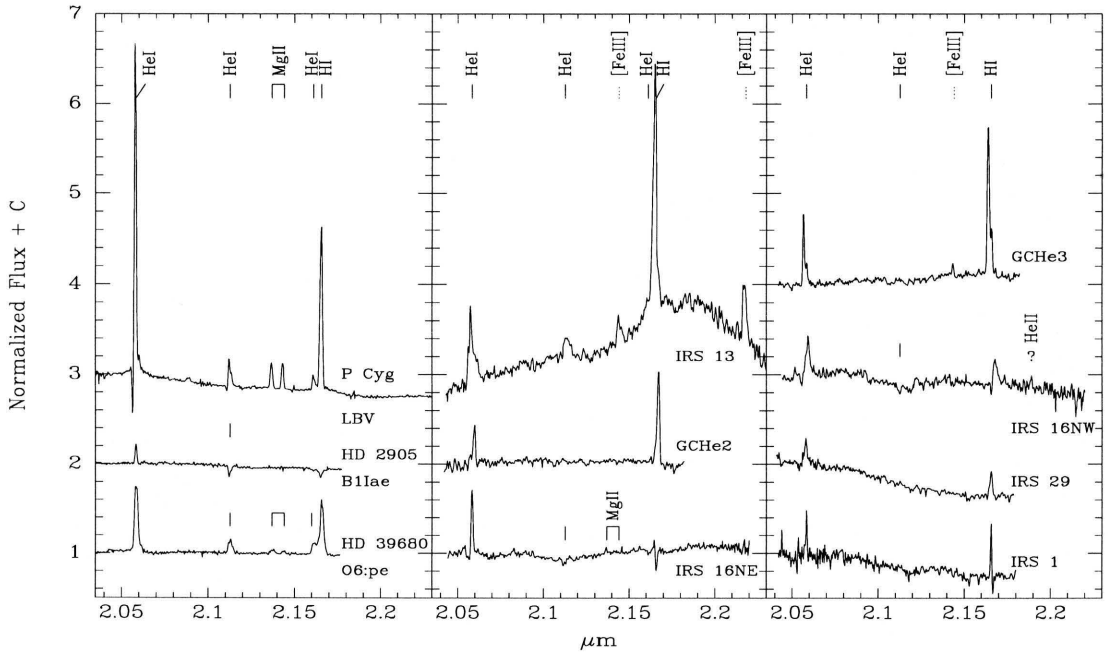

Figure 3.4: Narrow-Lined GC Sources with Selected Comparison Stars. These spectra are distinguishable from the WN classes by their relatively narrow ($< 500\,\mathrm{km/s}$) emission lines. Notable features include the He I 2.112/3 feature in the spectrum of IRS 13 and the Mg II 2.137 and 2.144 μm features in the spectrum of IRS 16NE. The [Fe III] 2.145 and 2.218 μm features are nebular. GCHe2, GCHe3, and IRS 29 have not had background correction. The spectra have been normalized to the continuum near 2.06 μm and shifted.

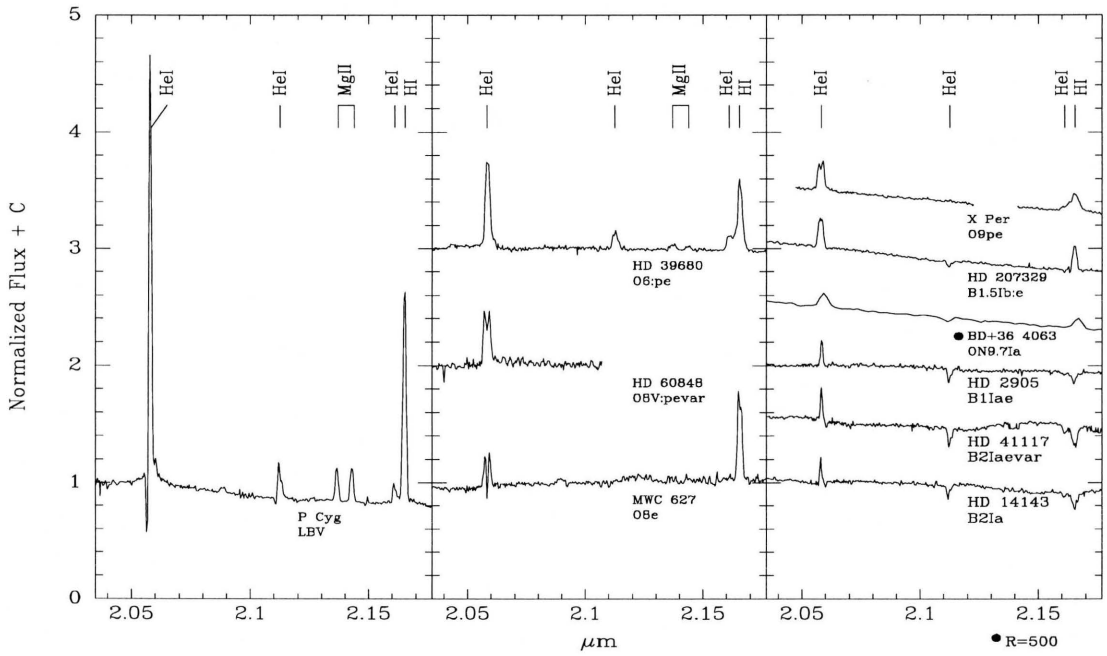

Figure 3.5: Comparison Stars with Significant He I Emission. Only these stars, apart from the WN series, had significant He I 2.058 μm emission. The spectra have been normalized and shifted. The spectrum of BD+36 4063 is relatively low-resolution; the 2.058 μm feature is comparable in strength to the neighboring spectra.

CHAPTER 4

STELLAR KINEMATICS

Abstract

The He I 2.06 μm images presented in Section 3.2 indicate that the He I stars can serve as kinematic tracers in the CO-depleted central 1/4 pc. Radial velocities from the spectra presented in Section 3.3 are used to confirm gas and CO kinematics and extend them to the neighborhood of the central region. A new mass constraint of $\lesssim 1.8 \times 10^6\,M_\odot$ for this concentration is derived from these data in Haller *et al.* (1996). These velocities are compared with those derived independently by Krabbe *et al.* (1995). In light of the discrepancy, new spectral data are searched for high velocity stars in the central region.

4.1 Introduction

The mass distribution in the central parsec of the galaxy is critical to our understanding of the region and the processes which occur there. Of particular interest is whether or not a central dark massive component exists and its nature and extent. This is particularly critical as *HST* is providing evidence for central dark-mass concentrations in other galaxies which may be massive black holes similar to AGN engines. However, even with *HST/WFPC2* the spatial scales which can be probed in other nuclei are thus far insufficent to rule out more extended dark-mass distributions such as clusters of stellar remnants. In the GC, we may be able to place uniquely tight constraints on the extent of the central dark mass and test theories for the development of central massive black holes.

However, the GC introduces a number of obstacles which prevent a determination of the mass distribution limited only by spatial resolution. The CO-bearing stars, both discrete and as an integrated background population, are very effective at probing the kinematics from relatively large radii in to $\gtrsim 8''$. At that point, however, measurement and interpretation of CO based kinematics becomes significantly more ambiguous. First, the volume in question is too small to have a significant number of distinguishable, luminous, CO-bearing stars as would be required for a discrete analysis. Second, the velocity dispersion rises sufficiently to blur the sharp CO-band features as stars with different velocities contribute to the aggregate light. Third, there is a CO-depletion region in which the CO band depths become too shallow for kinematic use (Sellgren *et al.* 1987). This occurs either because the background population loses the CO in the stellar atmospheres through dissociation or mass stripping, or because the background stellar distribution does not peak as sharply as a more luminous, non-CO-bearing population, which dilutes the CO absorption with additional continuum. For these reasons, CO kinematic measures

become increasingly difficult in the very central regions. Further, interpretation of measured dispersions is not straight forward near this depletion region because the region's structure is ambiguous (cf. Haller *et al.* 1996). For example, if the CO depletion is caused by dilution by an additional, featureless population, then kinematics measured from the CO stars throughout the region can be interpreted as valid tracers of the kinematics. However, if the depletion is complete in a spherical region in which atmospheric CO is dissociated, perhaps by a strong central UV source, then CO-absorbing stars seen within this radius are projected from larger radii where the velocity dispersion is lower, resulting in a tendency to underestimate the enclosed mass. Extensive models of the behavior of the CO dispersion in these and other geometries and comparison with other cluster properties such as the light distribution allow Haller *et al.* (1996) to derive confidently enclosed mass measures in to ~ 0.15 pc. However, a kinematic sample which does not have these complications, such as the He I stars, is obviously useful as a check and to sample even closer to the center of the depletion region.

A second technique which has proven reliable at larger radii is to measure kinematics from the emission lines of the ambient gas. Similar kinematic measures can be derived all the way into the central region (e.g. Lacy *et al.* 1991). However, ionized gas is subject non-gravitational influences which are expected to distort its systematic motions in a region of strong magnetic fields (see review by Morris 1994) and energetic phenomena like the GC. For this reason alone, gas kinematics are unacceptable probes of the gravitational potential in the central parsec.

4.2 Kinematics from 1994 Data

4.2.1 Velocities and Positions

The data described in Section 3.3 were analyzed for radial velocities of He I emission-line stars. The data were already wavelength calibrated. For this experiment, a number of He I emission sources which were clearly stellar were extracted and their emission profiles fit to derive radial velocities which were subsequently corrected for heliocentric motion. A step which was more important for this analysis than for the study of the stellar population was determination of the location of the He I source relative to the dynamical center near Sgr A*. These locations were determined by comparing the spatial information present in the long-slit spectra with a high quality image of the region provide by M. Rieke. In an iterative fashion, starting from where observing notes, encoded telescope-mount coordinates, or a simultaneous guider image indicated the slit position was intended to be, a vector was extracted from a smoothed and rebinned copy of the image and compared with the spatial axis of the spectrum. For MMT data in which the slit passed near at least one bright source, this procedure gave positions repeatable to better than an arcsecond. Comparison of spectral features at derived slit intersections confirms the technique. For the Bok data with the coarser spatial scale and wider slit, an accuracy closer to 2″ is achieved. In a few cases there were no high contrast sources and the slit location could not be definitively determined. With only one exception, these spectra did not have any stellar emission features and were probably well removed from the central cluster. These spectra will not be considered further. The one exception has two late-WN spectra which appear similar to spectra of a source near IRS 11 and AHH-NW which are available from other spectra, so it was redundant and not considered.

4.2.2 Systematic Biases

The velocities derived from the stellar emission lines are expected to be biased in two ways to a higher dispersion leading to an artifically high enclosed mass. The first bias is introduced by the winds in which this emission line is produced and the second by a selection effect to avoid confusion with ambient gas.

The He I 2.06 μm emission line is produced preferentially in a fast stellar wind (cf. Najarro *et al.* 1994). Correspondingly, the measured profiles are resolved and at least as broad as the expected velocity dispersion of the population. Through geometrical effects and increased error in profile fits, the measured velocities are expected to have more scatter than the intrinsic stellar velocities. We have endeavored to minimize the effect of this systematic bias in three ways. First, we have rejected from our kinematic sample those stars with He I 2.06 μm emission-line widths greater than 200 km s^{-1} because stars with narrower profiles tend to give velocities measured from profile fits closer to their intrinsic velocities. Second, we have used the highest spectral resolution available to allow better profile sampling and more accurate fits and to distinguish stars with unacceptably wide emission lines. Third, we interpret the derived velocity dispersion as an **upper limit**.

The point of this experiment is to derive velocities of a population affected only by the gravitational potential and not by non-gravitational influences to which gas responds. Although Figure 3.1*a* indicates that most of the He I emission is associated with stars, the spectra in Chapter 3 also show a large amount of emission from ambient gas in the region with clear systematic motions. Hence, it is essential to distinguish stellar He I emission from gas emission to avoid contamination of the derived velocity dispersion by non-gravitational motions. Several steps were taken to avoid including gas velocities in Table 4.1. First, the spatial dimension available in the long-slit spectra allow us to select sources which are spatially unresolved and

Table 4.1: Measured Radial Velocties from He I Lines

Source	Offset	FWHM [km/s]	v_{lsr} [km/s]
IRS 16NW1	−1″, 1″	180	−196
IRS 16NW2	−1, 1	320	433
IRS 29	−2, 1	250	−194
IRS 16NE	3, 1	170	34
GCHe5	−3, 3	150	−26
GCHe3	−2, −5	120	−239
IRS 13	−4, −2	210	−153
IRS 34	−5, 1	230	−174
between 10E & 16NE	8, 5	150	34
GCHe2	4, −7	220	180
E of IRS 9	7, −8	150	132
IRS 5	9, 10	150	85
E of IRS 11	−10, 12	180	−18

brighter in emission than their surroundings. Second, we can use the image to check that an emission source is associated with a bright star. Third, we can reject sources with the same velocity as the surrounding gas. The latter was done both by comparing with spectra extracted from nearby positions and by comparing with published gas velocities derived from other emission lines. However, this latter selection criterion introduces a bias away from the local gas velocity. Again, we minimized the influence of this effect by maximizing the spatial and spectral resolutions to reduce confusion and by interpreting the derived velocity dispersion as an upper limit.

4.3 Comparison with Krabbe *et al.* (1995)

Contemporary to our observations, a number of other groups observed the central parsec (Libonate *et al.* 1995; Blum *et al.* 1995b; Eckart *et al.* 1995; Krabbe *et al.* 1995). One of these groups, Krabbe *et al.* (1995) (hereafter K95), had sufficient

coverage and spectral resolution to perform a kinematic analysis similar to that described in the previous section. A comparison of our observations and results is in order.

K95 used three different instruments. FAST, a Fabry-Perot imager, was also used by Krabbe *et al.* (1991). This instrument provides 0.9″ (undersampled) images of the central 30″ with a spectral resolution of 950. K95 observed only the He I 2.058 μm line with this instrument. With 18 images of 250 s each spaced at 150 km s^{-1}, these observations should have samped the He I profiles well. Unfortunately, they present a velocity-integrated, continuum-subtracted image rather than spectral profiles. This image agrees very well with Figure 3.1*a* with comparable spatial resolution. It includes the field north of IRS 16 but is not very deep and probably added useful kinematic information only for the strongest sources (IRS 16, 13, 15, AF, and AHH-NW).

CGS4 is a long-slit spectrometer with a 3.″1 wide slit and resolution 650–1310 used for H and K. K95 list it as used for kinematics of IRS 7W, IRS 13E, IRS 15SW, IRS 15NE, IRS 9, and AF, but with this wide a slit, only the IRS 15, AF, and possibly IRS 13 observations are likely to be valid measurements. The IRS 7W and (mis-identified) IRS 9 emission sources are quite close to much brighter sources. A 3″ region around IRS 13 includes a tremendous amount of emitting gas at high velocities, but it is a very strong emission source so their data are probably dominated by the stellar emission.

3D is a very different instrument which is much more suited for these observations. All of the spectra K95 show are from this instrument and it contributed to most of their reported velocities. Hence, it is probably the most important instrument for this experiment. It is briefly described (Genzel *et al.* 1995) as an image slicing spectrometer which obtains 256 channel K-band spectra of a 16x16 grid of

0.″52 pixels with $\lambda/\Delta\lambda = 1000$ resolution on a NICMOS3 detector. Their net 45 minute exposure with 1″ resolution has unique advantages. We review the most pertinent differences between this instrument and Fspec and compare their observations with our own.

First, K95 have complete two-dimensional coverage of the field in uniform conditions in contrast to our collection of disjoint long-slit spectra which individually have only one spatial axis. This allows them to know directly where each spectrum is in the field whereas we reconstruct the position as described above. In addition to allowing more precise determination of source positions, their data are preferred for distinguishing fine spatial features. They can, for example, compare the spectrum from a point with spectra of neighboring points in any direction. This is very valuable in the most crowded and gas contaminated regions. They can also peak up and extract a spectrum directly on a bright continuum source like IRS 13 whereas our slit positions were always off the centroid of this source and our spectrum of this source is therefore weaker and more contaminated.

Second, their data cover a longer wavlength range. They covered the entire K-band in each spectrum whereas Fspec in high-resolution mode provides $\approx 0.08\,\mu$m of coverage in one grating setting. Hence, they did not need to splice together spectra taken at different times with different grating settings with the inherent errors in registration this entails. Specifically, their data would be much preferred for determining line ratios such as Br γ/He $I_{2.06}$. Their coverage to longer wavelengths is not valuable in this study because these stars are relatively featureless in this region.

Third, for part of these observations they used a tip-tilt guider (ROGUE) with similar scientific advantages as FASTTRAC described in Section 3.2 (although with an optical guide star). In principle, this should have given them significantly higher

spatial resolution except that the 0.″52 pixels clearly limit them to the net 1″ resolution they report.

Fourth, in spite of the 45 minute on source integration they used for the central 8 arcsec^2 and reduced spectral resolution, our data have significantly higher S/N. Presumably this is because the slit spectrometer is more efficient than an image slicer. This is most evident in the spectra of the weaker sources which we have in commmon. Indeed, they even sum all of their candidate "WC9/Of" and He I stars to bring the signal out of the noise. Although this was clearly unnecessary for the He I stars as their IRS 13, IRS 16SW, and IRS 16NE spectra have strong features, it is the only way the He II, C III, and C IV features show. This reduced S/N is particularly significant in analyzing the stars with weaker emission features both for emission properties and for kinematics.

Fifth, our data have significantly higher spectral sampling, 50 km s^{-1} pixel^{-1} rather than 300 km s^{-1} pixel^{-1}. As we have stresed in Section 3.5, this is essential in distinguishing the line widths and profiles to allow identification of WR, Oe, and narrow-line sources. As described in Section 4.2.2, high spectral resolution is valuable for kinematics for two reasons. First, a more precise fit to the line profile is possible with the better sampling; with a systemic velocity disperion of order 150 km s^{-1}, a spectral resolution element significantly wider than this is a significant handicap. Second, the wide-lined stars are poor and biased kinematic probes and can not be distinguished from the preferred, narrow-lined probes. They have subtracted a systematic shift of 90 km s^{-1} from He I 2.058 μm velocities to compensate for P Cyg absorptions.

Despite these varied differences in the data sets, we are primarily in agreement. We see similar kinds of stars and identify mostly the same sources and our spectra of the same sources are in good agreement. Exceptions are that we do not detect

"WC9/Of" stars as they claim and we do not agree with their kinematic results. The former discrepancy could arise from our emphasis on the He I line or incomplete spatial coverage. The latter is in the direction predicted based on the biases described above and likely illustrates that their data is inappropriate for this analysis. However, missing a few high velocity stars due to incomplete spatial coverage, although unlikely to systematically affect our results (we did not **avoid** high velocity stars), could have a significant impact. To address these concerns, we carried out additional observations aimed at continuous spatial coverage of a portion of the field where the K95 data indicated a number of "WC9/Of" stars. In selecting a target region, we ignored the velocities reported by K95 in order to continue to have an appropriate unbiased kinematic sample.

4.4 New Spectroscopy to Search for High Velocity Stars

On the nights of April 11–13 1995, we returned to the MMT with Fspec in high-resolution mode and the infrared guider. Figure 4.1 illustrates the dense spatial coverage of the central cluster in the spectra obtained over the course of this project. Observational and data reduction procedures were the same as described in Section 3.3. Figure 4.2 shows some sample data after atmospheric, background, and dispersion correction. Despite the systematic spatial coverage, the data have no identifiable, unresolved sources with abnormally high velocities which would have a significant impact on the derived kinematics. A search of the data for significant C III or C IV lines revealed that there are no sources with these lines comparable in strength to the weaker He I sources discussed in this work.

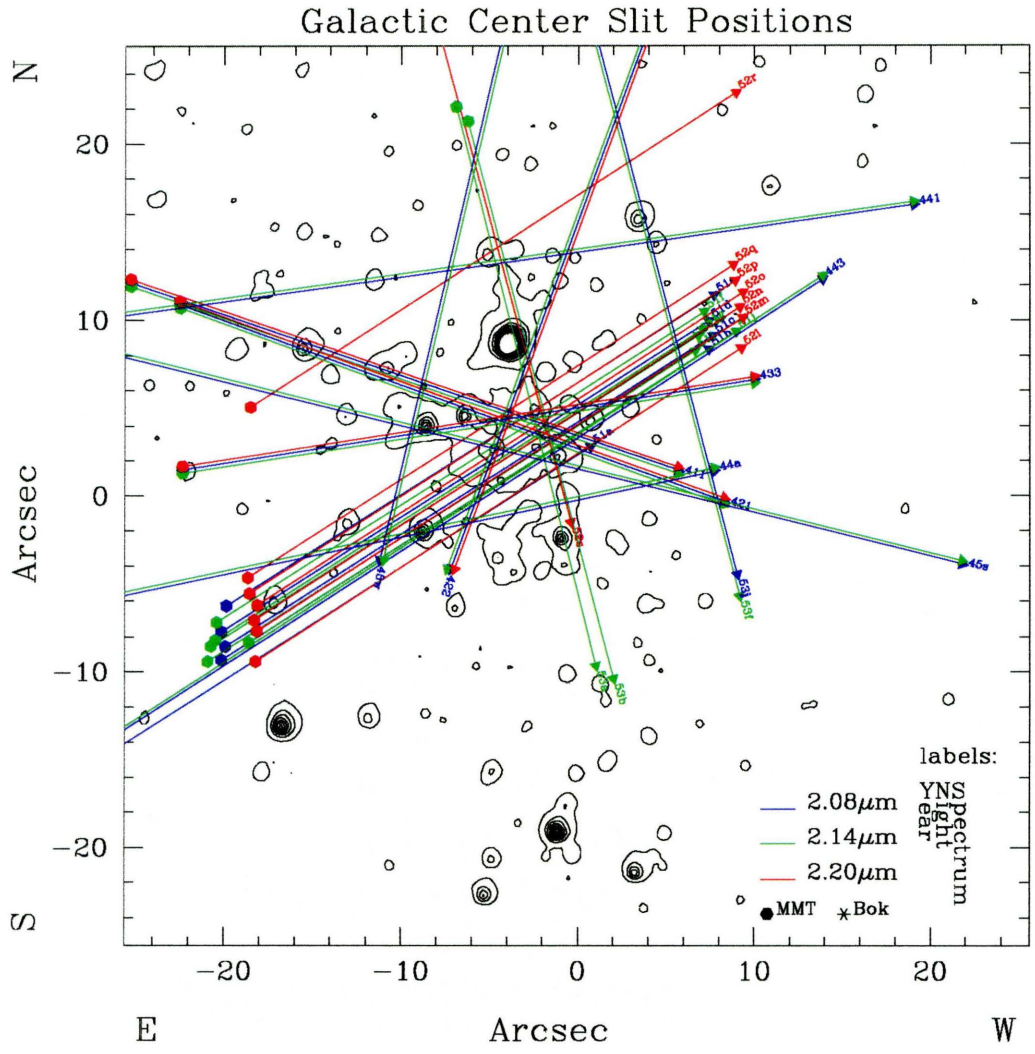

Figure 4.1: Confirmed Slit Locations, 1994–1995. This figure illustrates the fairly complete spatial sampling of the central cluster and shows where the slits were near various isolated sources. The background contours are of an image of the region provided by M. Rieke which was used to confirm the slit positions.

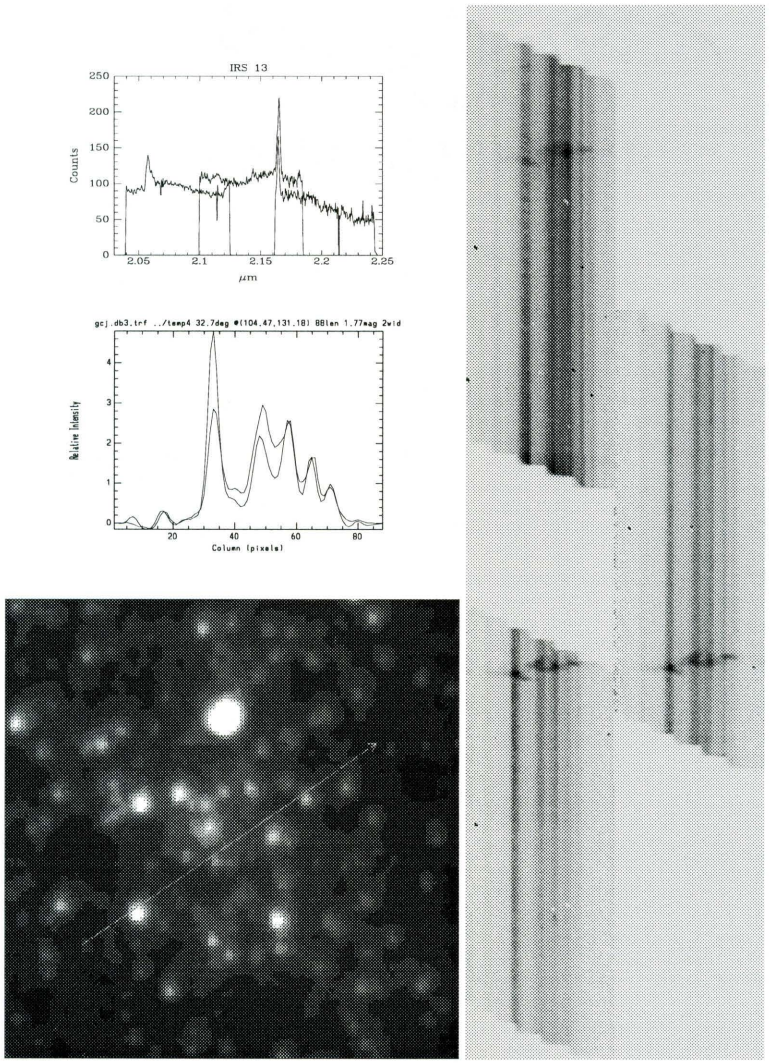

Figure 4.2: Sample Spectroscopic Data from the 1995 Observing Run. The image (courtesy M. Rieke) on the bottom left shows where the slit was located in the GC region for the three long-slit spectra on the right. IRS 7 is the brightest source in the image and IRS 9 is the bright source nearest the left end of the slit. The three spectra are of the same spatial location but with different grating settings. The top spectrum includes the He I 2.06 μm emission line, dominated by gas in this case. IRS 13's contribution can be seen above a white pixel defect. The middle spectrum is wavelength aligned and overlaps to cover the weaker He I 2.112 features which do not show well in the grayscale. The other prominent emission line is Br γ. The upper left panel shows a single column extraction from NE of IRS 13. Finally, the middle left panel compares the intensity distribution along the slit with a vector from the image after smoothing and rebinning. It allows one to identify the sources in the spectra, such as IRS 9.

4.5 Conclusions

The spectra described in Section 3.3 analyzed for radial velocities confirm and extend closer to the cluster center the kinematics derived from CO and gas observations. Data from all of these sources are combined with the light and CO distributions and detailed models (Haller *et al.* 1996) to derive a central dark component with mass $1\text{–}3.6\times10^6\,M_\odot$ which is possibly extended on a scale of 3 pc. This may be a massive central black hole or a collection of stellar remnants. The He I data are best interpreted as providing an upper limit on the enclosed mass due to systematic biases. The upper limit derived is substantially below that found by a similar analysis (K95). The datasets are compared and new MMT observations with Fspec densely sampling the central cluster do not indicate any overlooked high velocity He I sources or detectable C III/C IV sources.

Chapter 5

Stellar Population Models II: Persistent Star Formation and a Hotter IRS 16

G. H. Rieke & Peter Tamblyn

Abstract

The compact cluster of luminous, blue stars imaged in Section 3.2 is distinct from the nuclear populations in M31 and M32. Steady-state models for the population are thus less likely to apply. A very recent burst of star formation such as discussed in Chapter 2 is a possible reconciliation of the cluster with these other galaxy nuclei. Stellar population models are now required to meet the considerably higher temperatures for the IRS 16-like stars determined from the properties observed in Chapter 3. A somewhat extended, but damped, star formation history comes closest to producing a population with the observed overabundance of very luminous, warm stars with the observed red stars. However, the comparison sample reviewed in Chapter 3 indicates that only a fraction of such stars would exhibit He I 2.058 μm emission. The luminosities are also found to be almost unparalleled among warm Galactic stars. These problematic properties and the observed spatial distribution suggest that abnormal star formation or stellar evolution may be involved.

5.1 Introduction

The observations reported in Chapter 3 and contemporary observations (Libonate *et al.* 1995, Blum *et al.* 1995a, Blum *et al.* 1995b, Eckart *et al.* 1995, and Krabbe *et al.* 1995) clearly indicate that there is a large collection of He I emission stars in the central stellar cluter. The comparison sample presented in Section 3.3 finds close spectral analogues only among rare and mostly evolved massive stars. A comparison of this population with the nuclear populations in nearby galaxies and re-evaluation of stellar population models similar to those presented in Chapter 2 with this additional information are likely to provide considerable insight into the age or abnormality of the cluster.

5.2 Not Steady State

For comparison with the GC, we list properties of the nuclei of local group galaxies in Table 5.1. The black hole masses have been taken from Haller (1992), Lacy *et al.* (1991), Kormendy (1988), Lauer *et al.* (1992), and Richstone, Bower, & Dressler (1990) (we have assumed the value for M31 P1 to enhance its stability against tidal disruption); the core radii are from Rieke & Lebofsky (1987), Lauer *et al.* (1992), and Lauer *et al.* (1993). The absolute magnitudes at 2.2 μm have been interpolated from measurements available in the literature. To estimate upper limits to the central concentration of blue stars in the other galaxies, we have assumed that these stars have $B-V$, $V-R$, and $R-I$ colors of zero.

We have used the *HST/WFPC* measurements in Lauer *et al.* (1992) and Lauer *et al.* (1993) to estimate upper limits to the portion of the emission from the central 0.5 pc (diameter) that could arise from such stars, assuming that the remaining nuclear stellar population has colors identical to those observed just outside of the nucleus. In the case of M32, the Hopkins Ultraviolet Telescope data (O'Connell

Table 5.1: Nuclear Properties of Some Local Group Galaxies

Galaxy	$M_{BH}(10^6 M_\odot)$	Core Radius (pc)	M_K (10 pc)	$M_{V or B}$ (core)
Milky Way	~ 2	$\lesssim 1.2$	-15.5 to -16	~ -10.3
M31–P1	$\sim 1(?)$	1.4	——	> -4.9
M31–P2	~ 10	3.7	-15.3	> -5.1
M32	~ 3	cusp	-15.9	> -4.9

et al. 1992) show the nucleus to be very red between 2500 and 1500 Å, so these data would yield a limit even more stringent than the one listed despite their relatively poor angular resolution. For the Milky Way, we have summed published fluxes (DePoy & Sharp 1991; Rieke *et al.* 1989) to get a total $m_K = 7.5$ for the population of He I stars and assumed zero colors. The tabulated V or B magnitudes apply to the blue stellar component only, not to the integrated light from the nucleus. Although the nuclei of M31 (P1 and P2) and of M32 are very similar to that of the Milky Way in most respects, and bracket the properties of the Milky Way's nucleus, it is noteworthy that any nuclear blue stellar cluster in these galaxies must be at least 100 times less luminous than in our galaxy.

5.3 Further Integrated Constraints

An additional set of constraints on the He I emitting stars can be derived from far-infrared mapping of the GC. Davidson *et al.* (1992) show that the far infrared is compatible with a centrally concentrated blue or ultraviolet source or sources with a luminosity of $\sim 10^7\ L_\odot$; luminosities as large as $2 \times 10^7\ L_\odot$ appear to contradict their data. In the following, we will define a "blue" source to be one capable of heating the dust in the region, while a "UV" source can both heat the dust and excite the gas. Since any hot stars are observed in the Rayleigh-Jeans portion of their spectrum, we can derive a simple relation between the integrated K magnitude in blue and

UV stars and their luminosity (approximating their outputs as blackbodies):

$$L \approx 10^{\frac{7.5-m_K}{2.5}} \left(\frac{T}{21,400\ \mathrm{K}}\right)^3 \times 10^7\,\mathrm{L}_\odot. \tag{5.1}$$

We have assumed extinction at K equivalent to $A_V = 30$ and the extinction law of Rieke & Lebofsky (1985). For example, if we assume the temperature of the UV sources is 33,000 K and that they have an integrated magnitude of $m_K = 8.5$, their luminosity would be $1.5 \times 10^7\,\mathrm{L}_\odot$, nearly violating the upper limit permitted by the far-infrared observations. However, we estimate the integrated K magnitude of the prominent hot sources to be $m_K \sim 7.5$, so most of these sources must have temperatures well below 33,000 K to satisfy the luminosity constraint. If we set the temperatures of these sources to 20,000 K, they have a luminosity of $8 \times 10^6\,\mathrm{L}_\odot$, and at this temperature they can contribute only a small portion of the UV. To stay within the luminosity limit, the source of the UV must then produce $< 5 \times 10^6\,\mathrm{L}_\odot$, requiring it to have an integrated $m_K > 9.7$. Perhaps one of the bright He I stars, or a number of faint ones, could be hot enough to provide the UV. However, the majority of the He I stars must have effective temperatures of roughly 20,000 K, similar to that modeled for the AF star by Najarro *et al.* (1994). Since it is improbable that the He I stars are significantly cooler than 20,000 K, from this calculation they do appear to provide the majority of the blue photons that are effective in heating the dust that produces the far-infrared emission, even if they do not dominate the excitation of the gas.

Along with the RSGs in this region, one expects a population of hot, main-sequence stars that is adequate to provide the UV (Rieke & Lebofsky 1982). The number of these stars can be estimated by Monte-Carlo population syntheses such as those of Chapter 2. These calculations suggest the presence of, on average, roughly 600 late O to early B main-sequence stars, which would be adequate to provide the 10^{50} Lyman continuum photons required to excite the gas. The brightest of these

sources would be at $m_K \sim 13$. Although our observations leave open the possibility that the UV is provided by a minority of the He I stars, it appears more plausible that the gas is excited primarily by the hotter main-sequence stars in the young stellar population.

5.4 Additional Population Models

In Chapter 2, we used loose constraints on the properties of the "blue" luminous stars: they were required to match m_K within a factor of two, have $T_{\rm eff} > 5,000\,{\rm K}$, and the integrated population could not violate the UV or mass constraints. In light of the observations reported in Section 3.3, especially the comparison sample, it is tempting to place much more stringent constraints on matching the He I stars. However, we will first see that raising the minimum temperature is alone a very powerful constraint which is much less subject to remaining ambiguities of massive stellar evolution and K-band spectral properties. Morris *et al.* (1996) examines the K-band spectra of several "transitional" (OfI, Ofpe/WN9, WNL, B[e], and LBV) objects, a sample closely related to that presented in Section 3.3 despite a different motivation. They emphasize the sparse knowledge of these stars' role in massive stellar evolution, inter-relations, and "peculiarity". Specifically, "... peculiarity should *not* necessarily be implied in the formation and evolution of hot, massive stars that cannot (yet) be readily binned into a specific spectral subtype" [original emphasis and qualifier]. Although we believe that the broader samples in Hanson & Conti (1994) and Section 3.3 demonstrate the rarity of the combination of He I $2.058\,\mu$m emission and extreme luminosity, we agree that it would be premature to declare that the GC stars are individually peculiar. Monte-Carlo synthesis models similar to those presented in Chapter 2 which do not depend on more subtle stellar characteristics than L and $T_{\rm eff}$ are ideally suited to exploring whether the *collection*

of warm, luminous stars at the GC is peculiar.

From a synthetic burst perspective, the most important result from our data is that many of the stars with $m_K \leq 10$ are hotter than 15,000 K and hence more luminous than $4.5 \times 10^5\,L_\odot$. Figure 5.1 is similar to Figure 2.1 but is based on newer tracks from the same group for Z=0.04 with enhanced mass loss (Meynet *et al.* 1994) and the figure includes younger bursts which are now obviously required to meet the extreme luminosities of the GC stars. These newer tracks significantly reduce the impact of the UV characteristic temperature constraint because the most massive stars evolve to lower temperatures almost immediately. Figure 5.1 illustrates why, despite the reduced importance of the UV constraint, no single-burst models match all of the criteria in Table 2.1 and a minimum $T_{\rm eff}$ of 15,000 K for the IRS 16-like stars. Stars this luminous are present only at ages less than 5 Myr and, as stressed in Section 2.4, the RSG population is absent at these ages. Based on average quantities rather than randomly populated bursts, Krabbe *et al.* (1995) (K95) similarly exclude any single burst age unless RSGs are destroyed in preference to blue supergiants and AGB stars. Hence, we conclude that the GC population cannot be the result of a single, short star formation episode with a normal stellar distribution and normal stellar evolution.

However, the argument in Section 2.4.2 that a single burst must dominate the population needs to be reconsidered now that solo bursts are excluded. As proposed in that section, K95 find that a more complex star formation history can produce a more mixed population without violating the integrated constraints. They conclude that an earlier burst (Haller & Rieke 1989) produced RSG stars and a second, more persistent star formation episode, beginning 6–8 Myr ago with a decay time of 3–4 Myr, is responsible for $\sim$ 30 OBI and late-WR stars which are associated with the He I stars. Such models predict that the hottest, main-sequence stars in the

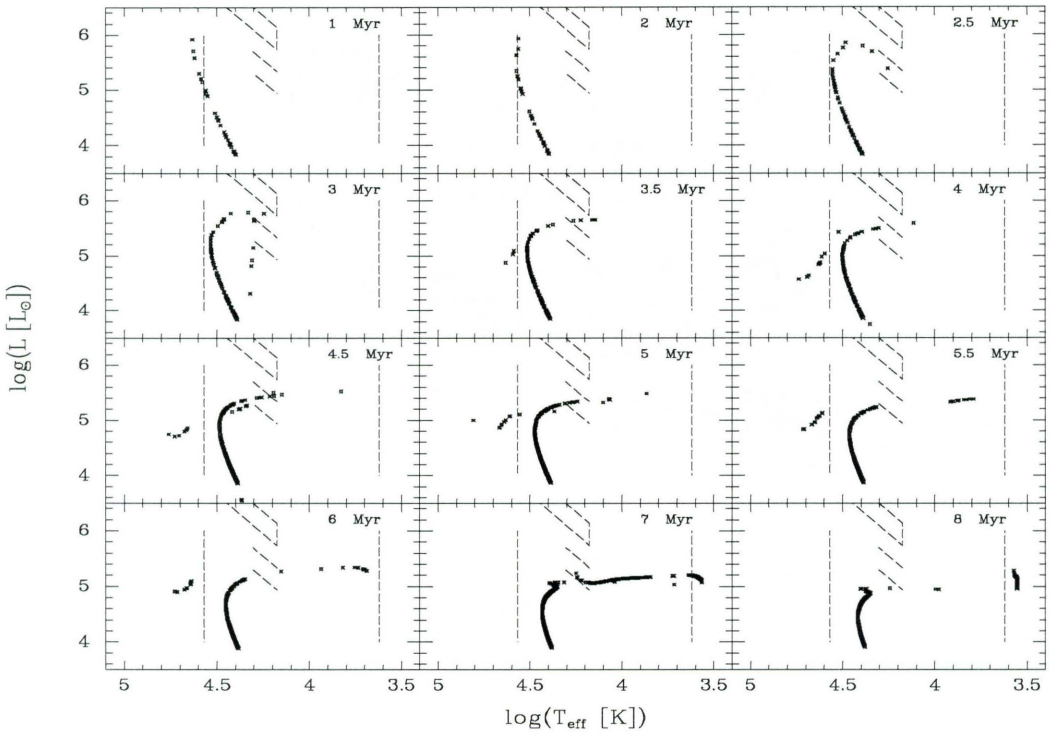

Figure 5.1: HR Diagrams of Bursts with Updated Tracks. The source tracks for these randomly populated bursts are from Meynet *et al.* (1994) for Z=0.04 and enhanced mass loss. The dotted lines are at $T_{\rm eff} = 4,170$ and 37,000 K as in Figure 2.1 and represent the regions of RSGs and the UV constraint. The rhombus is the location of the brighter He I sources with the cool edge at 15,000 K and top and bottom at $m_K = 8.8$ and 9.8 (d= 8 kpc, $A_K = 3.47$). Line segments at $m_K = 10.8$ and 11.8 (background) are also indicated for reference. Note that no stars are ever expected to match IRS 16NE well and that stars approach the region required to match IRS 16C,CC,NW, etc. only in bursts with ages ~ 3 Myr but that RSGs do not develop for quite some time later. Also note the large number of O stars near the main sequence expected for young bursts and that they are fainter at K than the $1''$ seeing background.

younger component dominate the UV instead of the He I emission stars. However, a smaller number of these hotter and more luminous stars is required in persistent formation models. We agree that such an exponentially decaying burst or a simpler two burst model with a much weaker second burst comes closer to meeting the burst criteria than a single burst. However, such models still do not predict the extreme luminosities, nor the ubiquitous presence of He I 2.058 μm emission in the luminous, warm stars.

Further tests of this model of persistent star formation will become possible as imaging and spectroscopy with spatial resolutions substantially finer than 1″ become routine. With the reduced confusion such observations provide, it should be possible to identify the OV stars from a young burst. Although very little temperature information is available from NIR photometry of hot stars, they can be effectively distinguished from red giants. Averaged luminosity functions of bursts similar to those presented in Figure 5.1 are shown in Figure 5.2 with stars cooler than 4,170 K distinguished. These could be used to determine if a young burst with few OV stars or an older burst with many BV stars dominates the UV. Failure to detect many hot stars brighter than $m_K \approx 14$ would indicate that the UV is dominated by very young stars (or a non-stellar source). This could also be tested with higher-resolution observations of the ionization state of the gas in the region. A UV-dominating young burst would have relatively few, dominant UV sources which might be discernable from ionization gradients. Eventually, high spatial resolution spectroscopy of the stars currently lost in the confusion may permit accurate determination of their spectral types in the manner of Hanson & Conti (1994).

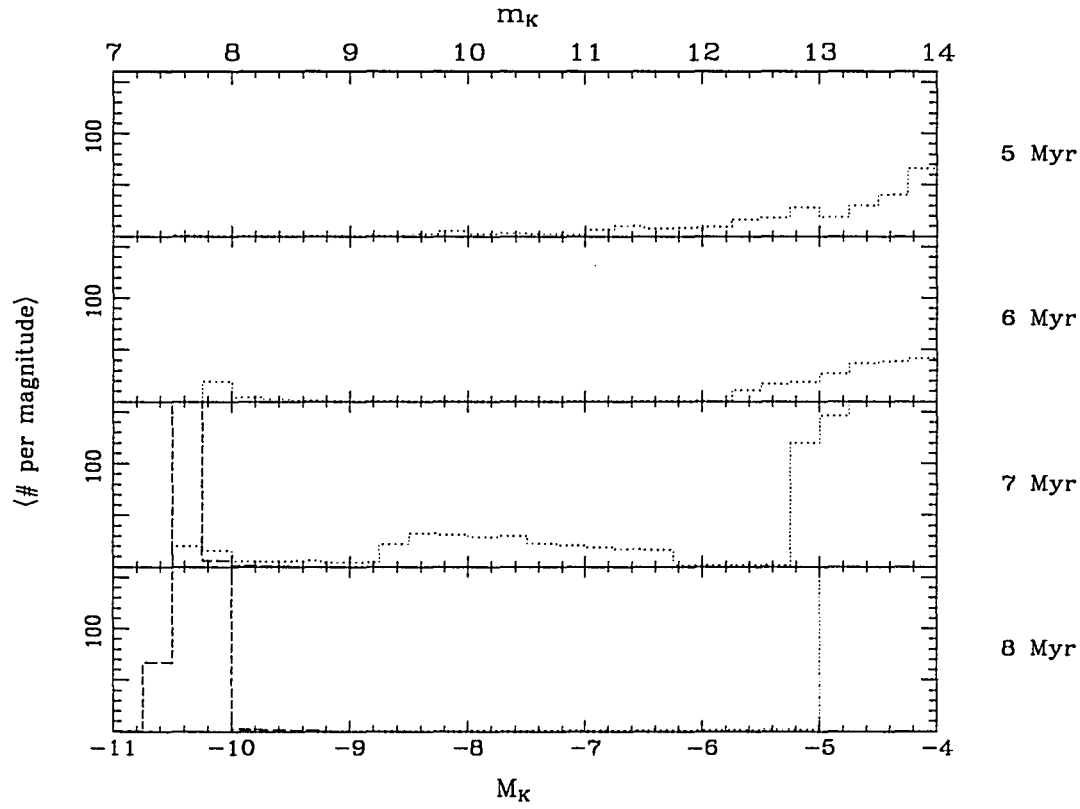

Figure 5.2: Predicted Luminosity Functions. The differential distribution of K magnitudes expected from UV-dominating bursts as in Figure 5.1 are plotted for stars hotter (dotted) and cooler (dashed) than 4,170 K. As higher-resolution observations of the region beat the confusion limit well below $m_K \approx 12$, the burst age may be discernable. The histograms for older bursts are truncated to emphasize expected dearth of intermediate brightness stars.

5.5 Line Emission and Luminosities

However, in evaluating the double (and extended) burst models we cannot ignore the results of Section 3.3 where we found that He I 2.058 μm emission is an unusual trait, even among very luminous or windy late-O stars. Figure 5.3 compares the region of the HR diagram occupied by the IRS 16 components with many of the optically classified comparison stars. What is immediately apparent, despite the bias in the comparison sample towards luminous and peculiar stars and the uncertainty in the temperatures of the IRS 16 stars, is that they are almost unique in the Galaxy. Also, neither $T_{\rm eff}$ nor L alone is enough to separate the emission sources, contrary to the assumption required to model the GC population as evolved from a normal but persistent star formation event. Further, the criterion used to create this plot, that some He I emission is detectable in high-quality spectra, is much more generous than the criteria for detection of He I emission in the GC stars; fewer stars would have solid markers if subjected to equally stringent criteria. The comparison stars plotted are from Table 3.2, Hanson *et al.* (1996), McGregor *et al.* (1988b), and Morris *et al.* (1996). Those with ambiguous spectra have been excluded. The stellar parameters, listed in Table 5.2, are from an uncritical and incomplete review of the available literature and should not be over-interpreted. Figure 5.4 further emphasizes the paucity of stars analogous to the IRS 16 stars: only a few comparable stars are seen in a relatively complete sample of an entire galaxy (the LMC). Note that the HR diagram presented by Blum *et al.* (1995a) has the IRS 16 components $\sim$ 1.7 magnitudes fainter than in these two figures. Although they assume 0.5 magnitudes less extinction at K, this discrepancy arises primarily from their fit for BC_K, which is about 1.2 magnitudes below a blackbody; this is attributed to the infrared excesses in their comparison stars. The fit is pulled down by η Car, HR Car, and S Dor. We can exclude such a large IR excess for the bright GC sources because of their

Rayleigh-Jeans NIR colors. The fainter sources may well have significant IR excesses if they are related to these LBVs.

The luminosities of the bright GC emission-line sources are enough to determine that they must be massive, and hence uncommon. Although the remaining ambiguity in $T_{\rm eff}$ for these stars allows an order of magnitude uncertainty in L, they still must be exceptionally luminous. Given a luminosity, we can establish a minimum mass for the radiating object by comparing to the Eddington Luminosity, $L_{Edd} = 4\pi GMcm_p/\sigma_T = 32,000\,\frac{M}{\rm M_\odot}\,\rm L_\odot$. This is the maximum luminosity an object with mass M can have in steady state because the opacity will always equal or exceed the Thompson opacity, σ_T. Applying this argument to IRS 16NE, which has $L > 10^6\,\rm L_\odot$, we derive a minimum mass over $30\,\rm M_\odot$. Although current data alone do not demonstrate that any of the other IRS 16 sources are quite this luminous, their masses must still be large. Further, a spread in effective temperatures is likely, and those which have higher temperatures than the minimum required to excite He I $2.058\,\mu$m emission may also be more luminous than $10^6\,\rm L_\odot$.

5.6 Spatial Concentration

The various independent high-resolution $2.058\,\mu$m emission images (Section 3.2; Eckart *et al.* 1995; Krabbe *et al.* 1995) also allow us to examine the spatial distribution of He I emitting stars. The original, larger scale image (Krabbe *et al.* 1991) combined with these new images of the central cluster show that the He I stars, especially the bright ones, are much more centrally concentrated than the stars (compare to continuum images such as in Eckart *et al.* 1993). A similar gradient in the WR fraction is seen in the dense core of the giant H II region NGC 3603 (Moffat *et al.* 1985). The crossing time of the central 1/4 pc of the GC at typical stellar velocities is only 1000 yr, hence the population should be well mixed on a

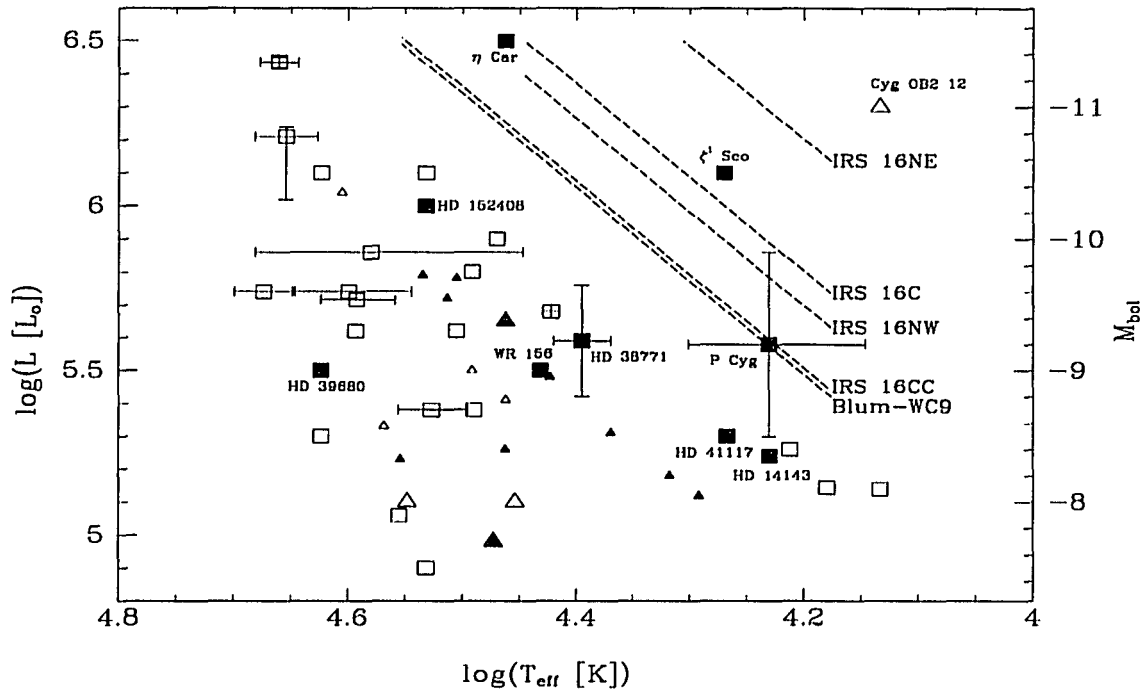

Figure 5.3: Luminous Galactic Emission-Line Stars Compared to the IRS 16 Sources. Filled symbols are comparison stars with the He I 2.058 μm emission line; open symbols are stars without the line or with only absorption in the line. Squares are used when both $T_{\rm eff}$ and L are available from the literature; small triangles are used when both had to be estimated from spectral type (Schmidt–Kaler 1982); large triangles are used when one had to be estimated. Error bars are indicated where available or where the literature has discordant values. The IRS 16 luminosities assume blackbodies at a distance of 8 kpc with $A_K = 3.47$. The extraordinary luminosities of the IRS 16 components are the most striking features. η Car, ζ^1 Sco and Cyg OB2 12 are known to be atypical stars. The figure also demonstrates that neither extreme luminosity nor $T_{\rm eff}$ alone determines the trait of He I 2.058 μm emission.

Table 5.2: Parameters of Selected Comparison Stars

Name	Spectral Type	$\log(T_{\rm eff}\,[{\rm K}])$	$\log(L\,[L_\odot])$	He I ?
Cyg OB2 12	B5Ia	4.13	6.3	n
HD 36371	B4Ia	4.13	5.14	n
HD 14134	B3Ia	4.18	5.14	n
HD 75149	B3Ia	4.21	5.26	n
HD 183261	B3II	4.22	4.61	n
HD 14143	B2Ia	4.23	5.24	y
HD 209008	B3III	4.23	3.74	n
P Cyg	B2pe/LBV	4.23	5.58	y
ζ^1 Sco	B1.5Ia+	4.27	6.1	y
HD 41117	B2Iaevar	4.27	5.30	y
HD 207329	B1.5Ib:e	4.29	5.12	y
HD 2905	B1Iae	4.32	5.18	y
HD 185859	B0.5Iae	4.37	5.31	y
HD 38771	B0Iab:	4.40	5.59	y
BD+36 4063	ON9.7Ia	4.42	5.48	y
HD 191781	ON9.7Ib	4.42	5.48	y
HD 37128	B0Iab:	4.42	5.68	n
WR 156	WN8	4.43	5.5	y
HD 191765	WN6	4.45	5.10	n
AS 268	WN8	4.46	5.26	y
AS 306	WN8	4.46	5.65	y
BD+59 2786	B0III	4.46	5.41	n
HD 177230	WN8	4.46	5.26	y
η Car	LBV	4.46	6.5	y
HD 313846	WN9	4.47	5.9	n
HD 50896	WN5	4.47	4.98	y
HD 209975	O9.5Ib	4.49	5.38	n
SAO 20924	B0III/O9e	4.49	5.5	n
WR 22	WN7	4.49	5.8	n
HD 210809	O9Ib	4.50	5.62	n
Roberts 89	WN7	4.50	5.78	y
X Per	O9pe	4.51	5.72	y
HD 151804	O8Iaf	4.53	6.1	n
HD 152408	O8:Iafpe	4.53	6.0	y
HD 193322	O9V((n))	4.53	4.9	n
HD 225160	O8e	4.53	5.79	n
HD 36861	O8III(f)	4.53	5.38	n
MWC 627	O8e	4.53	5.79	y
HD 192163	WN6	4.55	5.10	n
HD 60848	O8V:pevar	4.55	5.23	y
HD 214680	O9V	4.56	5.06	n
HD 194334	O7.5Ve	4.57	5.33	n
HD 14947	O5.5f	4.58	5.86	n
HD 190864	O6.5III(f)	4.59	5.62	n
HD 206267	O6V	4.59	5.72	n
HD 229232	O5e	4.60	6.04	n
HD 46150	O5V((f))	4.60	5.74	n
HD 190429	O4.5If+	4.62	6.1	n
HD 199579	O6V	4.62	5.3	n
HD 39680	O6:pe	4.62	5.5	y
HD 15558	O5.5III(f)	4.65	6.21	n
HD 15570	O4If+	4.66	6.44	n
HD 15629	O5V((f))	4.67	5.74	n

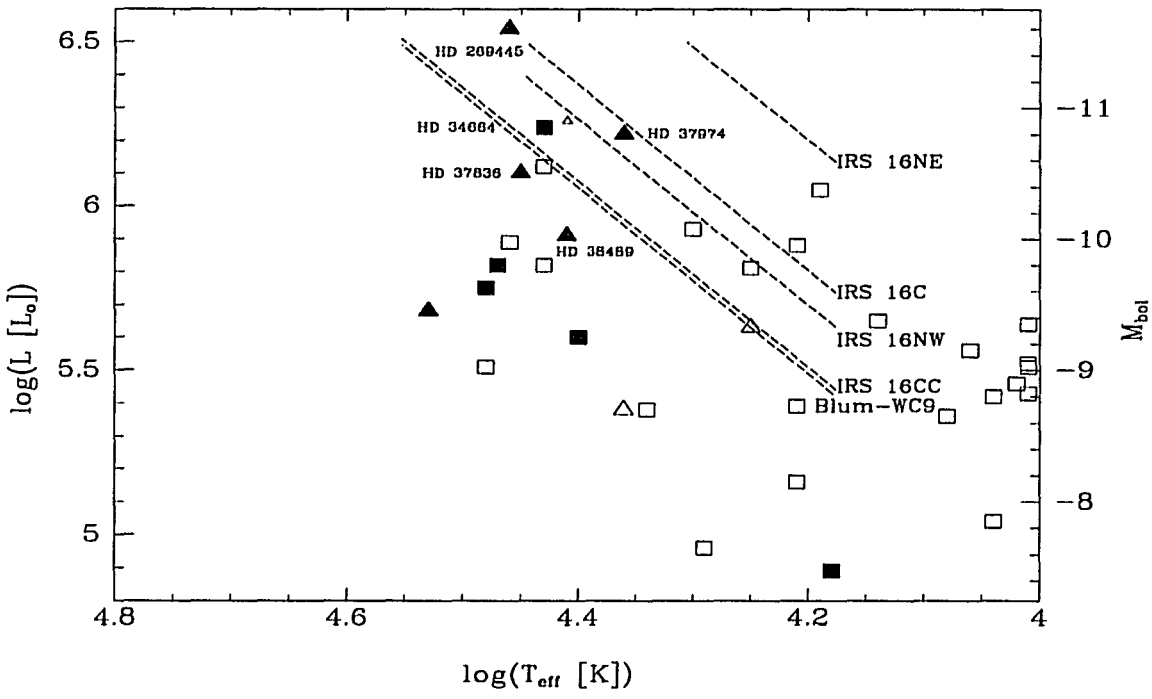

Figure 5.4: Luminous Stars in the Large Magellenic Cloud Compared to the IRS 16 Sources. As in Figure 5.3, filled symbols represent stars with the He I 2.058 μm emission line and open symbols represent stars without this emission line; squares are used for stars with well determined parameters while triangles or small triangles are used for stars with inconsistent colors. The LMC stellar parameters are from McGregor *et al.* (1988a); the luminosities of GC sources assume blackbodies at a distance of 8 kpc with $A_K = 3.47$. Note that even in a relatively complete sample of a galaxy's stars, only a few appear to be like the IRS 16 stars. This comparison also suggests somewhat hotter temperatures, near 25,000 K, for the emission stars, and consequently luminosities well above $10^6\,L_\odot$.

much larger scale. As the observed stellar properties are not well mixed, a second influence is required. The cluster relaxation timescale is of order 80 Myr (Lee 1993), hence the young stars are not mass segregated. A possibility is that the outer- and inner-most He I stars are not co-eval but from distinct bursts. In this picture, the RSGs and outer WR stars are slightly older. This is consistent with the population models which predict that older He I stars should be fainter: it is now recognized that the He I sources associated with IRS 9, 11, and 15 are not dominant continuum sources. One would also expect a correlation of line width with spatial location in the cluster if an earlier burst is less centrally concentrated. The older, wide-lined WRs would be typically observed with a larger projected separation from the cluster center. Figure 5.5 illustrates that this correlation is exhibited in the GC. However, this figure is constructed from data which have a selection bias towards finding large equivalent width and hence preferentially wide-lined stars at larger projected distances. If the young GC stars formed in two bursts, it is not obvious why the stars from a second burst would be trapped further down in the central potential. Another possibility is that some property of the central 1/4 pc enhances the proportion of sources with He I emission. This possibility will be examined in the next chapter.

5.7 Summary

The GC blue stellar population has an integrated $m_B \approx 7.5$; comparison with *HST* data on M31 and M32 indicates that the GC is either unique in some unknown way or not in a steady state. The observational demonstration that the bright blue GC stars are mostly He I emission sources and hence have $T_{\rm eff} \gtrsim 15,000\,{\rm K}$ also allows a more detailed examination of the complex star formation history scenario discussed in Section 2.4. New tracks from the same source as the tracks used in Chapter 2 significantly reduce the impact of the UV characteristic temperature con-

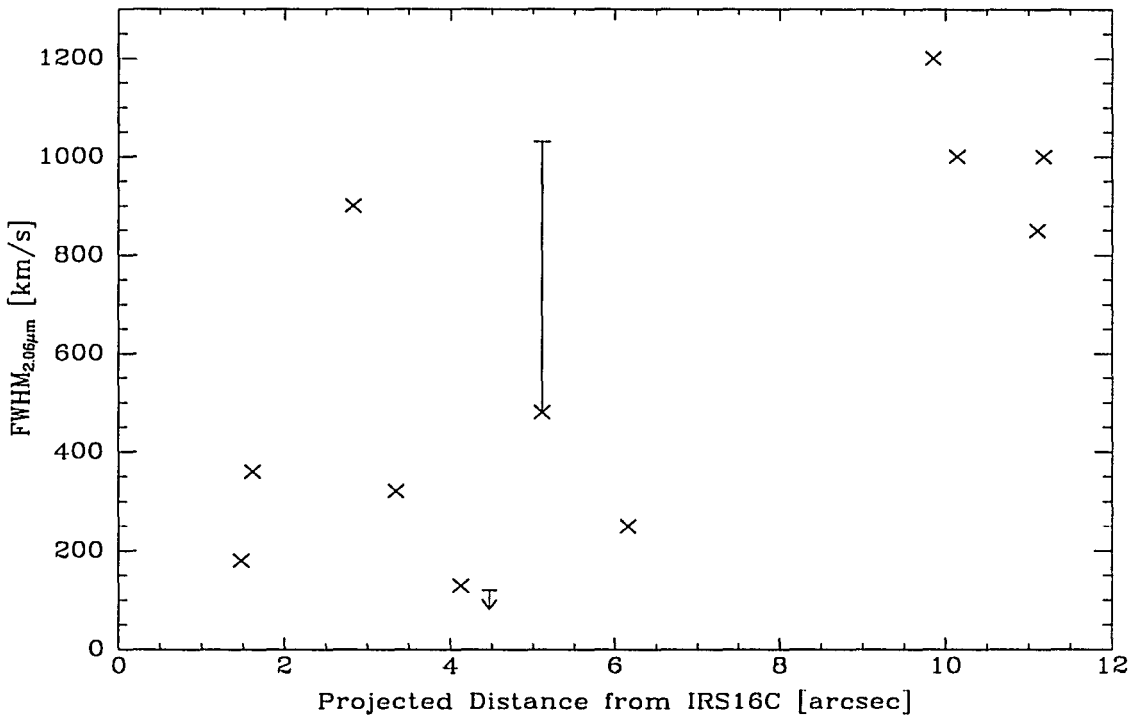

Figure 5.5: Correlation of Line Width with Projected Distance. The width (FWHM) of the He I 2.058 μm emission line is apparently correlated with projected distance from the center of the stellar cluster (near IRS 16C). This correlation is consistent with the two burst hypothesis. The projected distances are from Table 3.4; the line widths are from Table 3.3 and Najarro *et al.* (1994). The large error bar for IRS 13 reflects the FWHM measured by Blum *et al.* (1995a) from high quality data; we also saw a broad line base which we excluded from the profile fit.

straint but continue to have difficulty reproducing stars as luminous as IRS 16NE. Population models which make a large allowance for uncertainty in massive stellar evolution indicate that a persistent or episodic star formation history might be able to reproduce the GC stellar population without invoking unusual star formation or evolution. However, comparison with luminous Galactic emission-line stars demonstrates that the GC stars are nearly unique and hence cannot arise in such numbers from normal stellar evolution. The concentration of bright He I sources to the central 1/4 pc may hint to their origin.

CHAPTER 6

UNUSUAL STELLAR EVOLUTION

Peter Tamblyn[1], Fulvio Melia[1,2], G. H. Rieke[1], & M. Ruffert[3]

[1]Steward Observatory, University of Arizona, Tucson, Arizona 85721

[2]Theoretical Astrophysics Program, University of Arizona, Tucson, Arizona 85721

[3]Max-Planck-Institut für Astrophysik, Karl-Schwarzschild-Strasse 1, D-85740 Garching bei München, Germany

Abstract

The stellar population at the GC may arise from unusual stellar development unique to this region. Steady-state and time-dependent models of the influences of unique characteristics of the region are reviewed and developed. Most are rejected as either quantitatively implausible or equally applicable to the nuclei of M31 and M32, neither of which has a blue stellar population like the one in the GC. Most promising are a class of models with time dependence provided by star formation in the recent past. Interactions of the massive stars with one another, with Sgr A*, and with the mass-dominating population are unlikely to influence the population substantially. We speculate that the high stellar densities might alter star formation to increase the number of tight binaries or very massive stars. Tidal capture by low-mass stars may explain the central CO depletion region.

6.1 Introduction

In the previous two chapters, we found that the central 1/2 pc has a large number of luminous, warm stars. Some of these stars, (Blum-WC9 and AF) and probably most of the faint, wide-lined stars, are WR or very closely related stellar types. The remainder are probably also enriched and all have evolved off the main sequence. Similar populations are not seen in the nuclei of M31 or M32 (Section 5.2). Single-burst models are unable to produce these stars and the observed RSGs (Krabbe *et al.* 1995; Section 5.4). The stellar content of young clusters is consistent with this conclusion. Persistent- or double-burst models can reproduce the gross properties of the population, but several difficulties remain. First, without a physical motivation, it seems contrived to have had two recent star formation episodes, especially considering the region's current hostility to star formation (cf. Morris 1993). Second, the normal-burst models depend on an almost complete association of luminous, warm stars in the models with He I stars, but our comparison sample illustrates that He I emission is a rare characteristic even among luminous emission-line stars of the appropriate temperatures. Third, the GC population contains an anomalously large number of stars significantly more luminous for their effective temperatures than the members of an extensive comparison sample. These stars bring into question the ability of any sequence of normal star formation followed by normal evolution to match the GC population. Fourth, the burst scenario does not obviously explain the observed concentration in the central 1/2 pc. Not only is the spatial density of the emission-line stars much higher in the IRS 16 environs, but there is an apparent correlation of location with continuum and emission properties (Section 5.6). Specifically, the IRS 16 components are the brightest spatially unresolved He I stars and they have narrow line widths in contrast to the outlying members (AF, AHH-NW, IRS 15NE...) which are fainter and have broader emission

lines. These factors lead us to consider alternative hypotheses which depend on the region's unique characteristics.

6.2 Steady-State Models

The expectation that we are not viewing the nucleus of our galaxy at a special time is a strong argument in favor of steady-state models or cyclic models in which the period is much shorter than the age of the Galaxy. Several steady-state models have been proposed since the discovery of the bright sources. However, the population of bright blue sources within the central parsec of the Milky Way contrasts dramatically with the absence of such objects in the dense nuclei of other galaxies where we might expect to see them (Section 5.2). Although the Galaxy may be unique in some as yet undetected way which permanently sustains the population of blue objects, these observations argue strongly against models in which the luminous blue objects form in a steady-state process that does not require unique conditions. Several such models are briefly reviewed here in light of this new finding.

6.2.1 Ongoing Stellar Mergers

At the stellar densities implied by recent observations, $n_* > 10^7\,\mathrm{pc}^{-3}$ (Eckart *et al.* 1993; Haller *et al.* 1996; Krabbe *et al.* 1995), individual low-mass stars can repeatedly collide and merge to build up to more massive stars (Lee 1987). According to this interpretation, the bright stars seen are a steady-state population of these merger products. However, the *HST* observations of M31 and M32 rule this out for the warm stars because these nuclei do not exhibit luminous blue stars like in the GC despite otherwise similar populations and spatial distributions of stars. Krabbe *et al.* (1995) further argue that the luminosities of these sources indicate they are like the most massive stars, and stellar mergers cannot build up to such high masses during the short lifetime of the merged object. Initially, for low-mass main-sequence

stars, the typical collision interval of over 10^9 yr (Eckart *et al.* 1993) restricts the growth to a rate too slow to reach the implied masses. This rate would increase as the merger product departs the main sequence and expands its cross-section, but the life expectancy of the merger product is then very short. Hence, the decreasing stellar evolutionary timescale beats out the timescale for additional mergers and restricts the product masses to well below $30\,M_\odot$. However, as discussed in Section 5.5, a comparison with the Eddington limit indicates that the brighter GC stars must have masses at least this large if built from mergers of low-mass stars with unenriched abundances. A detailed model with ongoing stellar mergers including the evolution of the cluster through core collapse (Lee 1993) shows that masses $\gtrsim 20\,M_\odot$ are seen only in smaller numbers than the observed He I stars and only for a limited time ($\approx 3 \times 10^8$ yr) around core collapse when the cluster parameters are substantially more compact than currently observed.

6.2.2 Accreting Black Holes

Morris (1993) has suggested that the bright (red) sources are powered by matter accreting onto stellar remnant black holes. He argues that through gravitational settling, the space density of these remnants would be significantly enhanced and the probability of collision with a star large. He proposes that the product of such a collision would be a luminous accretion source in which the originally stellar material puffs up to red-giant proportions in response to the high luminosity. However, this model would apply equally strongly to M31 or M32. Formation of these accreting objects through an enhanced merger rate during a time-dependent dynamical event, such as core collapse of the central cluster, would be a possible explanation, but in this case the central objects would be much more strongly concentrated within the core than are the prominent IRS 16 components (Lee 1993).

6.2.3 Clusters

The source crowding and the extreme luminosity of the brightest GC sources has led to suggestions that these stars might be tight clusters rather than single objects. Indeed, Eckart *et al.* (1993) resolve IRS 13 into 5-10 components within 1″ diameter. However, lunar occultation data (Simon et al. 1990; Simons et al. 1990) show that the bright (at K) components of IRS 16 are dominated by point sources even with a 0.″02 $\sim$ 200 AU scale. This is a considerably finer resolution than even the 0.15″ achieved by Eckart *et al.* (1993). Hence, if sources such as IRS 16NE were to be sub-clusters, they would need to be much more compact than the IRS 13 group. Further, if this were the explanation for the IRS 16-like sources, we would expect to observe a large, dispersed population of individual stars with similar properties (except for brightness) which had evaporated from the sub-clusters. Although fainter, outlying He I sources have been identified, their emission line profiles are distinctly wider. Also, the equivalent widths of the IRS 16 He I emission lines are quite large compared to most of our non-WR comparison stars. Hence, it is likely that the He I sources dominate the brightness of the IRS 16 sources (excluding the extended IRS 16S). However, even the lunar occultation observations do not exclude tight (a $\ll$ 200 AU) binaries in which the He I source provides at least half the near-IR flux, but this is qualitatively different from the previously popular sub-cluster interpretation and will be discussed in detail below.

6.3 Time Dependence from Recent Star Formation

Given the independent evidence for recent formation of massive stars in this region (e.g., IRS 7, Lebofsky *et al.* 1982; it's tail, Yusef-Zadeh & Melia 1992; and a nearby maser, Yusef-Zadeh & Mehringer 1995), the most promising avenue for investigation

appears to be models in which the blue objects result from abnormal formation or evolution of massive stars due to the environment of the GC. According to this interpretation, the current state of the GC represents a short-lived (and possibly recurring) phase shared by other galactic nuclei. The distinction from M31 and M32 is only that they have not had recent nuclear bursts of star formation. The challenge is instead to understand what distinguishes the GC from other star forming regions.

Observationally, the distinguishing features of this population are a relatively cool integrated UV spectrum and a high concentration of very luminous stars, many of which have the uncommon trait of He I 2.058 μm emission. Various pieces of information independent of the stellar characteristics allow us to estimate the age of the star formation episode(s). Most persuasive for a very recent episode are the H_2O maser recently discovered at the intersection of the expanding [Fe III] shell with the surrounding molecular cloud (Yusef-Zadeh & Mehringer 1995) and the shell itself (Lutz *et al.* 1994). Assorted stars (IRS 7 and AF among them) also appear to be fairly normal products of a very recent star formation episode. Hence, it is fairly clear that evolved massive stars inhabit the region. However, as we showed in Chapters 2 and 5, the overall characteristics are inconsistent with the expected population from a single burst. We focus here on mechanisms suspected to increase the frequency or lifetimes of blue, evolved, massive stars.

6.4 Unusual Single Star Evolution

As briefly discussed in Section 3.4, it seems unlikely that the peculiar GC objects can be explained in terms of abnormal evolution caused by metallicity effects. This result seems to hold even if moderately elevated metallicities increase the atmospheric opacities and enhance the winds, although a better understanding of high-metallicity

massive stellar evolution would be desirable. The enhanced winds would increase the duration of the WR stage. However, the gas around the GC out of which these stars must have formed does not appear to have metallicity higher than twice solar (Shields & Ferland 1994), nor is there evidence in stellar spectra for a dramatic increase in metallicity within the central kpc (Tyson 1993). Finally, the population sampled in the surrounding 40 pc (Cotera *et al.* 1995) does not appear to be anomalous.

6.5 Influences of Other He I Stars

The spatial distribution of the He I stars suggests that close proximity to one another and/or location near the dynamical center is important to their formation or evolution. The extreme stellar density in the GC may increase the importance of a number of mechanisms which can affect massive stellar evolution. Mechanisms which are unimportant elsewhere may have dominant roles in this environment. All of these would be of greatest importance to post-main-sequence supergiant stars despite their comparative rarity (short evolutionary stage compared to main sequence) because they have much more distended and hence less tightly-bound atmospheres than do main-sequence stars. Although the observed spatial distribution suggests that location may be a dominant factor in determining whether a RSG is influenced, the proximity of several RSGs (IRS 7, IRS 9) indicates that the mechanism may operate on a timescale comparable to the RSG phase. Specifically, any mechanism suggested to create the anomolous concentration in the GC from normal RSGs must have a timescale shorter than a typical RSG lifetime to account for the relative excess of these stars, yet not so short as to make the presence of RSGs in the region troublesome.

If RSG envelopes are preferentially stripped, this would account for an enhanced

number of hot, luminous stars similar to the fainter He I sources; the bright IRS 16 sources are apparently too luminous to have ever experienced a RSG phase. The luminosity of a massive, core-helium-burning RSG would not be affected dramatically by the loss of most of its envelope (Arnett, private communication). The stripped object would be a hotter star, probably with somewhat enriched surface abundances. Traditional WR stars demonstrate that a massive star which has shed its envelope will be hot and luminous. Whether the resulting star appears as a WR star or more like an Ofpe/WNL star is a function of the new surface abundances: WR winds are driven by the substantially increased opacity of He-rich material. In contrast, low-mass, hydrogen-rich stars have an opacity which more closely follows Kramers Rule; the decreased temperature at the new surface layers permits ion recombination, increasing the opacity and leading to runaway expansion (Arnett; Renzini *et al.* 1992).

First we consider three consequences of the proximity of the known massive stars to one another. Although an extended envelope can be stripped by a nearby supernova (SN) if it is in a sufficiently tight binary (Livine, Tuchman, & Wheeler 1992), this mechanism is unlikely to play a significant role if the massive stars are as evenly distributed as the bright sources. The typical projected separation of the major IRS 16 components is at least 0.01 pc; hence, even a 1200 $R_\odot$ star would intercept $\sim 2 \times 10^{-6}$ of the 10^{51} ergs available in the kinetic energy of the ejecta. This would allow the liberation of less than a solar mass of envelope even from the tenuous hold of a RSG. The population models (see Figure 5.1) show that if the RSGs are from a single burst which dominates the region's UV with age ~ 6.5 Myr and a high mass IMF index of -3.3, then of order 230 supernovae should have gone off in the past few million years. If uniformly distributed through the central 1/2 pc, they would typically be ~ 0.1 pc from the nearest RSG and exert a negligible

influence. Indirect indications of these supernovae would be difficult to detect in this region due to other energetic phenomena.

Similarly, although massive stellar winds carry a significant amount of energy and momentum (mass-loss rates $\sim 10^{-5}\,M_\odot\,yr^{-1}$, terminal velocities $\gtrsim 1000\,km\ s^{-1}$; Conti 1988), the geometrical dilution at typical separations indicates this is not likely to account for the GC He I stars. Although the radiative power produced by an O star is $\sim$ 100 times the wind power and the intercepted UV could be a substantial ionization heating source in a nearby RSG's atmosphere, it would require an unrealistically high efficiency near unity to ablate even $10^{-6}\,M_\odot\,yr^{-1}$ in this manner with the expected typical separation. IRS 7's ablation by the composite UV and wind from IRS 16 (see Yusef-Zadeh & Melia 1992 and references therein) is a physical example of the process. Its mass-loss rate of $10^{-5}\,M_\odot\,yr^{-1}$ (Serabyn *et al.* 1991) is comparable to what would be expected without the external UV and wind sources, confirming that this process is inefficient when operating over scales $\approx 1/3\,pc$.

6.6 Influences of Sgr A*

A central massive object ($M \sim 10^6\,M_\odot$) associated with Sgr A* could disrupt stars which pass within a tidal radius (cf. Hills 1975)

$$r_t \sim \left(\frac{M_{co}}{M_*}\right)^{1/3} R_*. \tag{6.1}$$

For a RSG, this is less than $10^5\,R_\odot \approx 0.002\,pc$. In the 10″ (0.4 pc) around Sgr A*, there are approximately 5 RSGs and at least 9 blue stars (Rieke & Rieke 1988; Krabbe *et al.* 1991). It is unlikely that such a large fraction of the available RSGs would have passed this close to the central object during this short-lived phase. If Sgr A* strongly dominated the region's mass, it might be reasonable to propose that all these stars are on highly elliptical orbits with periastron within this radius, but

the light and mass distributions do not appear to be this centrally concentrated. If space velocities of these stars, which may be obtainable in the near future, are biased in this way, this would strongly argue that the other stellar orbits are also likely to be highly eccentric, which would influence the derived mass of the central object.

A sporadic influence of a central supermassive black hole also needs to be considered. The Sgr A geometry may indicate a recent explosion near the dynamical center (Yusef-Zadeh & Morris 1987). This explosive event must have been more powerful than a typical supernova unless preceded by a strong wind (Mezger *et al.* 1989). Theoretical studies (e.g., Hills 1975; Khokhlov & Melia 1996) indicate that stars from the mass-dominating population occasionally pass within the tidal disruption radius of Sgr A*, creating large, explosive events. Although typical event energies are $\approx 2 \times 10^{52}$ ergs and these occur every $\sim 10^4$ yr (Khokhlov & Melia 1996), the less common but more energetic events such as may be responsible for Sgr A East are more interesting in this context. A typical RSG would experience one of the 10^{53} erg events which are expected to occur every $\sim 10^5$ yr because the ejecta are distributed over a solid angle $\lesssim 0.2$ steradians. At a distance from Sgr A* typical of the IRS 16 stars of ~ 0.1 pc, enough of the explosive energy to remove $\sim 0.2\,M_\odot$ would be intercepted. This is inadequte to affect a RSG dramatically, and it is unlikely that all of the currently blue stars were significantly closer during one of these events.

6.7 High-Mass, Low-Mass Star Interactions

6.7.1 Space Density of Low-Mass Stars

Another possibility is that the extremely high density of low-mass main-sequence stars (and possibly stellar remnants) alters the evolution of massive stars in the

GC. Although the stellar density in this region must be very high, it is difficult to measure quantitatively, both because the light from the region is dominated by a small number of very luminous objects and because the mass is dominated by a central concentration of dark matter. As a result, it is difficult to measure either the light or the mass associated with the low-mass stars. Eckart *et al.* (1993) measure a small core radius (0.15±0.05 pc) and a central mass density of $\rho_c = 10^{7.7\pm0.5}\,M_\odot\,pc^{-3}$. Rieke & Lebofsky (1987) use a different technique and measure a core radius of $\sim$ 1.2 pc for low-mass stars, which would imply a stellar density in the central 0.2 pc an order of magnitude lower than the estimate of Eckart *et al.* (1993) for the total mass density. Moreover, the number and distribution of dark objects such as stellar remnants is unknown: current limits would allow a density as high as $\rho_c = 2 \times 10^8\,M_\odot\,pc^{-3}$ within the central 4″ radius if the central dark mass is not predominantly in the form of a black hole. Hence, the space density, n_*, of main-sequence stars and more compact objects is highly uncertain and may exceed $10^8\,pc^{-3}$. High stellar densities are also encountered in the cores of globular clusters, and two classes of mechanisms for stripping the envelopes from low-mass red giants in these systems have been studied. This section reviews the mechanisms of core ejection and common-envelope ejection, and indicates how they might apply to the GC region. We make estimates of the rates of these processes to determine which, if either, may play an important role in the GC.

6.7.2 Core Ejection

A consequence of collisions in which a relatively compact low-mass object (main-sequence star or stellar remnant) plunges through the envelope of a RSG can be that the dense RSG core is slingshot out of the dynamically slow envelope. This mechanism was studied in the context of red giants by Tuchman (1985) and Livine & Tuchman (1988) to explain the gas clouds observed in the GC by Lacy, Townes,

& Hollenbach (1982) (see also Davies, Benz, & Hills 1991 and Rasio & Shapiro 1991 for application to globular clusters). In the impulsive approximation, as used by these authors, the kinetic energy imparted to the core of mass M_c by the pull of the passing intruder of mass m with impact parameter b and relative velocity v_r is

$$\Delta E_c = \frac{2G^2 M_c m^2}{v_r^2 b^2}. \tag{6.2}$$

This must exceed the binding energy of the core to the envelope for ejection. For a model RSG with mass $15\,M_\odot$, kindly provided by Dr. S. Woosley, this binding energy is roughly 1.7×10^{48} ergs, yielding $b_{crit} \approx 10\,R_\odot$. This value is uncertain because the binding energy depends on the choice of core-envelope boundary. This result is markedly different from Tuchman's analysis primarily because the model RSG envelope profile is considerably steeper than the $\rho \sim r^{-1.5}$ for a red giant. An impulse approximation leads to a predicted interval between such close collisions for a RSG in a system with velocity dispersion σ_v of

$$\tau \gtrsim 1.3 \times 10^7 \left(\frac{n_*}{10^8\,\mathrm{pc}^{-3}}\right)^{-1} \left(\frac{\sigma_v}{170\,\mathrm{km/s}}\right)^{\alpha} \mathrm{yr} \tag{6.3}$$

in which α is just under 2. This estimate is very coarse because the freefall velocity at such small impact parameters is comparable to typical collision velocities, contrary to the impulse approximation. Nonetheless, it shows that this mechanism is unlikely to affect a large fraction of the GC RSGs during their $\sim 10^6$ yr life spans even if $n_* \approx 10^8\,\mathrm{pc}^{-3}$, in the upper range of what is allowed by observations.

6.7.3 Common-Envelope Evolution

In a sufficiently tight binary ($a \lesssim 1000\,R_\odot$; $P \lesssim 2.5$ yr for $M = 15\,M_\odot, m = 1\,M_\odot$), the secondary is eventually engulfed by the evolving supergiant's envelope. In this subsection we review the consequences of such a structure and look at two reasons why the requisite close binaries might be more likely to exist in the GC. Through-

out, we use primary and secondary to refer to the perturbed and perturbing stars, respectively.

Taam, Bodenheimer, & Ostriker (1978) showed how a neutron star companion orbiting in a RSG envelope can generate enough drag dissipation to accelerate a portion of the envelope to greater than the escape velocity. More recent work (see Livio & Soker 1988, Taam & Bodenheimer 1991, and references therein) replaced the neutron star with a low-mass main-sequence star such as would be more likely to be captured by a nuclear RSG. Although the timescales change, the envelope is still ejected efficiently on a timescale shorter than that of stellar evolution. These systems are distinguished from contact binary systems or W Ursa Majoris stars in that the binary's mass ratio is skewed so the envelope is not co-rotating with the secondary before contact (Livio & Soker 1988; Taam & Bodenheimer 1991). Hence, the secondary drags through the envelope and locally deposits orbital energy. The secondary spirals in through the envelope until it coalesces with the primary's core or until enough envelope mass has been ejected that the primary can settle within the (significantly reduced) orbit radius. The need to explain short-period evolved systems (low-mass X-ray binaries, binary radio pulsars, cataclysmic variables, and binary-nucleus planetary nebulae) has prompted increasingly sophisticated efforts to study common-envelope systems. The efficiency of orbital energy conversion for the liberation of envelope material, $\alpha_E \gtrsim 0.15$ (Taam 1993), is more than adequate to strip the envelope of a RSG. Physical effects which divert or dissipate energy, reducing α_E from unity, are envelope spin-up, acceleration of some material beyond escape velocity, and energy transport resulting in increased luminosity which is directly radiated from the system without internal conversion to mechanical energy (Taam *et al.* 1978). Although the competitions among the timescales for mass ejection, orbital decay, energy transport, and envelope spin-up are critical for deter-

mining whether the final state of the system is a short-period binary or coalescence, it has been shown for other systems (and compact evolved systems demonstrate) that most or all of the common envelope is lost. It is therefore reasonable to expect that similarly efficient envelope ejection would affect a RSG in the GC which has engulfed a low-mass secondary.

6.7.4 Tight, Coeval Binaries

In general, a large fraction of stars are formed in binaries. It is possible that this tendency is enhanced by the abnormal conditions under which stars form in the GC. The formation process may be akin to fragmentation of an accretion disk, rather than collapse of condensations from a molecular cloud. At the high densities involved, the collapsing protostars will be subject to perturbations by collisions or near misses with each other, and furthermore will have numerous interactions with the many low-mass main-sequence stars and remnants that populate the region. These perturbations could trigger instabilities that lead to enhanced binary formation in a manner analogous to the proposal of Bonnell (1994). He considers a rapidly rotating central object surrounded by a rotationally supported infalling disc of gas and shows that instability modes can cause formation of a self-gravitating secondary body in orbit around the central one.

6.7.5 Companion Capture

Due to the extreme stellar density, binaries can also be formed during the short life span of a massive star. The formation of binaries in dense stellar systems has been studied extensively in the context of globular cluster cores, and many of the same processes operate in the GC. Significant differences are introduced by the large mass ratios, large relative velocities, and short timescales relevant to the current problem. For instance, equilibrium arguments do not apply because a

massive star's lifetime is shorter than the equilibration timescale. Also, because of the high velocity dispersion, conventionally defined "hard" binaries, $E_{bind} \gg m\sigma_v^2$, are considerably harder than required to evolve into a common-envelope binary. In globular clusters, the soft binaries are of minimal importance because they have a low equilibrium density and little binding energy. We cannot ignore the "soft" binaries with $1/30 \lesssim E_{bind}/m\sigma_v^2 \lesssim 1$ because we are interested in the evolution of the binary systems themselves rather than their impact on the cluster energetics.

In general, binaries can be formed by transferring excess relative kinetic energy to a third body. A simple density argument (Binney & Tremaine 1987, p. 492) is sufficient to show that the rate at which massive stars in the GC participate in 3-body encounters which create a binary is vanishingly small. The only binary formation mechanism we need to consider is capture by conversion of orbital energy into tidal distortions of the distended target star.

6.7.6 Tidal-Capture Rate — Analytic Estimates

In this dynamically hot system, typically only penetrating encounters (collisions) remove sufficient orbital energy through tides to create a bound system. The perturbations induced by such a collision are not well approximated by conventional estimates of tidal distortion derived for a close pass, as discussed further below. Nonetheless, we will use initally the impulsive tidal approximation to estimate the orbital energy loss, ΔE_T, in the encounter because the uncertainty in the rate at which a RSG captures companions,

$$\mathcal{R} = \tau^{-1} = n_* \int_0^\infty f(\vec{v_r})\sigma(v_r)v_r d^3\vec{v_r}, \tag{6.4}$$

is still dominated by the uncertainties in the stellar density n_* discussed earlier.

To estimate roughly the capture cross-section, $\sigma(v_r)$, we can consider the excitation of $l = 2$ non-radial oscillations in the RSG envelope as presented by Fabian,

Pringle, & Rees (1975) (hereafter FPR), adapted for a distended star (Bailyn 1988). The problem has also been studied for larger impact parameters by analogy to stellar dynamical behavior (Spitzer 1987; see also Binney & Tremaine 1987, p. 438). The requirement for tidal capture can be expressed as (Davies *et al.* 1991):

$$\Delta E_T = \frac{GMM_{env}}{R} f^2 \left(\frac{m}{M}\right)^2 \left(\frac{R}{b}\right)^6 \geq \frac{1}{2}\frac{Mm}{M+m} v_\infty^2. \tag{6.5}$$

M, M_{env}, and R refer to the primary's mass, envelope mass, and radius. m is the mass of the impactor, b is the impact parameter, and v_∞ is the relative velocity of the stars before the encounter. Although a massive star spends only a small part of its life as a RSG, this is the only phase in which it has a non-negligible probability of capturing a companion because R^2 is very much smaller in the longer main-sequence phase. f is a "reduction factor" (FPR) to account for incomplete coupling between the collision frequency and the $l = 2$ mode of the RSG. FPR give limiting forms for f of $k\left(\frac{M}{m+M}\right)^{1/2}\left(\frac{b}{R}\right)^{3/2}$ for collisions in which this term is $\ll 1$ and the inverse exponential of this when it is $\gg 1$. We conservatively enforce continuity by switching to the latter form when $f = \exp(-f) \approx 0.567$. k is a constant in the range 2 to 3 which relates the fundamental frequencies of the RSG to its mass and radius.

The collision cross-section, $\sigma(v_r)$ in Equation 6.4 includes a term for gravitational focussing:

$$\sigma_{gf} = \pi b^2 \left[1 + \frac{2G(M_1 + m)}{v_r^2 b}\right]. \tag{6.6}$$

When the particles can be treated as point masses, M_1 is the mass of the primary. Obviously, for a penetrating encounter M_1 is reduced.

The relative velocity distribution, $f(v_r)$, can be related to the observable systemic velocity dispersion, σ_v, with some reasonable assumptions. For example, if both the RSG and impactor populations of stars have Maxwellian velocity distributions with

the same one-dimensional dispersion, σ_v, then $f(v_r)$ is a Maxwellian with dispersion $\sqrt{2}\sigma_v$ (Binney & Tremaine 1987, p. 485). In this case, the integration over v_r yields

$$\tau \sim 4 \times 10^6 \left(\frac{n_*}{10^7 \text{ pc}^{-3}} \right)^{-1} \text{ yr.} \tag{6.7}$$

As a massive star spends ~ 1 Myr in a very distended state (cf. Schaller *et al.* 1992), these calculations indicate that roughly one out of four of the RSGs in the GC will capture a companion. This is in the target regime mentioned in Section 6.5 which can explain the enhanced He I star population without making the presence in the region of RSGs such as IRS 7 problematic. Although the approximations used to derive this collision rate are intended for close passes rather than penetrating encounters and for a mass ratio closer to unity, this calculation is sufficient to show that an enhanced binary-capture rate is worth further examination.

6.7.7 Tidal-Capture Rate — Numerical Estimates

Three pieces of further research suggest that FPR's formulation of the reduction parameter, f, is accurate only for grazing encounters and that second-order effects dominate over the frequency coupling inefficiency when the stars collide. Detailed smooth-particle-hydrodynamics (SPH) simulations of parabolic encounters applicable to globular clusters (Davies *et al.* 1991) are in very close agreement with Equation 6.5 for near-grazing encounters but show that the reduction factor should remain closer to unity for more distant encounters (see Figure 6.1). Simulations by the same group show that the efficiency is over-estimated for encounters which penetrate within $b/R_{RG} \approx 0.7$. Two detailed piecewise-parabolic-method (PPM) hydrodynamic simulations conducted for this project by Dr. Ruffert similarly suggest that the energy loss saturates near the value predicted for grazing encounters.

Most of the collisions of interest for this analysis occur at a large fraction of the stellar radius where the cross-section is large but the energy transfer is still adequate

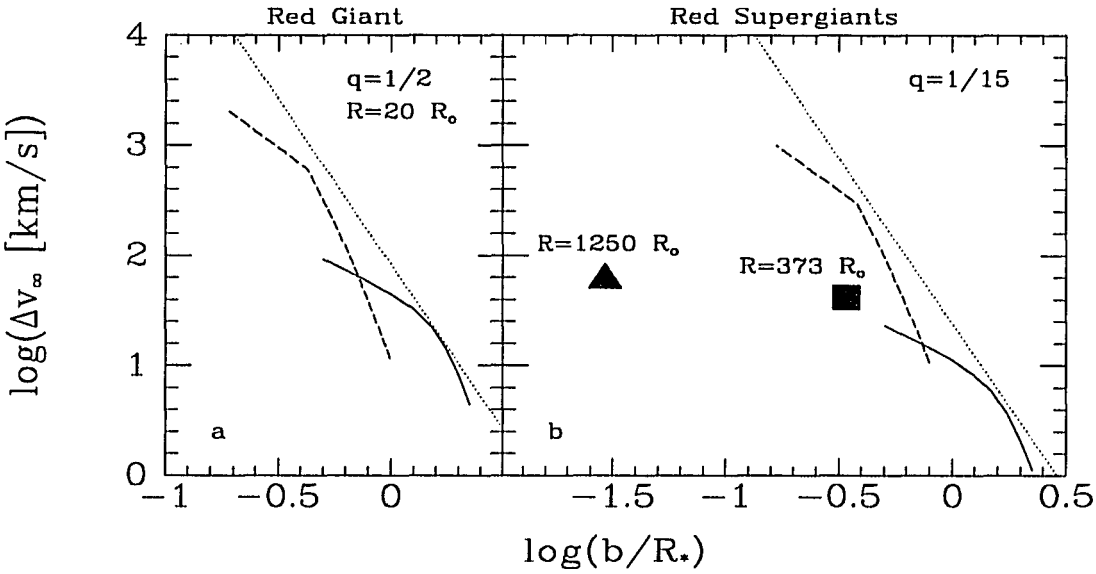

Figure 6.1: Comparison of Tidal Energy Loss Estimates.
a: The analytic approximation of FPR (dashed line) is compared with detailed hydrodynamical models (Davies *et al.* 1991, solid line). The simulations involved a $0.8\,M_\odot$, $20\,R_\odot$ red giant as a target and had a mass ratio, q, of 1/2. The dotted line is the FPR formulation with the reduction factor, f, set to unity. The excellent agreement with the latter at $\log x = 0.2$ shows that f should be nearly 1 for close, non-penetrating encounters, but the efficiency falls off even more steeply for collisions than estimated by FPR.
b: In this panel, the FPR approximation (dashed and dotted lines as above) is compared to Ruffert's hydrodynamical simulations (points). The Davies simulations have been shifted for $q = 1/15$ for comparison. In these plunging collisions, the energy loss is significantly over-estimated by FPR's formulae, even with f reflecting the frequency coupling inefficiency. However, the shifted Davies simulations would agree very well with the Ruffert points if extended, indicating a saturated dependence on impact parameter.

to result in a bound binary. An assessment of $v_{crit}(b)$ could be determined by simulating a large number of collisions with the same techniques used by Dr. Ruffert. However, a much simpler analysis of the dominant physical effect in this transition region suffices. Outside the star, the tidal distortion is geometrically simple but the collision timescale is too slow to excite the dominant oscillation mode; this is the factor FPR's f addresses. In plunging collisions, a detailed simulation is required to model the complex distortion. In between, an improved consideration of the tidal distortion geometry reveals the saturation of v_{crit}. Equation 6.4 with f set to 1 is simply the maximal tidal distortion energy at periastron. This can be extended numerically into the regime of collisions. To conduct this analysis, the model RSG is considered in a Cartesian grid and the tidal field introduced by the perturber at an arbitrary point and the resulting tidal distortions are computed for each bin and propagated to neighboring bins. The distortion is a compression or expansion in the direction to the perturber such that hydrodynamic stability is restored, $\nabla\vec{P} = \vec{F_o} + \vec{F_{pert}}$. The biggest potential flaw in this analysis is that it ignores the time dependence of the problem and assumes that maximal tidal distortion will occur, the factors which the FPR f is intended to address. However, there is good reason to believe that this is a good approximation because the distortion is no longer harmonic and the collision timescale is shorter than the thermal timescale; hence, the collision acts as a geometrical perturbation to the stellar structure. Consider by analogy a rubber ball which is bounced on a firm surface: the ball distorts geometrically ($ds \rightarrow ds'$) until the pressure gradient is sufficient to halt further compression rather than absorbing the energy of the impact through a thermal ($\vec{P}$) adjustment. The results of this analysis, presented in Figure 6.2, confirm that the reduced energy transfers in the Davies *et al.* (1991) and Ruffert collisions result from this more complicated distortion geometry.

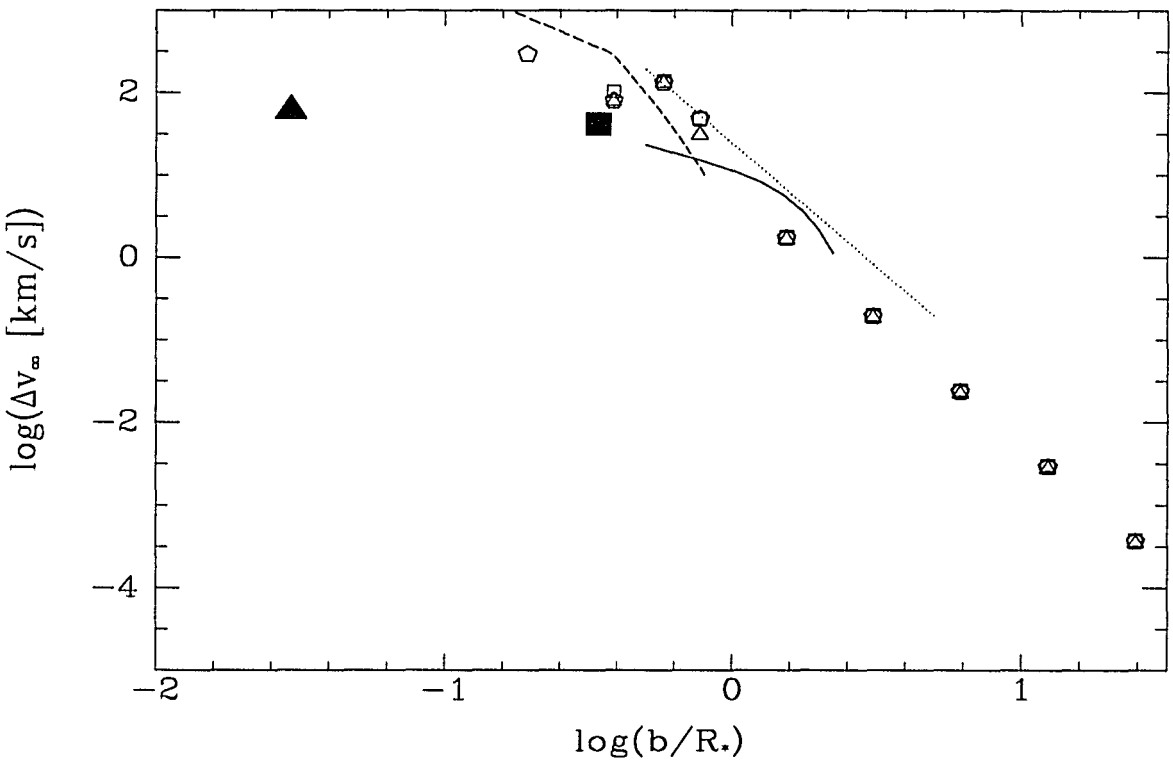

Figure 6.2: Estimated Tidal Energy Loss in Collisions. The second-order tidal estimates approximately connect the regime of close passes where the FPR approximation is valid with the highly damped, plunging encounters sampled by the hydrodynamic simulations of Ruffert. These calculations are based on a $1\,M_{\odot}$ impactor and a Woosley model RSG. The various open symbols illustrate the numerical stability of the code to different rejection criteria required by the coarse and unphysical binning of the target star. The filled symbols and lines are as in Figure 6.1*b*.

These disparate but consistent simulations were the basis for a three segment power-law fit to the capture cross-section:

$$\log \Delta v_\infty = \begin{cases} -0.15 \log b/R_* + 1.548 & \log b/R_* < -0.5689 \\ -1.006 \log b/R_* + 1.061 & -0.5689 \leq \log b/R_* \leq 0.197. \\ -5.294 \log b/R_* + 1.9065 & \log b/R_* > 0.197 \end{cases} \quad (6.8)$$

Integration with this cross-section predicts a capture timescale of

$$\tau = 42 \left(\frac{n_*}{10^8 \, \mathrm{pc}^{-3}} \right)^{-1} \left(\frac{m}{1 \, \mathrm{M}_\odot} \right)^{-1.1} \left(\frac{\sigma_v}{140 \, \mathrm{km/s}} \right)^3 \mathrm{Myr} \quad (6.9)$$

with weak dependences on M and R (taken to be $15 \, \mathrm{M}_\odot$ and $400 \, \mathrm{R}_\odot$). The indicated dependence on σ_v is only a first order estimate and would not apply for substantially different dynamical systems. This interval is much longer than the expected lifetime of a RSG. Hence, tidal capture of low-mass stars or remnants is unlikely to influence the evolution of massive stars in this region. As we have also seen that core ejection is inefficient in this system, it appears that any mechanism involving collisions with the background population (such as mergers or core exchange) will not explain the observed population. Tidal capture by lower-mass stars, which would have mass ratios closer to unity and longer life spans, may well be important, but is not expected to produce such luminous products. Gravitational settling and stellar mergers will enhance the fraction of higher-mass objects in the central regions (cf. Morris 1993; Lee 1987), and interactions with these more massive objects are individually more likely to result in capture. But such objects must be less numerous to remain consistent with the observed mass limits, and it is very unlikely that such massive objects even dominate the central mass. Hence the specific form of the mass-dominating population does not influence this result.

6.7.8 Tight Binaries — Survival

Especially because the relevant encounters are physical collisions, any binaries which are formed this way will be tight (as is always the case for tidal-capture binaries,

Lee & Ostriker 1986). If a common-envelope phase does not commence at once, it will do so shortly due to continuing tidal influences and the further evolution-driven expansion of the primary. There is a small probability that the binary system will interact with a third star (see the review by Hut 1985). As the pre-contact binary is "soft" in terms of the cluster dynamics, it would be more likely to lose binding energy in such an interaction ("Heggie's Law"). The equilibrium dissociation (evaporation) timescale in the region for these binaries (Binney & Tremaine 1987, p. 536) is

$$t_{evap} \approx 2 \times 10^7 \left(\frac{\rho_c}{10^8\,\mathrm{M_\odot pc^{-3}}} \right)^{-1} \left(\frac{a}{400\,\mathrm{R_\odot}} \right)^{-1} \left(\ln \frac{a}{400\,\mathrm{R_\odot}} + 2.5 \right)^{-1} \mathrm{yr}. \qquad (6.10)$$

Although this timescale is of importance to loose, coeval, massive-star binaries, it is slower than the progression from tidal capture to common-envelope evolution.

6.7.9 Common-Envelope Evolution — Observable Signatures

If the He I stars have experienced a common-envelope phase they may be spectroscopic binaries ($K_1 \sim 5 \sin i\,\mathrm{km\ s^{-1}}$, $K_2 \sim 100 \sin i\,\mathrm{km\ s^{-1}}$) or they may be rapidly rotating as a consequence of coalescence. Hjellming & Taam (1991) show that if the secondary emerges from the common-envelope phase before coalesence, the effects on the secondary will be minimal; the only peculiarity a post-common-envelope secondary would show would be a very short ($\lesssim 120\,\mathrm{day}$) period. If the final state is a merger, the orbital angular momentum at the time when the intruder touches the core is quite high, $L \gtrsim (Ga/(m + M_c))^{1/2} m M_c$; the separation a would be expected to be $\sim 10^{11}\,\mathrm{cm}$. In one extreme, if the resultant merger product remains as centrally condensed as the RSG core, the induced rotational velocity could be as high as $2000\,\mathrm{km\ s^{-1}}$. Despite this, the change in rotational velocity may not be detectable. Another limit is given by a uniform ball with the maximum size deduced for an IRS 16 component from $m_K = 8.8$ and $T_{\mathrm{eff}} \gtrsim 15,000\,\mathrm{K}$ of $170\,\mathrm{R_\odot}$, which would

have an induced rotation of only a few km s^{-1}. Also, the photosphere might rotate significantly more slowly than the central mass condensation. However, detection of anomously fast rotational velocity in an IRS 16 component would be strong support for the envelope ejection model discussed here.

6.8 High-Mass Binaries

Even in the field, the fraction of high-mass stars in binaries is high, at least 30% (see the review by Abt 1983) and possibly much higher. Smaller and more biased samples (Garmany & Conti 1980) indicate that among these binaries, mass ratios near unity and very short periods (days) are favored. A survey (Mantegazzen *et al.* 1980) finds orbital separations $a \sim 1.5(R_1 + R_2)$, where R_1 and R_2 are the stellar radii. In such tight binaries, stellar evolution can be dramatically influenced by mass transfer and mass loss (e.g., Podsiadlowski *et al.* 1992). This and other studies prompted by the unexpectedly blue progenitor of SN 1987A have used modified stellar evolutionary calculations which account for rapid mass transfer such as occurs with Roche Lobe overflow. Podsiadlowski *et al.* (1992) expect this to enhance to 30 – 40% of massive stars the fraction appearing as "helium stars", a group which are clearly analogous to the GC stars. Further, there is observational evidence of systems which are currently undergoing mass transfer (e.g., AZ Cas, Podsiadlowski *et al.* 1992) or obviously have done so.

The fraction of massive stars in binaries tight enough for significant interaction might be further influenced by unusual formation processes in the GC or by binary hardening in interactions with field stars. In manners yet to be identified, star formation conditions in this region may lead to an enhanced fraction of high-mass stars in tight binaries with other early-type stars. There is some observational support for this hypothesis. Although giant H II regions generally do not have strong

central concentrations, the massive star formation regions 30 Dor and NGC 3603 each have compact cores (R136 and HD 97950, respectively) composed of numerous massive stars (Moffat *et al.* 1985; Moffat *et al.* 1994; Drissen 1994) which should be compared to the GC central cluster. Several properties of these clusters are noteworthy. First, both have very high central stellar densities; estimates are seeing limited (even with *WFPC*!) but of order $10^5 - 10^7\,M_\odot\,pc^{-3}$, although they are not expected to have coincident concentrations of low-mass stars. Second, both have WNL stars in very tight binaries. Moffat *et al.* (1985) also note a pronounced concentration (steeper than the light concentration) of WRs in HD 97950 which they argue results from gravitational settling of the more massive WR progenitors. This work provides an alternate explanation: in the much denser core of NGC 3603, which is thought to be approaching core collapse, binary formation and common-envelope evolution may explain the enhanced WR frequency. Further, recent data (Drissen *et al.* 1995) find that the WRs in HD 97950 have 6 coeval O3V–III neighbors. As WRs are commonly thought to evolve *from* the most massive O stars, which in this coeval cluster are seen relatively unevolved, this can be interpreted to implicate a second influence (Hanson, private communication). We suggest this influence may be binary enhancement.

Even if the binary fraction or period distribution is not peculiar, frequent ($\tau \sim 10^5\,yr$) interactions of the expected fraction of high-mass binaries with the mass-dominating population will on average drive the high-mass binaries tighter. This would drive some binaries which would be wide enough to avoid mass exchange if they were in the field into a common-envelope phase. Unlike the high–low-mass binaries discussed in Section 6.7.5, the binding energy of high-mass binaries will exceed the cluster's characteristic dyanamical energy, $m\sigma_v^2$, and hence will on average be driven tighter in binary–field star interactions. Although the binding energy changes

slowly, it increases over the whole lifetime of the binary. Survival of hard binaries is very likely: they can not be gradually "evaporated" like soft binaries because most collisions will instead make them harder. Instead, it requires an atypical collision with an unusually high velocity star to drive the binary over the Heggie's Law watershed in one event. Hence, the high-mass binaries formed in the GC either through normal or biased star formation will be driven towards Roche Lobe exchange. However, the importance of these interactions should not be over-emphasized: most have a small influence on the binding energy. The timescale over which the binding energy changes by a characteristic energy $m\sigma_v^2$ (cf. Binney & Tremaine 1987, p. 539) is comparable to a massive star's lifetime (10^7 yr). Also, these estimates are coarse because the system will likely behave as a 3-body system for an interval which is significant compared to the time between interactions.

Although Roche Lobe overflow is likely the dominant process in these binaries given the tendency for binary hardening, it is still instructive to review other important processes in high-mass binaries. Several of the interactions between massive stars dismissed in Section 6.5 need to be reconsidered in this context because typical binary separations are much smaller than the separations between the known He I stars. Identifying the GC He I stars as binaries would also help (although only slightly) explain the extraordinary luminosities of the brightest sources. However, the He I source probably still dominates the near-IR of such a binary regardless of whether the companion is blue or red. Specifically, if the companion is a blue, main-sequence late-O star, it would be several magnitudes fainter in the NIR than the cooler primary. On the other hand, a red companion's contribution must be small because these sources have Rayleigh-Jeans spectra. Intermediate-temperature companions could contribute up to approximately equal flux without making the emission equivalent widths too problematic, but are strongly dis-favored by evolu-

tionary expectations. Most interesting in this context and most probable are binaries with companions of nearly equal mass which have either gone supernova during the RSG phase of the current He I star, or are late-O main-sequence stars.

At first assessment, it seems that if RSGs are in massive star binaries a significant fraction of the time, this could explain all of the observed blue stars by supernova stripping (Livine *et al.* 1992). However, the odds that each of the observed WR or "transition" objects were stripped during their RSG phases by a companion's SN are much smaller because the ratio of RSG to total lifetime for a massive star is $\sim 10\%$. Hence, the coeval binaries would need to have components with nearly equal masses.

In contrast, the potential, less massive, unseen O star companions would have continual winds and high UV fluxes. No coincidental timing is required for these influences to operate when the primary is extended. Hence, the possibility that the He I stars have been individually stripped by binary companions cannot be ignored. Using the same mass-loss characteristics as in Section 6.5 but a binary separation of $2000\,R_\odot$, the wind kinetic energy intercepted by the RSG would be enough to liberate substantial material, $\lesssim 10^{-3}\,M_\odot\,yr^{-1}$, if the conversion is efficient. The luminosity power is again about 100 times as much, but the conversion is probably substantially less efficient. Further, at such tight orbital separations, the RSG will overflow its Roche Lobe if the companion is also massive. Regardless of which influence dominates, it is clear that an O-star companion would have a substantial effect on the evolution of a RSG (cf. Podsiadlowski *et al.* 1992). Indeed, such binaries remain a viable explanation for field WR stars.

Considering that the binary fraction of OB and WR stars is generally subject to controversy, it seems ambitious to try to detect binaries among the luminous stars in this region which is relatively difficult to observe. However, adaptive optics

and space based NIR observations make it feasible to conduct meaningful searches for eclipses among the prominent members. The narrow emission lines also make a spectroscopic search plausible, but care must be taken to avoid confusion from crowding or intrinsic wind variations.

6.9 Application to Lower-Mass Red Giants

There has been considerable research on the influence of the GC environment on Red Giants (RGs) prompted by two observational clues. The first is the CO depletion region described in Chapter 4; an image can be found in Haller *et al.* (1996). The second is a series of mid-IR emission sources which were interpreted as stellar-mass clouds (Lacy *et al.* 1982) created by stellar collisions. Although these mid-IR sources are now thought to be part of a coherent structure (Lacy *et al.* 1991), the CO depletion region remains an important piece of the GC puzzle with uncertain explanation. Hence, it may be valuable to review how some of the mechanisms considered in this chapter apply to lower-mass RGs in the nucleus of our own and other galaxies.

In many respects, predictions for RGs are expected to be much more secure: our understanding of their evolutionary timescales and structure are much better than for RSGs, their lifetimes exceed the equilibrium timescales for GC dynamics, and these mechanisms have been directly modeled with RGs in the context of globular cluster core collapse. The important distinctions of this region from globular cluster cores for RGs are the much higher relative velocities and (presumably) stellar densities. The most important distinction from RSGs other than lifetime is in RG opacities and structure: a red giant of solar metallicity which loses partial envelope mass will rebound and appear as a lower-luminosity red giant. Although in detail the energy source is different, "red clump" stars are an adequate demonstra-

tion of this: after losing mass ascending the red-giant branch and the helium flash, moderate-metallicity low-mass stars populate the reddest part of what would be the horizontal branch in lower-metallicity populations, where it intersects the red-giant branch. Nearly complete envelope loss would break the opacity dependence that drives runaway expansion (Renzini *et al.* 1992) and leave a bluer object without CO absorption features. A central concentration of such objects would dilute the CO feature in a manner consistent with the observations. However, they would not have the WR-like characteristics which make the GC He I stars individually identifiable.

We briefly remind the reader that several models for unusual stellar development in the GC have been developed without resorting to recent star formation, and they have been thoroughly discussed by their originators and following papers. For example, the prediction of ongoing stellar mergers (cf. Lee 1993) certainly must apply to some extent. However, it is not expected to have any impact on the two observational traits discussed above because the merger process is expected to be almost completely efficient, yielding only a more massive star. Similarly, the model in which black holes aquire envelopes from collisions with red giants (Morris 1993) likely influences the GC region but is not relevant to these problems.

The CO layer in RGs in the vicinity of a strong UV source could be externally dissociated. If the He I stars, which may dominate the region's UV, are responsible, one would expect a stronger correlation between these stars' locations and the observed depletion region. For example, AHH-NW and IRS 15 are likely stronger UV sources than the AF star, but located outside the observed depletion region. External ionization from Sgr A* looks feasible given the spatial distribution, but the finding that stars dominate the UV makes this unlikely. Although a low-luminosity, harder-UV source at Sgr A* is consistent with the observations, it should be the softer, stellar UV which dominates the CO dissociation. The unseen main-sequence

O stars are a more promising source of external ionizing radiation. These stars may dominate the region's UV and are likely to be somewhat concentrated to the depletion region by gravitational settling.

Core ejection was first considered (Tuchman 1985) specifically to explain the GC mid-IR clouds, and would also account for a concentration of continuum sources in the densest regions which would dilute the CO absorption. In the original analysis, it was assumed that white dwarfs would be abundant and serve as the perturbing projectiles. We can consider as a limit that most of the central mass density is in the form of $0.8\,M_\odot$ white dwarfs and that the target RGs remain confined to this region throughout their RG phase. A more realistic model would consider stellar evolution and gravitational settling to estimate the white dwarf space density and realistic stellar orbits with a fraction of the RG phase in the densest regions. Equation 6.2 still applies, but the energy binding the envelope to the core is substantially lower. Accepting Tuchman 1985's "typical" RG parameters ($M = 2\,M_\odot$, $M_c = 0.62\,M_\odot$, $L = 6000\,L_\odot$, $\rho_{env} \propto r^{-\alpha}$ with $1 \leq \alpha \leq 1.5$), $BE \approx 1.5 \times 10^{46}$ ergs, yielding a $b_{crit} \approx 50\,R_\odot$. However, his $R \approx 580\,R_\odot$ (estimated from his Figure 2; implies $T_{\rm eff} \approx 2100$ K) RG is probably generous. A review of RG evolutionary tracks (e.g., Sweigart *et al.* 1989) suggests that a $50\,R_\odot$ star is more appropriate. Such a star, assuming the same envelope density profile, has about 10 times as much binding energy, requiring a collision 3 times as close. A coarse estimate of the interval between such encounters for a RG is

$$\tau \sim 6 \times 10^7 \left(\frac{n_*}{10^8\,\mathrm{pc}^{-3}}\right)^{-1} \left(\frac{\sigma_v}{140\,\mathrm{km/s}}\right)^{\alpha} \mathrm{yr}. \qquad (6.11)$$

Obviously, an integration considering the evolving envelope size and profile would improve this estimate, but since this must compete with the fast evolution in this upper portion of the RG branch, it is sufficient to show that this process does not have a significant influence on the population of low-mass stars. This result also

applies to intermediate-mass stars: although they are substantially more luminous and larger, the increased core mass compensates for the more extended envelope. The core–envelope binding energy is comparable and a similarly hard (and rare) kick is required to free the core. Hence, although core ejection is expected to occur often enough to contribute to creation of stellar-mass gas clouds, it is not expected to alter integrated properties such as the CO absorption depth significantly.

Although lower-mass stars also inflate to large cross-sections, the ratio of main-sequence to RG lifetimes beats the increased cross-section. Further, in this dynamically hot system, RGs capture only a small fraction of objects with which they collide, but more compact main-sequence stars can dump more than $200\,\mathrm{km\ s^{-1}}$ in relative velocity in a grazing encounter and hence most collisions result in capture. If white dwarfs dominate the central mass density and $n_* \approx 10^8\,\mathrm{pc^{-3}}$, a main-sequence star will collide with a white dwarf every $\sim 2\,\mathrm{Gyr}$. Hence, a large fraction of the Population II component should have captured companions. These companions would typically have orbits of only a few $\mathrm{R}_\odot$ and hence be engulfed in a common envelope during the giant phase of the primary. There are some data on field RGs which demonstrate that such tight binaries prevent evolution through the RG phase. Unlike samples of warmer stars, there are indications of a deficit of RGs in binaries with periods less than $\sim 1\,\mathrm{yr}$ (Griffin 1985; Duquennoy & Mayor 1991). If correct, this suggests that the shorter period systems undergo mass transfer or common-envelope evolution, preventing the primary from ever appearing as a RG.

Models considering realistic stellar orbits, binary dissociation rates, and a star formation history over the age of the Galaxy could be combined with improved constraints on the composition of the central mass excess to assess the significance of tidal capture to the central red-giant population. Three factors may reduce the fraction of low-mass stars with captured companions from unity: the fraction of the

central mass density in the form of stellar remnants may be significantly smaller than assumed here, some of the intermediate- and low-mass stars may be younger than the Galaxy, and most of their orbits could be spent in lower density regions.

It is now possible to test the mechanism of tidal capture with RGs in globular clusters with HST observations of core populations. For example, M15 has a deficiency of RGs in the central 6″ which explains the bluer core observable from the ground (Guhathakurta 1995). A bluer core is seen in many post-core-collapse clusters but not in less concentrated cluster cores. Hence, these data support tidal capture during core collapse. Further work on the statistics and distribution of RGs and blue stragglers in globular clusters will further constrain the capture efficiency.

As briefly reviewed in Section 4.1, the characteristics and cause of the CO depletion region are still poorly understood. It remains unclear whether a deficit of RGs exists, much less what fraction of expected RGs are absent, as the presence of a second, bluer population is a viable explanation for the entire effect. Nonetheless, capture of companions may provide a significant reduction in the central density of RGs, as well as explain the gas clouds. If the clouds are formed in this manner (they may instead be part of a coherent structure), they should have detectable expansion velocities and distorted morphologies like elliptical or butterfly planetary nebulae (Livio & Soker 1988).

6.10 Summary

Many models for the alteration of stellar evolution in the GC region have been reviewed and most have been found to operate too slowly to explain the collection of blue massive stars. We confirm what could be surmised from the extraordinary luminosities of several of the IRS 16 sources (see Figure 5.3), that single star evolution cannot be expected to produce this population. We can identify no sufficiently

strong interaction mechanism among the massive stars to modify their evolution, such as wind or supernova explosions. It also appears unlikely that outbursts by Sgr A* can account for the population. New numerical results indicate the same for tidal capture of low-mass stars or remnants by RSGs and for core ejection in collisions.

It therefore appears likely that the peculiarities of the observed population are a result of their conditions of formation. For example, tight, coeval binaries are a possible cause for anomalous evolution of massive stars. High-mass binaries are common in all environments and there is some evidence (in the dense cores of 30 Dor and NGC 3603) that tight binaries are more likely in dense star forming regions. Cluster evolution will also slowly drive high-mass binaries harder. Transfer to the secondary or expulsion from the binary of the primary's envelope is expected to leave a helium star consistent with the observed properties of the GC stars, although the luminosities of the brighter members remain problematic. Through binary evolution, the mass range from which WR-like stars can be drawn and the duration of this phase would be increased. According to this interpretation, the distinction of the GC from the nuclei of M31 and M32 is that the latter have not had recent episodes of massive star formation. Although difficult, a search for binaries among the He I stars could confirm these conclusions. Very high resolution observations of additional dense regions with recent star formation would also test this conclusion.

A second possibility is that unusual conditions of formation led to a distribution of stellar masses which is significantly different from that expected from a standard IMF. If so, then this concentration of stars which are analogous to the most extreme stars seen in other environments could arise from normal evolution of an abnormally high number of very massive and very luminous stars. This cluster may unexpectedly prove useful for studies of massive stellar evolution.

Tidal capture by lower-mass main-sequence stars is expected on an interesting timescale and can explain the observed gas clouds. The clouds should have observable signatures if they are expelled common envelopes. This process may also operate at a sufficient rate to reduce the spatial density of RGs measurably in the central 1/2 pc by accelerating their evolution to white dwarfs. A quantitative estimate of the effect will require more detailed analysis than is provided here. Such an analysis is of interest because this process could explain the decrease in CO absorption depth that is observed in the region.

Chapter 7

Concluding Remarks

7.1 Major Conclusions

The major results of this work are:

- The broad He I emission feature from IRS 16 arises from stellar winds associated with the bright stars.
- The bright blue sources at the GC are apparently evolved stars from a recent star formation episode.
- The bright blue sources' contributions to the region's ionization are poorly constrained, but the ionization is naturally explained by the large population of hotter, late-OV stars expected to accompany the evolved stars.
- Considered individually, the helium emission stars are not peculiar, although they are remarkable with very high luminosities for warm stars.
- As a group and in the context of the region's red population, the He I star population is inconsistent with the predictions of a single episode starburst model, even with generous allowances for the uncertainties in massive stellar

evolution. A starburst extended slightly in time provides more parameters but is a better fit.

- The nuclei of M31 and M32 do not have similar populations. This indicates that the GC is in some way unique or in a transitory state, ruling out many steady-state models for the blue sources.

- Expected influences on single star evolution cannot explain this peculiar population; interactions among the massive stars, or with the mass-dominating population, or with Sgr A* are not probable explanations.

- Unusual conditions of formation are speculated to lead to a higher fraction of luminous helium stars. The tight-binary fraction may be enhanced or there may be a strong predilection to very massive stars.

- We confirm that stellar interactions may cause the observed gas clouds and CO depletion region. We find that tidal capture into close binaries is the most likely mechanism.

- Kinematics derived from the He I population are consistent with those derived from CO-bandhead and gas kinematics. An upper limit on the central mass of $1.8 \times 10^6\,M_\odot$ is derived from these data alone, substantially lower than found by Krabbe *et al.* (1995).

Our proximity has allowed us to probe details of the GC which are unnoticed in more distant nuclei. With these details have come more perplexing problems. Having determined that the GC is in a transient state, how often does this state recur and what fraction of other nuclei share similar populations?

7.2 Future Directions

New observations will continue to add to our understanding of this region and the dominant processes in galactic nuclei, and to the questions we must address. We have seen that high spectral resolution is an important tool in K-band observations of the warm, luminous stars. Larger comparison samples with broader wavelength coverage and studies of the surrounding star formation areas with comparable resolution may be able to clarify the peculiarity of the individual stars. Adaptive optics and space based observations will make the crowding less of a problem. This will permit higher precision color determinations, deeper luminosity functions extending to the main sequence, searches for eclipsing and intrinsically variable stars, and less contaminated spectroscopy. Proper motion and high-resolution radial velocity measurements will allow characterization of the stellar orbits and mapping of the central mass distribution. Space-based observations of other galactic nuclei can extend the sample of nuclei in which we can test for the presence of similar populations beyond M31 and M32. Adding realistic star formation histories and stellar orbits to red-giant tidal-capture models will allow us to address whether the CO depletion region has an extent consistent with what this mechanism would produce.

We have shown that the bright He I sources in the GC are similar to extreme stars seen elsewhere but unique as a population. This population must arise from peculiar formation rather than from unusual stellar evolution unique to this region. The peculiarity of the warm population raises the issue of how star formation in dense galactic nuclei is different from formation in less dense regions.

REFERENCES

Abt, H. A. 1983, ARAA 21, 343

Allen, D. A., Hyland, A. R., & Hillier, D. J. 1990, MNRAS 244, 706

Backer, D. C. & Sramek, R. A. 1987, in AIP Conf. Proc. 155, The Galactic Center, ed. D. C. Backer, (New York: AIP), 163

Bailyn, C. D. 1988, Nature 332, 330

Becklin, E. E. & Neugebauer, G. 1968, ApJ 151, 154

Binney, J. & Tremaine, S. 1987, Galactic Dynamics (Princeton: Princeton)

Blum, R. D., DePoy, D. L., & Sellgren, K. 1995a, ApJ 441, 603

Blum, R. D., Sellgren, K., & DePoy, D. L. 1995b, ApJ 440, L17

Bonnell, I. A. 1994, MNRAS 269, 837

Castor, J. I., Abbott, D. C., & Klein, R. I. 1975, ApJ 195, 157

Close, L. M. & McCarthy, D. W., Jr. 1994, PASP 106, 77

Close, L. M., McCarthy, D. W., Jr., & Melia, F. 1995, ApJ 439, 682

Conti, P. S. 1988, in O Stars and Wolf-Rayet Stars, ed. P. S. Conti & A. B. Underhill, (Washington: NASA), 81

Cotera, A. S., Erickson, E. F., Colgan, S. W. J., Simpson, J. P., Allen, D. A., & Burton, M. G. 1996, ApJ in press

Crowther, P. A., Hillier, D. J., & Smith, L. J. 1995, A&A 293, 172

Davidson, J. A., Werner, M. W., Wu, X., Lester, D. F., Harvey, P. M., Joy, M., & Morris, M. 1992, ApJ 387, 189

Davies, M. B., Benz, W., & Hills, J. G. 1991, ApJ 381, 449

DePoy, D. L. & Sharp, N. A. 1991, AJ 101, 1324

Drissen, L. 1994, STScI Newsletter, 11-2, 7

Drissen, L., Moffat, A. F. J., Walborn, N. R., & Shara, M. M. 1996, ApJ in press

Duquennoy, A. & Mayor, M. 1991, A&A 248, 485

Eckart, A., Genzel, R., Hofmann, R., Sams, B. J., & Tacconi-Garman, L. E. 1993, ApJ 407, L77

Eckart, A., Genzel, R., Hofmann, R., Sams, B. J., & Tacconi-Garman, L. E. 1995, ApJ 445, L23

Eckart, A., Genzel, R., Krabbe, A., Hofmann, R., van der Werf, P. P., & Drapatz, S. 1992, Nature 355, 526

Eenens, P. R. J. & Williams, P. M. 1994, MNRAS 269, 1082

Eenens, P. R. J., Williams, P. M., & Wade, R. 1991, MNRAS 252, 300

Fabian, A. C., Pringle, J. E., & Rees, M. J. 1975, MNRAS 172, 15P

Forrest, W. J., Shure, M. A., Pipher, J. L., & Woodward, C. E. 1987, in AIP Conf. Proc. 155, The Galactic Center, ed. D. C. Backer, (New York: AIP), 153

Frogel, J. A., Persson, S. E., Aaronson, M., & Matthews, K. 1978, ApJ 220, 75

Frogel, J. A. & Whitford, A. E. 1987, ApJ 320, 199

Garmany, C. D. & Conti, P. S. 1980, in Close Binary Stars: Observations and Interpretation, ed. M. Plavec *et al.* (Dordrecht: IAU), 163

Genzel, R. *et al.* 1995, ApJ 444, 129

Griffin, R. F. 1985, in Interacting Binaries, ed. P. Eggleton & J. Pringle (Dordrecht: Kluwer), 1

Guhathakurta, P. 1995, unpublished

Güsten, R., Genzel, R., Wright, M. C. H., Jaffe, D. T., Stutzki, J., & Harris, A. I. 1987, ApJ 318, 124

Hall, D. N. B., Kleinmann, S. G., & Scoville, N. Z. 1982, ApJ 260, L53

Haller, J. W. 1992, Ph.D. thesis, University of Arizona

Haller, J. W. & Rieke, M. J. 1989, in The Center of the Galaxy ed. M. Morris (Dordrecht: Kluwer), 487

Haller, J. W., Rieke, M. J., Rieke, G. H., Tamblyn, P., Close, L., & Melia, F. 1996, ApJ 456, 194

Hanson, M. M. & Conti, P. S. 1994, ApJ 423, L139

Hanson, M. M., Conti, P. S., & Rieke, M. J. 1996, ApJS submitted

Henry, J. P., DePoy, D. L., & Becklin, E. E. 1984, ApJ 285, L27

Herbst, T. M., Beckwith, S. V. W., Forrest, W. J., & Pipher, J. L. 1993, AJ 105, 956

Hills, J. G. 1975, Nature 254, 295

Hjellming, M. S. & Taam, R. E. 1991, ApJ 370, 709

Hollywood, J. M. & Melia, F. 1995, ApJ 443, L17

Humphreys, R. M. & Davidson, K. 1994, PASP 106, 1024

Hut, P. 1985, in Dynamics of Star Clusters, ed. J. Goodman & P. Hut (Dordrecht: IAU), 231

Khokhlov, A. M. & Melia, F. 1996, ApJ 457, L61

Kormendy, J. 1988, ApJ 325, 128

Krabbe, A., Genzel, R., Drapatz, S., & Rotaciuc, V. 1991, ApJ 382, L19

Krabbe, A. *et al.* 1995, ApJ 447, L95

Kurucz, R. 1992, private communication

Lacy, J. H., Achtermann, J. M., & Serabyn, E. 1991, ApJ 380, L71

Lacy, J. H., Townes, C. H., Geballe, T. R., & Hollenbach, D. J. 1980, ApJ 241, 132

Lacy, J. H., Townes, & Hollenbach 1982, ApJ 262, 120

Lauer, T. R. *et al.* 1992, AJ 104, 552

Lauer, T. R. *et al.* 1993, AJ 106, 1436

Lebofsky, M. J., Rieke, G. H., & Tokunaga, A. T. 1982, ApJ 263, 736

Lee, H. M. 1987, ApJ, 319, 801

Lee, H. M. 1993, in The Nuclei of Normal Galaxies: Lessons from the Galactic Center, ed. R. Genzel & A. I. Harris (Dordrecht: Kluwer), 335

Lee, H. M. & Ostriker, J. P. 1986, ApJ 310, 176

Libonate, S., Pipher, J. L., Forrest, W. J., & Ashby, M. L. N. 1995, ApJ 439, 202

Livine, E. & Tuchman, Y. 1988, ApJ 332, 271

Livine, E., Tuchman, Y., & Wheeler, J. C. 1992, ApJ 399, 665

Livio, M. & Soker, N. 1988, ApJ 329, 764

Lutz, D., Krabbe, A., & Genzel 1994, ApJ 418, 244

Maeder, A. 1990, A&AS 84, 139

Maeder, A. & Conti, P. S. 1994, ARA&A 32, 227

Maiolino, R., Rieke, G. H., & Rieke, M. J. 1996, AJ 111, 537

Mantegazzen, L., Paolicchi, P., Farinella, P., & Luzny, F. 1980, in Close Binary Stars: Observations and Interpretation, ed. M. Plavec *et al.* (Dordrecht: IAU), 23

McGinn, M. T., Sellgren, K., Becklin, E. E., & Hall, D. N. B. 1989, ApJ 338, 824

McGregor, P. J., Hillier, D. J., & Hyland, A. R. 1988a, ApJ 334, 639

McGregor, P. J., Hyland, A. R., & Hillier, D. J. 1988b, ApJ 324, 1071

Melia, F. 1994, ApJ 426, 577

Meynet, G., Maeder, A., Schaller, G. Schaerer, D., & Charbonnel, C. 1994 A&AS 103, 97

Mezger, P. G., Zylka, R., Salter, C. J., Wink, J. E., Chini, R., Kreysa, E., & Tuffs, R. 1989, A&A 209, 337

Miller, G. E. & Scalo, J. M. 1979, ApJS 41, 513

Moffat, A. F. J., Drissen, L., & Shara, M. M. 1994, ApJ 436, 183

Moffat, A. F. J., Seggewiss, W., & Shara, M. M. 1985, in Dynamics of Star Clusters, ed. J. Goodman & P. Hut (Dordrecht: IAU), 467

Morris, M. 1993, ApJ 408, 496

Morris, M. 1994, in The Nuclei of Normal Galaxies: Lessons from the Galactic Center, ed. R. Genzel & A. I. Harris (Dordrecht: Kluwer), 185

Morris, M. & Yusef-Zadeh, F. 1987, in AIP Conf. Proc. 155, The Galactic Center, ed. D. C. Backer, (New York: AIP), 127

Morris, P. W., Eenens, P. R. J., Hanson, M. M., Conti, P. S., & Blum, R. D. 1996, ApJ in press

Najarro, F., Hillier, D. J., Kudritski, R. P., Krabbe, A., Genzel, R., Lutz, D., & Drapatz, S. 1994, A&A 285, 573

O'Connell, R. W. *et al.* 1992, ApJ 395, L45

Podsiadlowski, Ph., Joss, P. C., & Hsu, J. J. L. 1992, ApJ 391, 246

Rasio, F. A. & Shapiro, S. L. 1991, ApJ 377, 559

Renzini, A., Greggio, L., Ritossa, C., & Ferrario, L. 1992, ApJ 400, 280

Rich, R. M. 1990, ApJ 362, 604

Richstone, D., Bower, G., & Dressler, A. 1990, ApJ 118, 122

Rieke, G. H. & Lebofsky, M. J. 1985, ApJ 288, 618

Rieke, G. H. & Lebofsky, M. J. 1987, in AIP Conf. Proc. 155, The Galactic Center, ed. D. C. Backer, (New York: AIP), 91

Rieke, G. H. & Rieke, M. J. 1988, ApJ 330, L33

Rieke, G. H. & Rieke, M. J. 1994, in The Nuclei of Normal Galaxies: Lessons from the Galactic Center, ed. R. Genzel and A. I. Harris (Dordrecht: Kluwer), 283

Rieke, M. J., Rieke, G. H., Green, E. M., Montgomery, E. F., & Thompson, C. L. 1993, Proc. SPIE 1946, 214

Rieke, G. H., Rieke, M. J., & Paul, A. E. 1989, ApJ 336, 752

Schaerer, D. 1994, in Unsolved Problems in the Milky Way, ed. L. Blitz (Dordrecht: Kluwer), in press

Schaller, G., Schaerer, D., Meynet, G., & Maeder, A. 1992, A&AS, 96, 269

Schmidt-Kaler, T. H. 1982, in Landolt-Bernstein New Series, Vol. 2b, Astronomy and Astrophysics - Stars and Star Clusters, ed. K. Schaifer & H. H. Voigt (New York: Springer), 451

Sellgren, K., Hall, D. N. B., Kleinmann, S. G., & Scoville, N. Z. 1987, ApJ 317, 881

Serabyn, E. & Lacy, J. H. 1985, ApJ 293, 445

Serabyn, E., Lacy, J. H., & Achtermann, J. M. 1991, ApJ 378, 557

Serabyn, E., Lacy, J. H., Townes, C. H., & Bharat, R. 1988, ApJ 326, 171

Shields, J. C. & Ferland, G. J. 1994, ApJ 430, 236

Simon, M., Chen, W. P., Forrest, W. J., Garnett, J. D., Longmore, A. J., Grauer, T., & Dixon, R. I. 1990, ApJ 360, 95

Simons, D. A., Hodapp, K.-W., & Becklin, E. E. 1990, ApJ 360, 106

Smith, K. C. & Howarth, I. D. 1994, A&A 290, 868

Spitzer, L. Jr. 1987, Dynamical Evolution of Globular Clusters (Princeton: Princeton)

Sweigart, A. V., Greggio, L., & Renzini, A. 1989, ApJS 69, 911

Taam, R. E. 1993, in Interacting Binary Stars, ed. A. Shafter, (San Francisco: ASP), 208

Taam, R. E. & Bodenheimer, P. 1991, ApJ 373, 246

Taam, R. E., Bodenheimer, P., & Ostriker, J. P. 1978, ApJ 222, 269

Tamblyn, P. & Rieke, G. H. 1993, ApJ 414, 573

Townes, C. H. 1989, in The Center of the Galaxy ed. M. Morris (Dordrecht: Kluwer), 1

Townes, C. H., Lacy, J. H., Geballe, T. R., & Hollenback, D. J. 1983, Nature 312, 661

Tuchman, Y. 1985, ApJ 288, 248

Tyson, N. D. 1993, in Back to the Galaxy, ed. S. S. Holt and F. Verter (New York: AIP), 141

van der Hucht, K. A., Conti, P. S., Lundström, I., & Stenholm, B. 1981, Space Sci.Rev. 28, 227

Wade, R., Geballe, T. R., Krisciunas, K., Gatley, I., & Bird, M. C. 1987, ApJ 320, 570

Walborn, N. R. 1982, ApJ 256, 452

Werner, M. W., Becklin, E. E., Stauffer, J., & Lee, T. 1991, BAAS 23, 830

Werner, M. W. & Davidson, J. A. 1989, in The Center of the Galaxy, ed. M. Morris (Dordrecht: Kluwer), 423

Yusef-Zadeh, F. & Mehringer, D. M. 1995, ApJ 452, L37

Yusef-Zadeh, F. & Melia, F. 1992, ApJ 385, L41

Yusef-Zadeh, F. & Morris, M. 1987, ApJ 320, 545